Thesis for the Degree of Master of Science
with a major in Textile Engineering
The Swedish School of Textiles
2020-08-24
Report no. 2020.14.07

Preparation of films and nonwoven composites from fungal microfibers grown in bread waste

Maximilian Benedikt Maria Köhnlein

Visiting address: Skaraborgsvägen 3 • Postal address: 501 90 Borås •
Website: www.hb.se/en/The-Swedish-School-of-Textiles

Description: Thesis submitted for the Degree of Master of Science in Textile Engineering

Title: Preparation of films and nonwoven composites from fungal microfibers grown in bread waste

Author: Maximilian Benedikt Maria Köhnlein

Submission Date: 24. August 2020

Contact: koehnlein.maximilian@gmail.com

Supervisor: Akram Zamani

Examiner: Nawar Kadi

Department: The Swedish School of Textiles

Keywords: bread waste, chitin, chitosan, filamentous fungi, film, fungal cell wall, fungal microfibers, glucosamine, mycelia, N-acetyl-glucosamine, nonwoven, wet-laid

ABSTRACT

Unsold bread makes up a signification fraction of waste occurring in Swedish supermarkets. This thesis seeks to address the problem of food waste, by cultivating filamentous fungi on bread waste and producing chitinous films and nonwovens from them.

Rhizopus delemar was cultivated on bread waste in liquid-state fermentation in order to obtain mycelia biomass. The biomass was processed by alkali or protease treatments to disrupt the fungal cells and remove proteins and fats. Afterwards it was subjected to a bleaching treatment to remove lignin fractions of bread residues. The treated biomass was then subjected to a grinding treatment for a homogeneous dispersion of mycelial fibers, where the dispersion was confirmed by microscopic images. The chemically and mechanically processed biomass was used for the preparation of films and nonwoven composites by employing a wet-laid papermaking process. The films exhibited plastic-like features, due to their brittleness and their smooth upper surface.

Films and nonwoven composites were characterized on their tensile properties, surface water contact angle and their surface morphology by scanning electron microscopy. Treating fungal biomass by alkali and then bleaching resulted in films with a tensile modulus of 3.38 GPa and an ultimate tensile strength of 71.50 MPa. These are the highest reported tensile properties for mycelia derived films to date. Water contact angle measurements confirmed a hydrophobic quality of mycelial films. Scanning electron microscopy showed a very dense and even surface without an obvious fibrous morphology.

Fungal biomass and viscose fibers together form a rigid nonwoven composite, in which fungal biomass takes over the role of a natural eco-friendly binding matrix. Flexural rigidity measurements were out of bounds and need to be confirmed by future studies.

Additionally, a second strain of fungi, Fusarium venenatum, was cultivated on bread particles in water suspension in order to determine optimum growth conditions for future scale-up investigations.

POPULAR ABSTRACT

Unsold bread makes up a significant fraction of waste occurring in Swedish supermarkets. This thesis seeks to address the problem of food waste, by cultivating filamentous fungi on bread waste and producing films and textiles from them. Filamentous fungi can be grown in liquids and are made up entirely of mycelium.
A filamentous fungus was grown on bread mixed with water in order to obtain mycelium biomass. The biomass was processed by chemical treatments to remove proteins and leaving the fibrous part of the fungi. Afterwards it was bleached to break down lignin parts from left over bread particles. The treated biomass was then subjected to a grinding treatment to break up entangled mycelium. From this biomass, films and nonwovens were produced by using a papermaking process.
Treating fungal biomass by enzymes or alkali and then bleaching resulted in films with exceptionally high tensile properties, which have not been reached before. Water contact angle measurements showed that the films do not absorb water, when a drop is placed on their surface. Microscopic images showed a very dense and smooth surface of the films. Fungal biomass and viscose fibers together form a rigid structure, in which fungal biomass acts as a natural eco-friendly binder.

ACKNOWLEDGEMENT

This thesis was conducted as part of the research project “Sustainable Fungal Textiles: A novel approach for reuse of food waste”. The project is financed by VINNOVA. The project is a collaborative effort between University of Borås, KTH Royal Institute of Technology, Sahlgrenska University Hospital, RISE Research Institutes of Sweden and Karolinska Institute

I want to thank Sofie Svensson and Jorge Ferreira at the Department of Resource Recovery and Building Technology for their support and collaborative effort through this project. Also, a big thank you to everyone of the staff and fellow researchers working in the labs at University of Borås. Many thanks to Nawar Kadi for the examination of this thesis. I also want to thank Michael Magnusson and his team at RISE Institute in Stockholm for the support they offered me during my stay there.
My sincerest gratitude goes to Akram Zamani for her supervision of this thesis and her continued support throughout the project.

Scanning electron microscopy was performed by a project partner at KTH Royal Institute of Technology.
Determination of GlcN and GlcNAc concentrations was done by Sofie Svensson at University of Borås.

TABLE OF CONTENTS

LIST OF ABBREVIATIONS

Abbreviation	Explanation
AIM	alkali insoluble material
ATCC	American Type Culture Collection
DD	degree of deacetylation
FE-SEM	field emission scanning electron microscope
FPU	filter paper units
FTIR	Fourier transform infrared spectroscopy
GHG	greenhouse gas
GlcN	glucosamine
GlcNAc	N-acetyl-glucosamine
HPAEC	high performance anion exchange chromatography
HPLC	high performance liquid chromatography
rcf	relative centrifugal force
RI	refractive index
rpm	rotations per minute
SEM	scanning electron microscopy
ssNMR	solid state nuclear magnetic resonance
VMNC	viscose-mycelia nonwoven composite
vvm	volume of air per volume of liquid per minute
WCA	water contact angle

LIST OF FIGURES

LIST OF TABLES

1 INTRODUCTION

1.1 PROBLEM DESCRIPTION

Unsold bread is among the top contributors of waste occurring in supermarkets (Brancoli et al., 2017). In Sweden, most of this waste is currently used for the production of biogas or it is incinerated for energy recovery (Eriksson et al., 2015). This project investigates the possibility to use bread waste as a substrate for cultivation of filamentous fungi, which are then used to produce films and nonwoven composites. Filamentous fungi are a well-known group of organism in biotechnology and are used for the production of a wide array of high-value products, such as antibiotics, ethanol, pigments or protein-rich food (Money, 2016; Wiebe, 2002). Filamentous fungi are also interesting to research due to their high contents of chitin in their cell wall. Chitin is a load bearing component in the exoskeletons of insects and crustaceans and in the cell wall of fungi. Chitin and its deacetylated derivative chitosan show many beneficial characteristics; among others antimicrobial properties, wound healing promotion and metal ion chelation.(Islam et al., 2017; Knezevic-Jugovic et al., 2010)

Nowadays, chitin is mostly won by processing shell wastes of crustaceans such as shrimp. However, shellfish waste as a chitin source poses some disadvantages. It is dependent on seasonal and local availability of shellfish and chitin is isolated by demineralization via dilute hydrochloric acid and protein-removal by dilute sodium hydroxide solution (Muñoz et al., 2018). Fungi as a chitin source offer a seasonal and local independence. Furthermore, chitin can be isolated from fungi by mild alkali or enzymatic treatment. (Ghormade et al., 2017) Lastly, filamentous fungi are low-demanding in terms of nutritional requirements. In fact, it has been shown, that they can be grown on industrial waste or food wastes, which are rich in starch and sugars, such as blackstrap molasses (M. Jones et al., 2019), spent sulfite liquor (Johnson and Carlson, 1978) or bread waste (Gmoser et al., 2019; Nair et al., 2017).

Chitosan is commonly derived from chitin by deacetylating it in a concentrated alkali solution at elevated temperatures. However, filamentous fungi of the order of zygomycetes are known to have significant amounts natural chitosan in their cell wall (Bartnicki-Garcia, 1968). Chitosan is known to promote wound healing and acts as an antimicrobial agent. Previous research has shown that wounds exhibit higher bursting strength when they are healing in the presence of chitosan. Chitosan is also known to chelate metal-ions, especially in water. Therefore, it is already used industrially in filters for the purification of a wide array of liquids, e.g. in the beverage industry as well as the textile and agriculture industry. (Desbrières and Guibal, 2018; Morin-Crini et al., 2019)

Fungi have been studied before for the production of chitinous films. However, the most used fungus is the common white champion mushroom (Janesch et al., 2020; Nawawi, 2016). Here, (nano-)fibers are isolated from the fruiting body. Another proposition is the use of filamentous fungi, since they exhibit an inherent fibrous

structure, due to their mycelial growth (M. Jones et al., 2019). This fibrous structure can then be readily used for the preparation of films.
The research at hand seeks to combine the repurposing of food waste (here bread waste) for cultivation of filamentous fungi with the production of chitinous films and nonwovens, which can potentially be applied for wound healing and water filtration purposes. In order to obtain useful films and nonwoven materials, their tensile properties have to be studied and optimized. Additionally, former studies use an alkali treatment for protein removal of the fungal cell wall (Janesch et al., 2020; M. Jones et al., 2019; Nawawi et al., 2020a). This study proposes a novel approach by hydrolyzing proteins in the fungal cell wall via enzymes. The advantage of this method is an even more environmentally friendly hydrolysis treatment, since the waste obtained is neither highly acidic nor alkaline. Additionally, it is expected that by future research, the hydrolyzed protein fractions from fungi can be recovered and processed into protein-rich food products or animal feed. This would drastically lower the amount of waste occurring during the processing of filamentous fungi.

All in all, the research at hand seeks to develop high-value chitinous films and nonwovens from filamentous fungi while reducing the environmental impact of the preparation process to a minimum.

1.2 RESEARCH QUESTIONS

The following questions guided the research throughout the project. Some of those questions served as a starting point of the thesis, while others arose during experiments, when certain phenomena or problems were observed.

- Can a wet-laid papermaking process be used for the production of films from fungal fibers?
- Can fungal fibers be used as a natural binder for wet-laid viscose nonwoven textiles?
- What influence do concentrations of chitin and chitosan have on tensile properties of wet-laid films from fungal biomass?
- What effect do protein-removal processes, such as alkali or enzyme treatment, have on properties of wet-laid films?
- What influence do bread particle residues have on those properties?
- Can bread particle residues be removed or reduced post cultivation by bleaching or enzymatic treatments?

The research at hand worked with two strains of fungi: *Rhizopus delemar* CBS 145940 and *Fusarium venenatum* ATCC 20334. The first strain was already investigated on its cultivation on bread medium and how it would perform in a scale-up in a previous research (Bucuricova, 2019). Therefore, the cultivation experiments of *F. venenatum* were guided by the following goals:

- Define cultivation conditions on suspended bread medium for maximum fungal growth.
- Investigate the effect of bread liquification on fungal growth

1.3 LITERATURE REVIEW

1.3.1 BREAD WASTE IN SUPERMARKETS

Brancoli et al. (2017) identified bread to be the main contributor to supermarket food waste in Sweden. According to Stenmarck et al. (2011) there are a number of reasons for the problem of food waste occurring in supermarkets. The main contributors being the customer's demands on freshness and perceived quality as well as expectations to have full shelves at any operating time of the supermarket. Unpackaged, freshly baked bread is especially sensitive to those demands since supermarkets do not disclose a best before date. Brancoli et al. (2017) and Stenmarck et al. (2011) come to the finding that freshly baked bread is the main contributor to waste in the overall category of bread and pastries. Gmoser et al. (2019) claim 7-10% of globally produced bread products end up as waste.

In light of the recent focus on the carbon footprint of consumer products and services, it is in everyone's interest to reduce overall food waste (Garnett, 2011). Currently, bread waste from supermarkets in Sweden is handled via incineration for energy recovery or anaerobic digestion to produce biogas. In some cases bread is taken back by the supplier and repurposed as pig feed (Eriksson et al., 2015).

An alternative option is to repurpose food wastes for the biosynthesis of high-value products via the cultivation of fungi. Cultivations of fungi on bread waste have been studied by Nair et al. (2017) where the fungi *Neurospora intermedia*, *Aspergillus oryzae*, *Mucor indicus* and *Rhizopus oryzae* were used for the production of ethanol in liquid state fermentation. Gmoser et al. (2019) conducted research on the cultivation of edible fungi *Neurospora intermedia* on bread waste. They showed that through a two-step fermentation process of liquid- and solid-state fermentation, fungi can be used to produce an array of high-value products such as ethanol, nutrient-rich animal feed and pigments.

1.3.2 INTRODUCTION TO FILAMENTOUS FUNGI

Discussion about the classification of life-forms on earth are still ongoing. However, the currently accepted proposal is a classification of two domains: *Eukaryota* and *Prokaryota* (cell-based species with and without a cell nuclei, respectively). *Eukaryota* are further divided into the five kingdoms of *Animalia*, *Chromista*, *Fungi*, *Plantae* and *Protozoa* (Ruggiero et al., 2015). Subdivisions of kingdoms are called phyla. The former phylum of fungi *Zygomycota* is of great interest to this thesis since these fungi are known to contain chitin and chitosan in their cell wall. Fungi formerly belonging to the recently abandoned phylum *Zygomycota* are now reclassified either to *Mucoromycota* or *Zoopagomycota*. (Spatafora et al., 2016).

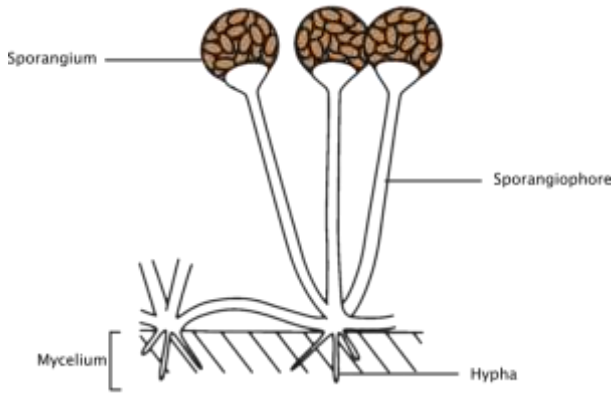

Figure 1 Schematic of filamentous fungi (based on Piepenbring (2015), licensed under CC BY-SA 3.0)

The term *filamentous fungi* is not used for a strict taxonomical classification but is a more general description of eukaryotic microorganisms which exhibit the growth of mycelium as part of their life cycle. (Kinsey et al., 2003) The mycelium is the fungal network structure which penetrates its surrounding substrate and absorbs nutrients (see *Figure 1*). Mycelium (pl. mycelia) is built of subunits called hyphae, which are the singular branches of mycelia. Through hyphae fungi secrete enzymes into their surroundings, which break down nutrients (e.g. starch into glucose monomers). These are then absorbed through the cell wall and are used for biosynthesis. Hyphae which grow outside nutrient medium into regions of air form sporangiophores, which are used for asexual reproduction via spore propagation.
The production of enzymes makes filamentous fungi a widely used organism in biotechnological processes. Next to the production of enzymes they are also used to produce e.g. polysaccharides, pigments, antibiotics, ethanol and lipids. (Money, 2016)

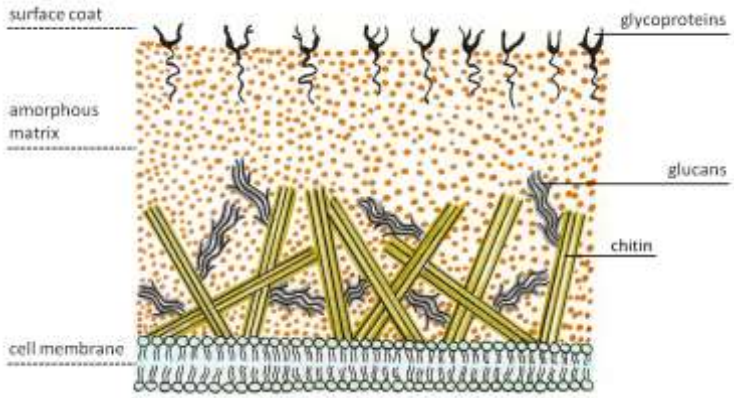

Figure 2 Cell wall structure of filamentous fungi (based on Maya (2013), licensed under CC BY 3.0)

As previously mentioned, the interesting trait of filamentous fungi to this thesis is their cell wall, which is known to contain chitin and chitosan for some phyla. The cell wall of filamentous fungi exhibits a composite structure, consisting of an amorphous matrix and a structural component as illustrated in *Figure 2*. The amorphous

matrix is made up of a complex of polyphosphates, polyglucuronic acid and polysaccharides among others. Zygomycetes also exhibit chitosan as part of the amorphous matrix. The chemical constitution of the structural components varies, depending on the taxonomy of fungi. Among others it can consist of chitin and β-glucans. (El-Enshasy, 2007)

Bartnicki-Garcia (1968) established a classification of eight fungi groups related to their chemical cell wall composition. Fungi belonging to the former class of *Zygomycetes*, which are now reclassified among the phyla *Mucoromycota* and *Zoopagomycota*, were found to have chitin and chitosan as the main components in their cell wall. Bartnicki-Garcia reports on *Mucor rouxii* (phylum: *Mucoromycota*) with a concentration content of 9.4%[1] and 32.7% of chitin and chitosan respectively. Liao et al. (2008) report on the chitin content of *Rhizopus oryzae* (phylum: *Mucoromycota*) ranging from 12% to 19%. The phyla of *Chytridiomycota, Ascomycota, Basidiomycota* and *Deuteromycota* were classified by Bartnicki-Garcia into the group *Chitin-Glucan*. Barbosa and Kemmelmeier (1993) found chitin contents of 27% in the cell wall of *Fusarium graminearum* (phylum: *Ascomycota*). *Fusarium sulphureum* was found to have a chitin content of 39% according to Barran et al. (1975).
Former zygomycetes are also known to contain high amounts of glucuronic acid and polyphosphates in mycelia. *Mucor rouxii* was found to contain 11.8 wt% glucuronic acid and 23.3 wt% phosphate (Bartnicki-Garcia, 1968). Glucuronic acid and (poly)phosphates are anionic compounds, which bind to the cationic chitosan polymers. The ionic bonding between those compounds makes them insoluble in conventional alkali and acid treatments, which are commonly applied for the isolation of chitin and chitosan (Gow et al., 2007, p. 46; Zamani et al., 2007). However, chitosan was shown to have a temperature dependent solubility in dilute sulfuric acid. This temperature dependent solubility is not shared with alkali insoluble cell wall compounds such as chitin, glucuronic acid and phosphate. This characteristic allows a liberation of polyphosphates as soluble phosphates and thereby a purification of chitosan (Zamani et al., 2007).

1.3.3 SOURCES AND STRUCTURES OF CHITIN AND CHITOSAN

After cellulose, chitin is the second most abundant natural polymer with more than 1000 tons generated annually by nature. It occurs in fungal cell walls as well as in exoskeletons of crustaceans and insects as a stress-bearing component. (Kumirska et al., 2011) Since chitosan is not as readily available as chitin in nature, it is mostly derived by the deacetylation of chitin. The deacetylation of chitin to chitosan is industrially achieved by alkali treatment. Commonly sodium or potassium hydroxide solutions with concentrations of 30-50% (w/v) are used at elevated temperatures (100-140°C) to produce alkali-insoluble material (AIM). Alternatively, an enzymatic process is possible in which deacetylases are used (Martinou et al., 1998).

[1] all percentages given as percent dry weight of the cell wall

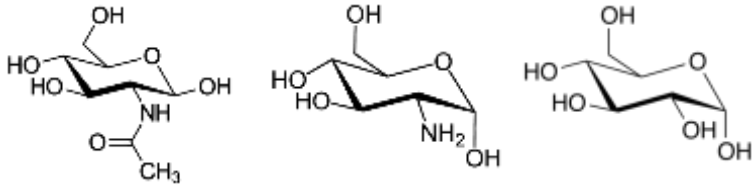

Figure 3 Molecular structures of N-acetyl-glucosamine (left), glucosamine (middle), glucose (right)

Chitin and chitosan are lineally structured polysaccharides made up of randomly distributed glucosamine (GlcN) and N-acetyl-glucosamine (GlcNAc) units in β-(1→4)-linkage. The chemical structures of both monomers are shown in *Figure 3*, together with glucose. The proportion of GlcN to GlcNAc units in the polymer chain determines if the structure is referred to as chitin or chitosan. The ratio of GlcN units is also expressed as the degree of deacetylation (DD) (Kumirska et al., 2011). If a polymer chain contains 60-100% GlcNAc units, it is referred to as chitin. A polymer chain with 60-100% GlcN is called chitosan, as illustrated in *Figure 4* (Roberts, 1992). However, a 100% deacetylation is hardly attainable without process modification, because polymer degradation sets in during the chemical treatment as well (Islam et al., 2017; Zamani, 2010).

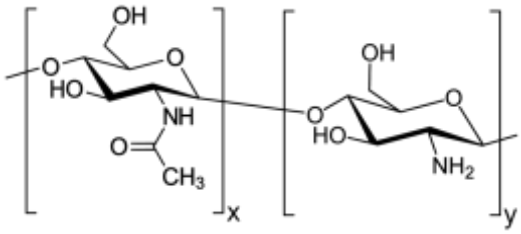

Figure 4 Simplified polymer structure of chitin and chitosan. x > 60% = chitin, y >60% = chitosan. True distribution of monomers is random

On an industrial scale, the main source for chitinous components is currently the shell-waste of crustaceans. However, fungi offer significant advantages as a chitin source compared to crustaceans. Fungi can be grown seasonally and locally independent and the obtained chitin can be tailored to a more specific molecular weight. Chitin derived from crustaceans is often subject to a wider variety in molecular weight. Additionally, fungal cultivation can be achieved on low value substrate and even waste products, which can make the chitin production a more cost-effective and ecological option. Isolation of chitin from shellfish wastes also comes with a hydrochloric acid treatment to remove minerals first before protein removal via alkali treatment can be done. Fungi on the other hand require a mild alkaline treatment to remove proteins. (Jones et al., 2020; Muñoz et al., 2018)

1.3.4 APPLICATIONS OF CHITIN AND CHITOSAN

Chitin and chitosan are nontoxic to humans as well as biodegradable which make them an attractive alternative to synthetic polymers. Further characteristics are their biocompatibility and antimicrobial effects, making them a strong candidate for in vivo applications. The great abundance of chitin in nature also makes it a cheap and easily obtainable polymer. (Islam et al., 2017) Chitinous structures also show wound healing properties. In their review on fungi and crustacean chitin for wound healing applications, Jones et al. (2020) list a number of interactions between various cell types and chitin or chitosan. For example, chitosan coagulates with red blood cells and attracts macrophages, which decompose dead cells. Furthermore, Chung et al. (1994) propose a mechanism in which chitosan interacts with lysozyme, an enzyme transported by the body to the wound during inflammation. Chitosan is degraded by lysozyme into GlcNAc monomers. These monomers then promote collagenase activity in the wound, which leads to higher wound bursting strength. Chitinous powders and wound dressings have been used in research investigating properties of wound healing, tissue engineering and burn healing (Chung et al., 1998; Islam et al., 2017). The hydroxyl and amine groups present in chitosan also make them a good adsorbent for complex metals, metal ions or organic chemicals such as pesticides, dye residues and drugs. This has led to the use in filtration of industrial waste waters from the textile, agriculture or beverage industry among others. (Desbrières and Guibal, 2018; Morin-Crini et al., 2019) For more comprehensive reviews of industrial applications of chitin and chitosan see Kim (2011) and Morin-Crini et al. (2019).

1.3.5 INTRODUCTION TO THE WET-LAID PROCESS

The production of flat structures, such as films from fungal mycelia is best facilitated by a wet-laid process, adapted from papermaking. Once fungal biomass has been dried it exhibits a very brittle nature, which makes other means of textile production highly problematic (Hamlyn and Schmidt, 1994). The drying of fungal mycelia causes the fibers to collapse and thus lose their swelling capabilities. Strong non-covalent bonds between dry chitinous fibers are not broken up by re-wetting without destroying the filamentous morphology at least partly. (Nawawi, 2016) Circumvention of this problem has been found in freeze-drying fungal biomass, which prevents the aforementioned collapse of fibers (Nawawi, 2016; Sagar et al., 1991, 1987). However, this method was not applied in the study at hand.

The wet-laid process originates from paper making and has later been adapted by the textile industry to produce wet-laid nonwoven textiles. However, a distinction between the terms nonwoven and paper is still necessary, since their means of bonding and resulting properties can differ greatly. SS-EN ISO 9092 (2019) defines the paper making process and its products as follows:

> "[Paper making is a] process of producing a thin material by pressing together, short, refined cellulose fibres formed on a screen from a water suspension of these fibres, and drying them, with hydrogen bonding as the predominant mechanism holding the web together […] The refined fibres plus the self-bonding that occurs between cellulose fibres during drying distinguish paper from wet-laid nonwovens."

Inversely, the wet laid nonwoven process is then defined as a “process where cellulose or other fibres are engineered to a level of structural integrity primarily by physical and/or chemical means other than hydrogen bonding” (SS-EN ISO 9092, 2019). Coming back to the similarities between the two technologies, there are three steps of the wet-laid process: fiber dispersion, web formation and drying & bonding (Wilson, 2010). In the case of paper making, a pulping process precedes the fiber dispersion. Pulping refers to mechanical or chemical treatments of wood in order to break up structural bonds between lignin, hemicellulose and cellulose. The resulting fibrous structure of pulp makes paper making possible.

Fiber Dispersion

Fiber dispersion is a crucial step in achieving a homogeneous wet-laid product. Fibers which occur in bundles need to be broken up into singularly free-flowing fibers. This is done by applying shear forces on a fiber suspension. In a conventional paper making process, shear forces are applied by a blunt rotor blade. The energy input of shear forces is controlled by the agitation time and agitation speed of the rotor blade. (Hubbe and Koukoulas, 2016)

Wet-Laying

Wet-laying is done by separating water and fibers through drainage by passing the suspension through a wire screen. Drainage is done on an industrial scale by a moving screen belt (also called a fourdrinier wire) or on lab-scale with a static screen. The main difference between a moving and a static screen is the control over fiber orientation in the wet-laid product. A static screen only allows for the wet-laying of isotropic structures. A moving screen belt can introduce oriented shear forces on the fiber suspension, thereby making it possible to produce webs with anisotropic characteristics. (Ek et al., 2009; White, 2007)

The established lab-scale paper making uses a so called handsheet former. Drainage is done by emptying a column filled with fiber-water suspension through gravitational force (*Figure 5*). Fibers are held back by the wire screen, while water passes through it. Once the water column is drained, draining force on the wet-laid web disappears (TAPPI T 205 sp-12, 2018).

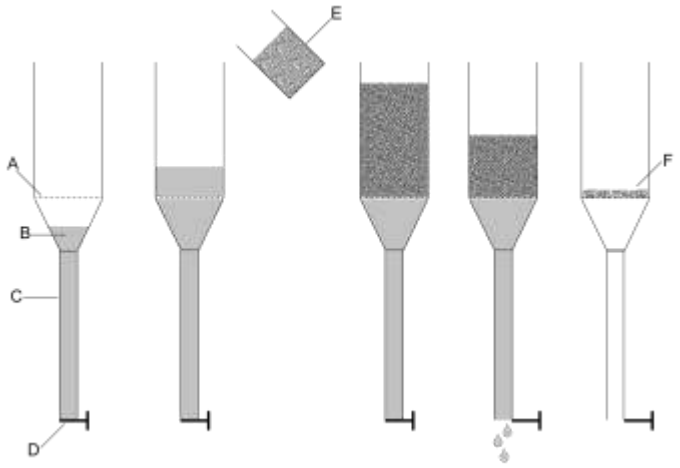

Figure 5 Schematic of the wet-laid process using a handsheet former. The column is first filled with water till above the wire screen. Then a fiber-water suspension is added. Drainage is started after the suspension has been agitated. A wet-laid web remains on the wire screen
A: wire screen, B: water, C: drainpipe, D: drain valve, E: fiber-water suspension, F: wet-laid web

The alternative method of web forming is done by vacuum filtration, using a Büchner funnel. In this method, drainage is done by forcing the water through a wire screen via a partial vacuum. This method is commonly applied in research concerning the preparation of films and nanopapers from nanofibrillated cellulose (Berglund, 2019; Ma et al., 2020). The method was later adapted for the preparation of films from fungal biomass (Appels et al., 2020; Janesch et al., 2020; M. P. Jones et al., 2019; Nawawi et al., 2020a). The main difference to the first method lies in the continued application of draining force, even after the water column has been removed. Wet-laid films can therefore be reduced to a lower water content compared to handsheet forming. However, this also causes a higher entanglement of fibers and the wire screen, as was observed in this study.

Drying and Bonding

Excess water in the wet-laid web is removed by applying pressure. This increases structural integrity by allowing hydrogen bonds to form between fibers. After pressing the remaining water is removed by heat or airflow. Paper and other cellulosic wet-laid structures might not need additional bonding for sufficient structural integrity. However, most nonwoven textiles require bonding through mechanical, thermal or chemical means.

Mechanical bonding is done by needle punching or hydro-entanglement. In the latter highly pressurized water jets are directed on the web surface to cause fiber entanglement. Chemical bonding is done by applying bonding agents such as latex. Commonly water-soluble latex is used, since it can be added during the dispersion process already. Thermal bonding is done by melting thermoplastic components in the web and thereby creating binding points. (Ek et al., 2009; White, 2007; Wilson, 2010)

1.3.6 PRODUCTION OF FILMS FROM FILAMENTOUS FUNGI

In this section a distinction needs to be made between so called *in situ* produced films and films produced through other means. *In situ* production of wet-laid films refers to films prepared from fungal mycelia, which in itself exhibits a fibrous structure and does not necessarily require a fibrillation step to isolate this fibrous structure. The term was introduced by Smelcerovic et al. (2008). On the other hand, the majority of recent studies about film preparation from fungal biomass focuses on films prepared from chitinous (nano)fibers. Chitinous fibers are mostly isolated from fruiting bodies of fungi fit for human consumption, i.e. common white champignon mushroom *Agaricus bisporus* (Janesch et al., 2020; M. Jones et al., 2019; Nawawi et al., 2015; Nawawi, 2016; Nawawi et al., 2019, 2020a, 2020c).
On the other hand, the majority of in situ production of films from filamentous fungi consists of various steps, illustrated in *Figure 6*. Some treatments bear resemblance to the three major steps in production of paper or wet-laid nonwovens, discussed in the previous section.

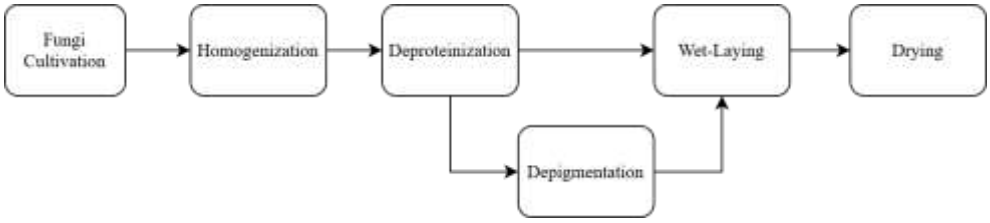

Figure 6 Schematic process of film preparation from fungi

First fungal biomass is cultivated in liquid-state fermentation. By keeping the fungi permanently submerged in liquid media, it is kept entirely in mycelial growth and does not develop sporangiophores or other structures which are not mycelial.
Cultivation of fungal biomass usually lasts 2-4 days, after which the biomass is harvested by separating liquid media from biomass. The biomass is then washed and mechanically and chemically processed in order to prepare it for wet-laying. Wet-laying is done either by employing a handsheet former or by vacuum filtration with a Büchner funnel.
The last step is drying of the films. This is done in consecutive steps, where the first one is the removal of excess water by pressing the wet-laid film between blotting papers. Afterwards, the film can be dried via high pressure at room temperature or by applying heat during pressing. The following sections give a detailed review of studies previously done on the matter of wet-laying of filamentous fungi.

1.3.6.1 CULTIVATING FUNGAL BIOMASS

The idea to produce flat structures from filamentous fungi can be traced back to a patent filed by Van Horn et al. (1957), where they present methods to produce pure mycelial films as well as composite sheets made from fungal biomass and wood pulp. They cultivated fungi of the order *Mucorales* in liquid dextrose-glycerol medium at 24-29°C, keeping the medium aeriated by an undisclosed method. Harvesting was done after 70 hours of cultivation, achieving a dry biomass yield of 5 g/l

media. Following the classification of Bartnicki-Garcia (1968), the fungi belongs to the Chitin-Chitosan group.
Johnson and Carlson (1978) worked with *Fusarium* sp. (Chitin-Glucan) and *Mucor rouxii* (Chitin-Chitosan) and cultivated them on diluted spent liquor medium. Sulfite liquor is used to delignify wood in the pulping process. Nowadays spent sulfite liquor is recycled so it can be reused multiple times. Before recycling was introduced, it was considered a waste product, containing high amounts of lignin and carbohydrates (Benjamin et al., 1969).
Jones et al. (2019) also investigated a sugar-rich waste product as cultivation media. Mycelia was cultivated on blackstrap molasses, a byproduct of sugarcane molasses. It is proposed as a low-cost option for cultivation, which offers similar or even better biomass yields than nutrient malt extract medium. Blackstrap molasses was diluted with water to a concentration of 100 g/1 l. Mycelia of *Allomyces arbuscula*, *Trametes versicolor* (both Chitin-Glucan) and *Mucor genevensis* (Chitin-Chitosan) were cultivated in shake flasks in liquid media for 14 days at 25°C and a constant shaking rate of 50 revolutions per minute (rpm).
Wales and Sagar (1990) cultivated among others *Neurospora crassa* and *Trichoderma viride* (both Chitin-Glucan) in shake flasks with malt extract-peptone liquid medium for 48 hours at 30°C and 400 rpm. Appels et al. (2020) cultivated mycelia of *Schizophyllum commune* (Chitin-Glucan) in the dark for 7 days. The cultivation was kept in 2 l shake flasks with 1.2 l minimal medium at 30°C and 200 rpm.

Studies which used fruiting bodies of fungi as a chitinous biomass source received them through a food-vendor and did not perform cultivation themselves. Among the most frequently used fungi were *Agaricus bisporus* (Janesch et al., 2020; M. Jones et al., 2019; Nawawi et al., 2015; Nawawi, 2016; Nawawi et al., 2019, 2020a, 2020c), *Daedaleopsis confragosa* (Nawawi et al., 2015, 2020a) and *Ganoderma tsugae* (Su et al., 1999, 1997). All three fungi belong to the phylum *Basidiomycota*, containing chitin and glucan in their cell wall.

1.3.6.2 MECHANICAL AND CHEMICAL TREATMENT OF BIOMASS

Fungal biomass is generally treated mechanically and chemically to prepare it for wet-laying of films. Mechanical treatment is done to homogenize the biomass by breaking up larger agglomerations and reduce mycelial fiber length if desired. Chemical treatments are done mainly to remove protein fractions from the fungal cell wall. Other effects of chemical treatments are removal of minerals or partly deacetylation of chitin into chitosan.

Homogenization

In early studies homogenization was done by a pulp disintegrator, where agitation is introduced by a stirring rod with blunt rotor blades. Prior to homogenization, an alkali treatment was employed for deproteinization. (Johnson and Carlson, 1978; Van Horn et al., 1957; Wales and Sagar, 1990)
A more recent method developed by Nawawi et al. (2015) uses a kitchen blender for homogenization. After 5 minutes at high speed blending, the slurry is heated to 85°C for 30 minutes in a water suspension of 1:30 w/v. The biomass is then cooled down

to room temperature again and centrifuged at 9000 rpm for 15 minutes at 18°C. The supernatant is poured away and the biomass precipitate is kept for further treatment. The same process was applied in studies of Janesch et al. (2020), Jones et al. (2019) and Nawawi et al. (2020a).
Appels et al. (2020) went directly for the wet-laid process, without homogenizing the mycelial biomass prior. The mycelia cake was suspended in 800 ml of water and then wet-laid in a Büchner funnel using a coffee filter.

Chemical Treatment

The most common treatment to remove protein fractions from the fungal cell wall is done with NaOH. Chitin as well as chitosan are alkali insoluble, making the alkali treatment an easy method to isolate chitinous fractions. The resulting biomass is commonly called alkali-insoluble material (AIM).
Wales and Sagar (1990) prepared a 2M NaOH solution, which was added to the fungal biomass at a concentration of 100 ml NaOH per 1 g dry biomass. The biomass was left for 2 hours at room temperature and then washed until neutral.
Su et al. (1999, 1997) employed an alkali treatment with 1M NaOH solution at 85°C for 24 hours and an alternative treatment at 90°C for 4 hours to expose the chitinous cell wall. (Su et al., 1997) used a 0.1% hypochlorite solution for depigmentation on neutralized alkali treated biomass. After bleaching the biomass residue, it was again neutralized.
The deproteinization process from Nawawi et al. (2015) was again reproduced by Janesch et al. (2020), Jones et al. (2019) and Nawawi et al. (2020a). The centrifuged residue from the homogenization process was treated with 1M NaOH at 65°C for 3 hours. Hydrolyzed substrate was cooled to 25°C, neutralized by repeatedly centrifuging and re-dispersing in water. Finally, a 0.8% w/v suspension with water was created and blended for 1 min to achieve a homogeneous suspension again. Nawawi et al. (2015) did not perform bleaching treatment, due to a suspected depolymerization effect on chitin.
However, (M. Jones et al., 2019) used 1M H_2O_2 and 1M HCl for a post-alkali treatment. Alkali treated *A. arbuscula* biomass was treated in a solvent ratio of 1:15 at room temperature for 1 hour. The treatment did not affect elemental or sugar composition but was successful in removing calcium salts from the biomass. Calcium was present in fungal cell walls, due to its content in the molasses medium used for cultivation.
Janesch et al. (2020) followed the initial alkali treatment with a second cycle of NaOH treatment to deacetylate chitin into chitosan. For this, they did a comparative study in which NaOH concentration and treatment time was varied. All deacetylation was done at 100°C. 20, 40 and 60% w/v NaOH solutions were prepared to treat fungal biomass for 1 hour each. 40% NaOH treatment was also prolonged to 2 hours in a second trial.

1.3.6.3 WET-LAYING OF FILAMENTOUS FUNGI

Su et al. (1999, 1997) produced mycelia films via vacuum filtration through filtration paper. The wet-laid film was freeze dried, after which a circular membrane with a 7 cm diameter and a thickness of 0.1-0.2 mm was achieved.

Nawawi et al. (2020a, 2020b, 2015) produced films with a final grammage of 80 g/m^2 and a diameter of 90 mm. The biomass was mixed with water to a 0.8% w/v concentration and vacuum filtered through qualitative filter paper. The films were subsequently pressed between two blotting papers under 5 kg (estimated to correspond to 7.7 kPa[2]). Then the films were hot pressed at 120°C for 3 hours under 5 kg. Janesch et al. (2020) and Jones et al. (2019) again followed Nawawi et al. for the film production. However, Jones et al. altered the hot pressing step to 120°C for 15 minutes under 500 kg (estimated to correspond to ca. 400 kPa). Janesch et al. reached final grammages of 10 - 85 g/m^2, whereas Jones et al. produced films with 50 g/m^2. It is worth mentioning, that while Nawawi et al. produced specimens with 90 mm diameter, Jones et al. produced specimens with 125 mm and Janesch et al. specimens with presumably 55 mm diameter. Nonetheless, they all describe the application of a 5kg weight for pressing. This difference in applied pressure might have had an effect on tensile properties of films.
As previously mentioned, Appels et al. (2020) went for the most direct production method. The mycelium was transferred from shake flasks to a Büchner funnel after mixing it with 800 ml water. The mycelium was filtered through a coffee filter and afterwards transferred to a flat cellophane covered surface to dry at room temperature and 50% relative humidity.

1.3.6.4 PREPARING NONWOVEN COMPOSITES WITH FUNGAL BIOMASS AS A BINDER

Johnson and Carlson (1978) prepared paper sheets with mixtures of fungal biomass and wood pulp. The paper sheets were prepared according to an earlier version of TAPPI T 205 sp-12 (2018) via a handsheet former. Mycelia-paper composites were produced with grammages of ca. 60 g/m^2 and mycelia concentrations from 5 to 50%. In their study about metal ion adsorption, Wales and Sagar (1990) prepared biomass composite structures by the conventional wet-laid method, where a mixture of mycelia and cellulose based fibers was suspended in water using a disintegrator. The fibers were mixed with mycelium in a ratio of 60% dry weight mycelium and 40% cellulose-based fibers. The composites were then wet-laid using a handsheet former. A second method employed a polyester nonwoven which was impregnated with mycelia by placing the nonwoven on top of the handsheet former's wire screen and then letting the fungal biomass impregnate the nonwoven during drainage. The composites were dried over night at 30°C.
Nawawi (2016) prepared nonwoven composites by mixing flax fibers and fungal biomass. Flax fibers were soaked in water over night for pretreatment. The fungal biomass was added in various concentrations of 5, 10 and 20% w/w to create a fiber mixture. To minimize gradient effects of binder distribution during wet-laying, a layer-by-layer method was employed, where the first layer was poured into the funnel, fully dewatered and then the next layer was poured on top. This process was repeated until composites with > 5 mm thickness were achieved. These composites were hot pressed under 1 MPa pressure at 120°C for 3 hours to achieve a 1 mm thick composite.

[2]estimations on pressure during drying were made by the author of the thesis

For a study on metal-ion adsorption properties Janesch et al. (2020) prepared 50 g/m² nonwoven composites by mixing fungal chitin-glucan isolate with cellulose microfiber sludge in a 20:80 dry weight ratio. A 0.1% w/w dispersion was created by adding water to the mixture and then blended for a total of 5 minutes for homogenization. The vacuum filtered composites were then cold pressed under 5 kg between two blotting papers and afterwards hot pressed at 120°C for 1 hour under 5 kg (both weights are estimated to correspond to ca. 4 kPa).

1.3.7 CHARACTERIZATION OF FILMS

1.3.7.1 CHITIN AND CHITOSAN CONTENTS

Since the main active component in fungal mycelia sheets is chitin and/or chitosan, their concentration in wet-laid films need to be measured. By Kjeldahl nitrogen level method, total nitrogen concentration in biomass can be determined (Kjeldahl, 1883; SS-EN ISO 3188, 1978). In this method all nitrogen is removed from the organic matter and precipitated in the form of ammonia salts. Su et al. (1997) reported the total nitrogen concentration via Kjeldahl method. By a conversion factor of 14.5, they arrived at a chitin content of 50 wt% in *Ganoderma tsugae* films after NaOH treatment. However, this method is flawed, since the conversion factor gives only an estimate and the degree of deacetylation (DD) of glucosamine cannot be determined. A differentiation between chitin and chitosan concentrations is therefore not possible.
More recent studies determine elemental concentrations via carbon, hydrogen, nitrogen, sulfur, oxygen analysis (CHNSO). Glucosamine concentrations are determined directly via high performance anion exchange chromatography (HPAEC). Furthermore, DD is determined by solid state nuclear magnetic resonance (ssNMR), by which concentrations of chitin and chitosan can be determined individually. For confirmation of chitin concentrations, Fourier transform infrared spectroscopy (FTIR) is employed to determine functional groups in molecules. (Janesch et al., 2020; M. Jones et al., 2019; Nawawi et al., 2015, 2020a)
Jones et al. (2019) determined chitin and chitosan concentrations of *Allomyces arbuscula* after NaOH treatment at 11.4 and 2.3 wt% respectively. A subsequent H_2O_2, treatment resulted in 17.2 and 1.6 wt% of chitin and chitosan. Alternatively, HCl post-treatment resulted in 14.0 and 3.9 wt% chitin and chitosan concentrations. *Mucor genevensis* films contained 12.8 and 10.0 wt% chitin and chitosan after NaOH treatment, confirming the classification to Chitin-Chitosan. *Trametes versicolor* was omitted in the analysis of chitin and chitosan contents, since N-contents were very low at 0.3 wt% of total mass, while glucose concentration made up 86.3 wt% of total sugar composition. This suggests that *T. versicolor* consists mainly of glucan and very little chitin.

Studies, which worked with *A. bisporus* fruiting bodies as a chitin nanofiber source, reported chitin concentrations of 36-49.6 wt% after deproteinization via NaOH (Janesch et al., 2020; M. Jones et al., 2019; Nawawi et al., 2019).
Nawawi et al. (2019) reported significantly higher chitin concentrations for the fruiting body's cap in comparison to the stalk (36 and 41 wt% respectively). Janesch et

al. (2020) was successful in deacetylating fungal chitin to chitosan by a second NaOH treatment. Chitosan concentrations up to 38.9 wt% after alkali treatment in 60% NaOH at 100°C for 1 hour were achieved.
Janesch et al. (2020) and Jones et al. (2019) also reported a chitosan content of 7.3 wt% and 11.5 wt% respectively after initial NaOH treatment in *A. bisporus* films. This suggests partial deacetylation is already happening at the first NaOH treatment, since *A. bisporus* does not contain chitosan fractions in its natural state (Michalenko et al., 1976). Similar results of partial deacetylation after NaOH treatment can be expected in the treatment of mycelia.

1.3.7.2 TENSILE PROPERTIES

Johnson and Carlson (1978) performed tests on bursting strength, tensile strength, tearing strength and strain at break. They state that physical influences, such as uneven surface structures, often had a dominating effect on tensile properties compared to the mycelium composition. Nevertheless, they were able to show that mycelial biomass contributes positively to the elasticity of wood pulp-based sheets with the highest strain at break of 2.4% reported for a wood pulp sheet containing 20% of *Saprolegnia ferax* mycelia.
Wales and Sagar (1990) performed tensile tests in both dry and wet state. *T. viride* - manila hemp composite sheets showed a peak load of 5.4 N (wet) and 48.7 N (dry) whereas conventional filter paper had a peak load of 1.0 N (wet) and 31.9 N (dry). Unfortunately, the specimen thickness was not disclosed, otherwise the results could be converted to ultimate tensile strength. *Table 1* lists all relevant results of tensile tests from previous studies.

Table 1 Ultimate tensile strength (σ_{UTS}), Young' s modulus (E), strain at break (ε) of films prepared from various fungal mycelia and fruiting bodies. All films were dried under pressure except for Appels et al.

Fungi	Fiber Size	Treatment	Drying Method	σ_{UTS} (MPa)	*E* (GPa)	ε (%)	Source
S. commune mycelia	microfibers	H_2O	air drying	11.2	1.26	1.2	(Appels et al., 2020)
		1% glycerol*		9.6	0.95	1.4	
		2% glycerol		12.3	1.05	2.2	
		4% glycerol		10.1	0.69	3.8	
		8% glycerol		6.4	0.12	14.9	
		16% glycerol		3.6	0.02	23.7	
		32% glycerol		1.8	0.003	**29.6**	
A. arbuscula mycelia	microfibers	NaOH	4 kPa cold + 400 kPa hot	16.0	1.80	0.9	(M. Jones et al., 2019)
		$NaOH + H_2O_2$		19.2	1.90	1.0	
		NaOH + HCl		14.3	1.70	0.9	
M. genevensis mycelia	microfibers	NaOH		**24.7**	**1.90**	1.5	
T. versicolor mycelia	microfibers	NaOH		0.9	0.70	0.1	
A. bisporus fruiting body	nanofibers	NaOH		97.6	6.50	1.8	
		NaOH	7.7 kPa cold + hot	**204.4**	**6.90**	5.3	(Nawawi et al., 2020a)
D. confragosa fruiting body	nanofibers	NaOH		65.3	1.20	**13.2**	
A. bisporus fruiting body	nanofibers	100% flax composite	1 MPa hot	1.6	0.3	0.8	(Nawawi, 2016)
		95% flax composite		7.2	1.50	0.6	
		90% flax composite		9.4	1.30	1.0	
		80% flax composite		21.6	3.20	1.1	

Appels et al. (2020) showed that soaking *S. commune* films (chitin-glucan) in glycerol over night increased the strain at break drastically. With a treatment of a 32% aqueous glycerol bath, a strain at break of 29.6% was achieved. Expectedly, stiffness was reduced to at the same time to 0.003 GPa, which is a more than 99% decrease compared to untreated films (1.26 GPa). Interestingly, a 2% glycerol treatment lead to an increase in tensile strength (11.2 vs. 12.3 MPa) as well as almost doubling the strain at break (1.2 vs. 2.2%), compared to films not treated with glycerol. Stiffness was slightly decreased from 1.26 to 1.05 GPa.
Tests of Jones et al. (2019) showed that tensile properties of *A. arbuscula* films (chitin-glucan) can be slightly increased by bleaching treatment via H_2O_2. Tensile strength, Young's modulus and strain at break are all improved by the treatment, which was applied to remove inorganic calcium impurities, stemming from the cultivation medium. The removal of calcium then led to an increase in hydrogen bonding between microfibrils. Films from *M. genevensis* yielded the highest tensile properties of mycelia derived films with a tensile strength of 24.7 MPa and a Young's modulus of 1.90 GPa, suggesting that chitosan concentration correlates positively with tensile properties. On the other hand, *T. versicolor* mycelia films showed very low tensile properties, providing further evidence that glucan acts merely as a binder and chitin and/or chitosan are the main stress bearing components. Nawawi et al. (2020a) showed that fruiting body derived films from *D. confragosa* exhibited exceptionally high strain at break of 13.2% with a glucan concentration of 98.9 wt%.

The highest tensile strength and stiffness to date of fungi derived films was reported by Nawawi et al. (2020a): Films prepared from chitin-nanofibers derived from *A. bisporus* fruiting body, exhibited a tensile strength of 204.4 MPa and a Young's modulus of 6.90 GPa. Results of Jones et al. (2019) confirm that fruiting body derived films exhibit much higher tensile strength and stiffness compared to mycelia derived films with a tensile strength of 97.6 MPa and a stiffness of 6.50 GPa. They propose, the large difference between fruiting body and mycelia derived films stems from a much higher chitin content in *A. bisporus* films, reporting a chitin and chitosan content of 30.8 and 11.5 wt%, respectively. However, a major influence might also lie in the size of fibrils. SEM images of Jones et al. show, that while fruiting bodies exhibit nanofibrillar structure after treatment via NaOH and mixing, mycelia show a microfibrillar structure after being subjected to the same treatment.
The stark difference between tensile properties of *A. bisporus* from Jones et al. (2019) and Nawawi et al. (2020a) could also be partially a result of differing drying treatments. Cold pressing was done under the same conditions. However, Jones et al. did hot pressing at 120°C for 15 minutes under 500 kg. Nawawi et al. applied 120°C for 3 hours under 5 kg and left the films to cool off at room temperature over night under the same weight. The higher pressure during drying could be a reason for lower tensile properties. Also, it is not clear if Jones et al. left their films to cool off at room temperature under sustained weight. If this step was omitted, it could be another source of diminished tensile properties.
Lastly, Nawawi (2016) showed that fruiting body derived chitin nanofibers can be used as a natural binder for flax fibers. Highest tensile properties were achieved for a composite consisting of 80 wt% flax fibers and 20 wt% *A. bisporus* chitin nanofibers. This composite showed 13.2 times higher tensile strength and 10.9 times higher stiffness compared to pure flax nonwovens.

Regarding specimen dimensions, Jones et al. (2019) and Nawawi et al. (2020a) performed tensile tests with dog bone shaped specimens with 10 mm gauge length and 2 mm parallel width at the narrow part. The testing speed of the tensile tester was at 1 mm/min. Appels et al. (2020) did tensile tests with type 5A dog bone specimens according to SS-EN ISO 527-2 (2012), which is the same specimen shape used in the study at hand. The specimen's gauge length is 20 mm and its parallel width 4 mm. Testing speed was 2 mm/min.
For tensile testing of nonwoven fungi-flax composites, rectangular shapes of 80 mm length and 15 mm width were cut out with a handsaw. Testing speed was kept at 1 mm/min and the gauge length was set to 50 mm. (Nawawi, 2016)

1.3.7.3 WATER CONTACT ANGLE

Appels et al. (2020) determined a water contact angle (WCA) of 129° for *S. commune* mycelia derived chitin-glucan films, which were dried at room temperature and not subjected to any chemical treatment. Treatment of these films with increasing concentrations of glycerol resulted in a decrease of WCA. After treatment for 24 hours in an 8% glycerol solution, the WCA decreased to 86%. A 32% glycerol solution resulted in a WCA of 49°.
Nawawi et al. (2020a) prepared films of NaOH treated fruiting bodies from *A. bisporus* and *D. confragosa* and reported WCA of 66° and 55° respectively. In a second study Nawawi et al. (2020b) differentiated between films prepared from the stalk and cap of the fruiting body of A. bisporus. However, all films showed similar WCA of ~65°. The water droplets were left on the films' surface and maintained their shape 1 hour after placement.
Jones et al. (2019) reported WCA on NaOH treated mycelia films of 106° (*A. arbuscula*) and 101° (*M. genevensis*). A subsequent treatment of *A. arbuscula* films with H_2O_2 reduced WCA from 106° to 79° and HCl treatment lead to a reduction of WCA to 84°. The decrease of WCA after H_2O_2 or HCl treatment is explained by the removal of lipid residue, which is still present after NaOH treatment. Films prepared from fruiting bodies of *A. bisporus* and treated with NaOH showed a significantly lower WCA of 87°, which is explained by missing lipid fractions in fruiting body derived films. Still, their results show a significantly higher WCA of *A. bisporus* films compared to Nawawi et al. (2020a). This difference might stem from the difference in hot-pressing treatment, where Jones et al. applied a pressure of ca. 400 kPa whereas Nawawi et al. used a pressure of ca. 7.7 kPa.

2 MATERIALS AND METHODS

Figure 7 outlines the general process from cultivation of fungi on bread waste over chemical and mechanical processing to the wet-laying of films and nonwoven materials. The following subsections give a detailed presentation of the materials and methods used in the individual steps.

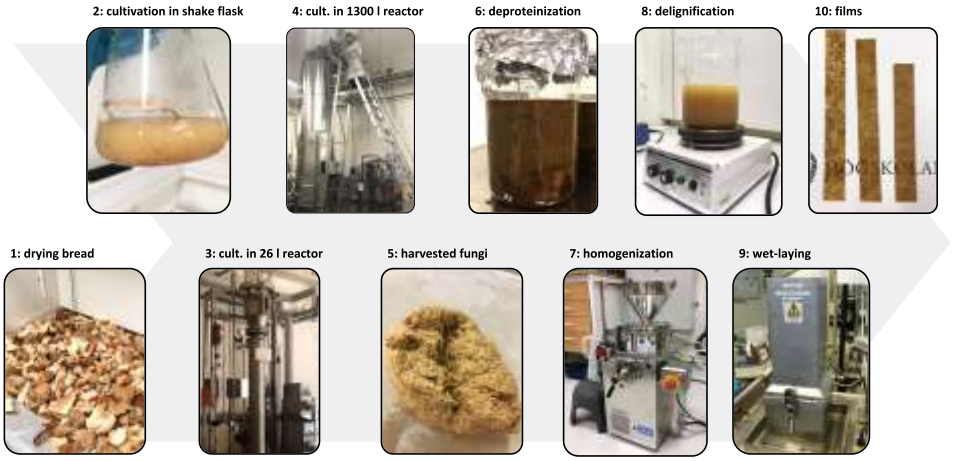

Figure 7 Method for film preparation from filamentous fungi

2.1 FUNGI SPECIES

Studies on production of films and nonwoven composites where conducted on *Rhizopus delemar* CBS 145940. Optimum growth conditions on liquid bread media were already studied by Bucuricova (2019) and therefore the cultivation could be scaled-up directly in order to achieve sufficient biomass to conduct all experiments on the same batch. *Rhizopus* belongs to the former phylum Zygomycota, which is known to contain chitin and chitosan in its cell wall (Bartnicki-Garcia, 1968; Tai et al., 2010).

Fusarium venenatum ATCC 20334 (American Type Culture Collection, Manassas, VA, USA) was selected as a second fungi from which chitinous biomass could be sourced. The chitin-glucan complex in its cell wall is known to result in high tensile strain of wet-laid films. Additionally, chitin contents can be deacetylated to chitosan by prolonged alkali treatment. (M. Jones et al., 2019) Other selection criteria for *F. venenatum* was its biosafety level and filamentous growth. Additionally, *F. venenatum* is a well-known species of fungi and is used as the main ingredient for the meat substitute products *Quorn*™ (Wiebe, 2002).

2.2 CULTIVATION SUBSTRATE

Bread was collected from a nearby *ICA* supermarket in Borås, Sweden. The bread, which comprised bread loafs, buns and puff pastries was removed from sales areas due to drying or superficial blemishes. There were no visible marks of the bread going bad due to mold. Sweet pastries and similar products containing large amounts

of fruits or custard were omitted, since they were suspected to prolong the drying process significantly and cause clogging problems during grinding.

2.2.1 SUBSTRATE PREPARATION

The bread was collected over the course of one week. For drying, the bread was torn into roughly palm sized pieces, then spread out flat to dry at room temperature for 2-3 days as shown in *Figure 8*. Afterwards the bread was placed in a ventilated drying cabinet at 60°C for 6 hours. The dry bread was ground with a cutting mill (*SM 100*, Retsch, Haan, Germany) to a particle size of < 3 mm. Until used for cultivation, the bread was stored in airtight plastic bags at -18°C.
In later cultivation trials with *F. venenatum*, the bread was sieved to a particle size < 1 mm before adding it to the water in order to minimize the undigested bread fraction remaining in the biomass after harvest.

Figure 8 Bread preparation process. Loafs and buns collected from supermarket (left), torn apart to dry (middle), dried, milled and sieved to particle size < 1 mm (right)

2.2.2 SUBSTRATE ANALYSIS

The dried and milled bread particles were analyzed for water content by weighing triplet samples of 10 g bread in aluminum dishes. The specimens were dried in an oven at 70°C over night. Afterwards, they were dried at 105°C for 2 hours. Then the specimen weight was measured using a digital balance (*AEJ 200-4CM*, Kern, Balingen, Germany). The concentration of water was determined by the following equation:

$$C_W = \frac{m_{pre} - m_{post}}{m_{pre}} * 100\%$$

Where C_W is concentration of water, m_{pre} is mass of bread pre drying and m_{post} is mass of bread post drying.
Analysis of nutrient contents of bread was omitted in this thesis. Instead, the bread was assumed to have the same nutrient concentrations which were established by Bucuricova (2019). Her research was concerned with the work of bread collected from the same supermarket in Borås under the same selection criteria. Bucuricova (2019, p. 17) obtained results concerning ash, carbohydrate, starch and nitrogen contents shown in *Table 2*. Protein concentration was derived from total nitrogen concentration by a conversion factor of 5.49 (Mariotti et al., 2008). Total carbohydrates made up 72.30 wt% of dry bread. Of this fraction, 55.50 wt% consisted of glucan, including starch.

Table 2 Nutrient concentrations of bread substrate taken from Bucuricova (2019, p. 17)

Component	Concentration (wt%)
Ash	2.40 ± 0.01
Starch	52.50 ± 0.04
Total carbohydrates	72.30 ± 0.09
Arabinan	6.60 ± 0.04
Galactan	1.80 ± 0.01
Glucan	55.50 ± 0.11
Mannan	6.80 ± 0.03
Xylan	1.60 ± 0.02
Nitrogen	2.30 ± 0.02
Protein	12.80 ± 0.02

2.2.3 SUBSTRATE HYDROLYSIS

Bread particles were later found to cause disturbances in wet-laid biomass films. Therefore, an experiment was conducted which investigated the possibility to break down bread particles via enzyme treatment and then cultivating fungi on a liquified bread medium. A large fraction of undigested bread particles in fungal biomass was found to be seed shells and other lignocellulosic components, which is why cellulase was used to break down those seed shells. Amylase was used to hydrolyze starch to sugars. Protease was used to break down protein fractions to polypeptides.

For enzymatic hydrolysis, granular *Protamex*® protease from Bacillus sp. (Sigma-Aldrich) was used in concentrations of 10 mg/g dry substrate. Liquid α-amylase (*Spezyme CL WB*, Genencor) was used in concentrations of 4 µl/g dry substrate. Liquid cellulase *(Cellic® CTec2*, Novozymes, Bagsværd, Denmark) was used with a concentration of 45 µl/g dry substrate. Its enzymatic activity was previously established to be 220 FPU/ml according to Adney and Baker (2008). All enzyme concentrations were kept the same throughout all enzymatic experiments throughout this thesis. Enzyme solutions were prepared by suspending them in sterile ultrapure water and then passing them through a CA 0.20 µm syringe filter (*GVS North America*, Sanford, ME, USA).

In a 150 ml Erlenmeyer flask, 1 g non-sieved bread particles were sterilized in 50 ml ultrapure water suspension (2% w/v). All sterilization processes were carried out with an autoclave (*VB-150* and *VX-95*, Systec, Linden, Germany). The pH was not adjusted prior to hydrolysis. The following enzyme combinations were carried out in duplicates:

1) Cellulase 2) Protease 3) Cellulase + Protease
4) Amylase 5) Amylase + Cellulase 6) Amylase + Protease
7) Amylase + Cellulase + Protease 8) no enzyme (control)

For enzyme hydrolysis the Erlenmeyer flasks were put in rotary shaking water bath (*OLS 200*, Grant Instruments, Cambridge, UK) at 100 rpm shaking speed and 55°C

for 15 hours. The hydrolyzed substrate was vacuum filtered using a Büchner funnel and grade 5 qualitative filter paper (*Munktell*, Ahlstrom-Munksjö, Helsinki, Finland) with a stated filtration speed of 1000 ml/min. The filtrate was collected in plastic tubes and stored at +4°C until use.
Since amylase treatment resulted in promising yields of soluble solids, it was tested with different bread concentrations in water suspension (2%, 5%, 10%, 15%, 20% w/v). Hydrolysis was performed in a static water bath at 70°C for 2 hours. This time, the bread particles were not sterilized before enzymatic treatment. Static water bath treatment was chosen this time with a large scale process in mind, where constant agitation of liquids might not be possible. To speed up the filtration process, hydrolyzed substrate was passed through a steel wire sieve (< 1 mm particle retention) to separate macro-sized particles. Afterwards the substrates were vacuum filtered by the same procedure mentioned before.
Cultivation experiments with amylase treated bread did not lead to the desired results (results are shown in section 3.3.2). Therefore, bread particles were hydrolyzed by a combination of amylase and protease. 5%, 7.5% and 10% w/v bread suspensions were prepared, to which amylase and protease were added. Substrate and enzyme solutions were not sterilized prior to hydrolysis. The hydrolysis was carried out in static water bath at 50°C for 4 hours. The substrate was passed through a steel wire sieve and then through grade 5 qualitative filter paper via vacuum assisted filtration.

For analysis of insoluble solids fraction, residue cakes were dried at 70°C over night and then weighed. For analysis of soluble solids fraction, 10 ml of filtrate from each specimen was dried at 70°C for 3 days in plastic tubes and weighed.
Recovery fractions of insoluble and soluble solids were calculated by the following equation after subtracting empty weights of filter paper and plastic tubes respectively:

$$insoluble\ solid\ fraction = \frac{m_{dry\ cake}}{m_{bread}} * 100\%$$

$$soluble\ solid\ fraction = \frac{m_{dry\ filtrate}}{m_{bread}} * 100\%$$

Where $m_{dry\ cake}$ is weight of dried filter cakes, m_{bread} is weight of bread pre hydrolysis and $m_{dry\ filtrate}$ is weight of liquid filtrate residue after drying.
Concentration of soluble solids (g/l) in filtrate was calculated by the following equation:

$$soluble\ solid\ concentration = \frac{m_{dry\ filtrate}}{vol_{filtrate}}$$

Where $vol_{filtrate}$ is volume of liquid filtrate before drying.

Additionally, glucose concentrations (g/l) were determined via high-performance liquid chromatography (HPLC). For all following HPLC analysis, 1.5 ml of filtrate was centrifuged with a microcentrifuge (*Heraeus™ Fresco™ 21*, Thermo Fisher Scientific, Waltham, MA, USA) at 14000 rpm for 8 minutes. The supernate was then passed through a CA 0.20 µm syringe filter. HPLC analysis was carried out by a hydrogen-ion based ion-exchange column (*Aminex HPX-87H*, Bio-Rad, Hercules,

CA, USA), running at 60°C and using 0.6 ml/min of 5 mM H_2SO_4 as mobile phase with a refractive index (RI) detector.

2.3 CULTIVATION OF *RHIZOPUS DELEMAR*

The following sections are concerned with the cultivation of the fungus *Rhizopus delemar* on bread waste particles. Previous research done by Bucuricova (2019) was concerned with the investigation on how *R. delemar* would grow on bread waste and the optimization of cultivation parameters such as bread particle concentration in suspension, pH of medium and cultivation time. In the project at hand, the process was scaled up to produce a maximum of fungal biomass in order to obtain enough material for trials on chemical treatments and wet-laying of films. The following experiments were conducted in sterile conditions.

2.3.1 CULTIVATION ON BREAD PARTICLES IN 1.3 M^3 BIO-REACTOR

Rhizopus delemar was grown on agar plates (17 g/l agar, 20 g/l glucose, 4 g/l peptone, pH 5.5) at 35°C for three days. Afterwards the plates were stored at +4°C for a maximum of 30 days until inoculation. Adjustment of media pH was done in all experiments with 1/% H_2SO_4 and 0.5 M NaOH. The pH was monitored with a glass pH electrode (Jenway, Staffordshire, UK) connected to a pH meter (*PW 9420*, Philips, Amsterdam, Netherlands).

Batch cultivation in 1.3 m^3 air column bioreactor was scaled up in a three-step process. The first cultivation step was done in 3 Erlenmeyer flasks (250 ml). A suspension of 100 ml ultrapure water and 4.5 g of bread particles (4.5% w/v) was adjusted to pH 5.5 and then sterilized. *R. delemar* spore suspension was prepared by adding 20 ml of sterile ultrapure water to one agar plate. By scraping the surface gently, fungal spores were suspended in water. 4 ml of spore suspension was transferred to each shake flask, resulting in a 2% spore concentration. Shake flasks were kept in rotary shaking water bath at 35°C, 100 rpm for 24 hours.

A total of 300 ml pre-inoculum from Erlenmeyer flasks was used to inoculate a bubble column airlift reactor[3] with a volume of 26 l (Bioengineering, Wald, Switzerland). Bread medium was prepared by sterilizing 20 l ultrapure water and 900g bread particles separately and mixing shortly before inoculation. The liquid bread medium was then added to the bioreactor without pH adjustment. The cultivation was run at 35°C for 38 hours. Aeration was set to 1 vvm (volume of air per volume of liquid per minute) and then increased to 1.5 vvm 12 hours after inoculation.

For the third step in scaling up, a 1.3 m^3 airlift bioreactor[4] *(*Knislinge Mekaniska Verkstad AB, Kristianstad, Sweden) was prepared by filling the vessel with 25 kg of dry bread and ca. 800 l of tap water. The bread was planned to be fed into the reactor vessel by mixing 5 kg batches with 135 l of tap water in the pumping system

[3] In a bubble column reactor, gas is introduced at the bottom of the vessel and travels through the continuous liquid phase. The gas is used for agitation and for a continuous gas exchange (Ferreira et al., 2017).

[4] An airlift reactor is built with a second internal tube. By introducing gas at the bottom of the reactor, a circular motion of the liquid phase is created, where liquid travels upward inside the inner tube und travels downward outside the inner tube (Ferreira et al., 2017).

of the reactor. However, after feeding half of the bread, the mixture thickened to a point where it could not be carried by the pumping system anymore. The second half of bread was then added manually through a funnel inlet at the top of the reactor. The bread-water mixture was sterilized in the reactor by introducing 167 kg of steam into the reactor. Additionally, 20 kg of sterile bread was added to the reactor through a funnel. With a total estimated water volume of 967 l, a bread concentration of ca. 4.65% w/v was reached. Inoculation was done with 20 l of biomass - liquid mixture (pH 2.47) taken from the 26 l bioreactor. The cultivation was run at 35°C with an aeration of 0.5 vvm for 22h. For measurement of pH as well as glucose and ethanol concentrations via HPLC, 100 ml samples were taken 0, 2, 4, 6, 9, 12, 14, 16 and 21 hours after inoculation, without duplication. Since the pH of medium dropped continuously after inoculation (pH_{t0} 4.39), 4M NaOH was successively fed through a funnel into the vessel until pH 4.88 was reached at t = 9h.
Harvesting of biomass was done prematurely 22 hours after inoculation because of a suspected contamination in the bioreactor. The harvesting was initiated by separating biomass from liquid medium by manual sieving. Excess water was removed by pressing the biomass in a pillow cloth by hand. Afterwards the biomass was purged with tap water via suspension to remove undigested bread particles. Purging was done three times.
The purged biomass was then pressed in a pillow cloth again to remove as much water as possible. Then it was packaged in plastic bags of ca 1 kg each and stored at -18°C until further use.

2.3.2 CULTIVATION ON SYNTHETIC MEDIUM IN 26 L BIOREACTOR

In the 26 l bubble column bioreactor, a fed-batch cultivation was performed with *R. delemar* on synthetic medium. Synthetic medium was prepared according to the following recipe and adjusted to pH 5.5:

30 g/l glucose
5 g/l yeast extract
3.75 g/l $NaNO_3$
2.25 g/l $MgSO_4 * 7 H_2O$
1 g/l $CaCl_2 * 2 H_2O$
3.5 g/l KH_2PO_4

To prepare the pre-inoculum, 3 Erlenmeyer flasks (250 ml) were prepared with 100 ml of medium each and inoculated with 2 ml spore suspension of *R. delemar*. The spore suspension was made by adding 20 ml of ultrapure water to one agar plate of *R. delemar*. After inoculation the flasks were kept in a water bath at 35°C, 100 rpm for 24 hours.
To start cultivation in the 26 l bioreactor, 20 l of synthetic medium was sterilized in 4 glass bottles, containing 5 l of medium each. The pre-inoculum together with synthetic medium was then fed into the reactor. Air flow was set to 1vvm and temperature to 35°C. The first harvest was done after 24 hours by removing 14 l of biomass-medium suspension and then replenishing with 15 l of fresh synthetic medium to promote biomass growth again. The harvested biomass was separated from liquid

medium by sieving and then washing with 15 l of distilled water. Afterwards excess water was removed by pressing the biomass by hand.
In total, 5 harvests were done in various time intervals, where the second harvest was done 16 hours after replenishing with medium, the third harvest after 8 hours, the fourth harvest after 16 hours and the fifth harvest after 8 hours.

2.4 CULTIVATION OF *FUSARIUM VENENATUM*

The first run of cultivations of *Fusarium venenatum* was done in fed-batch to determine the cultivation time for maximum biomass yield (g dry biomass/g bread). Afterwards fed-batch cultivation was compared to batch cultivation, to see how a batch process would influence biomass yield. In a fed-batch process, medium is fed to the cultivation in defined time intervals. In a batch process, all medium is provided at the start of cultivation.
For many microorganisms a fed-batch process results in higher biomass yields compared to a batch process. This is based on the so called Crabtree effect, in which an excessive presence of glucose causes a metabolic shift in microorganisms from respiration to fermentation in aerobic conditions. During respiration, glucose is fully metabolized to water and CO_2 whereas during fermentation glucose is metabolized to ethanol and CO_2. (De Deken, 1966; Swart et al., 2020) The presence of ethanol in turn diminishes biomass growth by disrupting the physical structure of cell wall membranes (Goldstein, 1986).

2.4.1 FED-BATCH CULTIVATION IN SHAKE FLASKS

All following cultivation experiments were done in sterile conditions. *Fusarium venenatum* was grown on agar plates (17 g/l agar, 20 g/l glucose, 4 g/l peptone, pH 5.5) at 27-30°C for three days. Afterwards the plates were stored at +4°C for a maximum of 30 days until inoculation.
Fed-batch experiments were done in 500 ml cotton-plugged Erlenmeyer flasks in rotary shaking water bath with 30°C, 100 rpm. An Erlenmeyer flask was filled 200 ml ultrapure water and sterilized. Bread particles were portioned into 2 g for each flask and sterilized separately. For preparation of spore suspension, 10 ml of sterile ultrapure water was added to each *F. venenatum* agar plate. 4 ml of spore suspension was transferred to each shake flask, resulting in a 2% spore concentration.
The fed-batch process was carried out by adding 2 g of sterilized bread (1 wt%) in 24 hour intervals until harvest (*Table 3*). All experiments were carried out in duplicates.

Table 3 Time plan of F. venenatum *fed-batch experiments*

Sample	Time (h)				
	0	24	48	72	96
1	+ 2g bread	Harvest	-	-	-
2	+ 2g bread	+ 2g bread	Harvest	-	-
3	+ 2g bread	+ 2g bread	+ 2g bread	Harvest	-
4	+ 2g bread	+ 2g bread	+ 2g bread	+ 2g bread	Harvest

Liquid medium samples for HPLC analysis were taken at t = 0 and 24 hour intervals from thereon, shortly before new bread batches were added to the flasks. At harvest, fungal biomass was separated from liquid medium by sieving. By pressing the biomass by hand, excess water was removed. Afterwards the biomass was dried at 70°C over night to determine the dry biomass yield.

For confirmation of biomass yield results, the fed-batch experiment was repeated with 48 and 72 hour cultivations. To minimize bread residue in harvested biomass, bread particles were sieved to a particle size of < 1mm prior to inoculation. During harvest the biomass was resuspended in distilled water after initial separation of biomass from liquid. Undigested bread particles were removed by letting them sediment and decanting the biomass through a sieve. This purging process was done three times. The gradual removal of bread residue is shown in *Figure 9*. Afterwards the purged biomass was dried at 70°C over night for determination of dry weight.

Figure 9 Bread residue sediments during purging of F. venenatum *biomass after 48 h fed-batch cultivation. From left to right: purging cycles 1, 2, 3*

2.4.2 BATCH CULTIVATION IN SHAKE FLASKS

Batch cultivation was first done with a suspension of bread particles in water. A second trial was made by hydrolyzing bread particles via enzymes and then using the hydrolyzed substrate as cultivation medium.

2.4.2.1 BATCH CULTIVATION ON BREAD PARTICLES

For batch cultivation, 2% and 3% w/v bread media were prepared in 500 ml cotton-plugged Erlenmeyer flasks with bread particles (sieved to particle size < 1mm) and 200 ml ultrapure water. The suspension was adjusted to pH 5.5 and then sterilized. Afterwards inoculation followed with *F. venenatum* spore suspension.

Cultivations with 2% bread substrate were run for 48 h, 3% bread substrate cultivations were run for 72 hours. One flask of the 72 hours run broke and its biomass was lost. Therefore, no standard deviation is shown in the results in this instance.
The biomass was harvested by initial sieving from liquid medium and then purging thrice via suspension in tap water. The biomass was dried at 70°C over night to determine dry weight yield.

2.4.2.2 BATCH CULTIVATION ON HYDROLYZED BREAD

During large-scale experiments of *R. delemar* it was observed that not all bread particles could be digested by the fungi. Those particles could also not be removed completely by a purging process with water after harvesting. Therefore, it was investigated how fungi would grow on a substrate which was prepared by hydrolyzing bread to obtain a liquified bread medium without any macro-sized particles.
Bread solutions were prepared by hydrolysis via amylase as described in section 2.2.3. The solutions were diluted to a soluble solid concentration of 20 g/l, adjusted to pH 5.5 and sterilized. 50 ml of diluted bread substrate was filled into a 150 ml Erlenmeyer flask and inoculated with 4 ml spore suspension of *F. venenatum*.
For the first trial, eight copies of cultivations were kept for 24 hours in a rotary shaking water bath at 30°C, 100 rpm. A second trial was conducted with six sample copies in which the cultivation time was extended to 48 hours. In both instances, biomass was separated from liquid by sieving and then purged thrice by water suspension. The purged biomass was dried at 70°C over night.
The biomass yield from those experiments was much lower compared to cultivations with bread particles. This was most probably due to missing proteins in the cultivation medium. Therefore, a third trial was made, using a substrate of bread hydrolyzed via amylase and protease. Soluble solid concentration was kept at 20 g/l and all cultivations were harvested 48 hours after inoculation. This experiment was conducted in quadruplicates.

2.5 ANALYSIS OF BIOMASS METABOLITES

Fungal metabolites were analyzed via high-performance liquid chromatography (HPLC). Analysis was done on contents of acetic acid, ethanol, glucose, glycerol, lactic acid and other sugars.

2.6 BIOMASS TREATMENT

Biomass obtained from the cultivation done in the 1.3 m^3 bioreactor was used for chemical treatment to expose the chitinous structures of filamentous fungi. A comparison of alkali treatment against a protease treatment was done. As a control experiment, autoclave treatment was done as well, where it was expected that the protein structures would not be removed entirely from fungal cell walls.
For homogenizing before chemical treatment, the biomass-water suspension was in all following experiments run once through a disc mill grinder (*MKCA6-5J*, Masuko Sangyo, Kawaguchi, Japan) with a gap size of +50 µm and a rotation speed of 1500 rpm, using the *MKE #46* grinding disc set. The gap size indicates the shift from a

zero position, where the grinding discs touch each other lightly. A positive gap size then means an open gap. A negative gap size means the grinding discs being pressed onto each other lightly or hardly, depending on the given value.
Afterwards the grinder was cleaned with 0.5 l tap water to remove biomass residues from the grinder. The cleaning effluent was added to the biomass suspension to recover lost biomass. This biomass suspension was subjected to various types of treatments. *Table 4* lists all relevant biomass treatments, which are discussed in the following sections and will be again used for coding of wet-laid films. If the sample code shows a number at its end, this indicates the number of grinding cycles the biomass has been subjected to. For example, Alk15 is biomass which was treated via alkali and then ground 15 times.

Table 4 Sample codes for chemical treatments on R. delemar *biomass. A number at the end of sample codes indicates the number of grinding cycles the sample was subjected to*

Treatment	Sample Code
autoclave + grinding	Aut
protease + grinding	Enz
NaOH + grinding	Alk
NaOH + grinding + bleaching	AlkGB
NaOH + bleaching + grinding	AlkBG
protease + grinding + bleaching	EnzGB
protease + alkali + grinding	EnzAlkG
R. delemar on synthetic medium: NaOH + grinding	synthAlk

If not described differently, the chemically treated biomass was purged by initial separation from liquid residues and then resuspension in 2 l of tap water once after which a second sieving followed. The sieving was carried out with by hand with a steel wire sieve (50 µm mesh size). Biomass dry weight after treatment was determined by drying one sample of each beaker at 70°C over night. The filtrate was measured for pH level.

2.6.1 AUTOCLAVE TREATMENT

Autoclave treatment was done as a control experiment, in which biological activity would be deactivated but non-chitinous fractions of the fungal cell wall would largely remain. The following experiment was carried out in duplicate.
In a 5 l glass beaker 250 g wet biomass (20.20 wt% dry content) was suspended in 1.3 l tap water. The homogenized suspension was autoclaved at 121°C for 20 minutes. The suspension was then sieved to remove water and then purged by suspension in 2 l tap water and sieving. The remaining inactivated biomass (IB) was stored at +4°C until further use.

2.6.2 PROTEASE TREATMENT

The following experiment was carried out in quadruplicates. A 5 l glass beaker was filled with 562 g of wet biomass and 2.425 l of tap water. The homogenized biomass suspension was preheated to 60°C in a water bath. 10 mg/g dry biomass *Protamex*®

protease granulate was directly added to the beaker without pH adjustment. The biomass suspension was stirred thoroughly by hand to distribute the enzyme evenly. Hydrolysis was carried out in a static water bath at 60°C for 4 hours. Afterwards water was removed by sieving and the remaining non-hydrolyzed material was purged by suspension in 2 l tap water and sieving. The liquid residue after treatment, assumed to contain a large fraction of proteins, was stored in glass bottles at +4°C for analysis of liquid and solid residues.

2.6.3 ALKALI TREATMENT

The following experiment was carried out in quadruplicates. In a 5 l glass beaker 562 g wet biomass was suspended in 2.225 l tap water and homogenized. A 200 ml 60-80 g/l NaOH solution was prepared in reference to the suspension's volume. The NaOH solution was added to the biomass suspension and distributed evenly by stirring to reach a final concentration of 4 g/l NaOH. The biomass-alkali mix was autoclaved at 121°C for 20 minutes.
For neutralization, alkali insoluble material (AIM) was separated from alkali solution by sieving. AIM was resuspended in 3 l tap water and sieved again, repeating the neutralization three times. After the third neutralization cycle, pH indication paper showed a pH of 7 to 8, which was deemed sufficient for safe handling and to stop further degradation of biomass. One of the samples was measured by a pH electrode after neutralization, which showed a pH of 10.07. The liquid residue was stored in glass bottles at +4°C for analysis of liquid and solid residues.

2.6.4 GRINDING TREATMENT

The biomass obtained from autoclave, alkali and protease treatment was subjected by a grinding process. Before grinding, all biomass suspensions were diluted with tap water to a concentration of 30 g dry biomass/l. The biomass was then homogenized by running it through the disc grinder once with a gap size of +50 µm.
Since the grinder has a minimum working volume, the quadruplicates of Alk and Enz were each poured together to make duplicate batches before homogenizing. Afterwards the biomass was ground in multiple grinding cycles by repeatedly passing it through the grinder and collecting the ground biomass through an outlet. The grinding was performed in a contact mode by gradually adjusting the position of the lower grinding stone to -70 µm with a rotor speed of 1500 rpm. For the grinding treatment, the same *MKE #46* grinding disc set was used as explained in section 2.6, which is shown in *Figure 10* along with the grinding machine itself. After cycles 1, 5, 10 and 15 a portion of ca. 500 ml (Aut) and ca. 800-900 ml (Alk and Enz) was separated into plastic bottles and stored at +4°C until used for wet-laying.
After initial wet-laying experiments with autoclaved, alkali and enzyme treated biomass, grinding cycles above 15 were investigated on their influence on tensile properties of films. The grinding process was kept the same but ground biomass was collected after different numbers of grinding cycles. Up to 40 cycles were investigated with taking intermediate samples after i.e. cycles 10, 20, 30 and 40.

Figure 10 Disc mill grinder with feeding funnel on top (left), dismantled grinding disc pair (right)

2.6.5 INVESTIGATION OF TWO-STEP CHEMICAL TREATMENTS

To further improve tensile properties of films produced from fungal biomass, several experiments were conducted on *R. delemar* biomass. Zamani et al. (2007) showed that AIM can be further purified by treatment with dilute sulfuric acid to release phosphates. Afterwards the alkali and acid insoluble material (AAIM) is treated a second time with NaOH to remove sulfuric acid remains.
Next to a purification of chitosan, other treatments, such as celllulase or protease treatment and bleaching, were applied to decrease the fraction of bread particles in biomass films and their detrimental effect on tensile properties.
Bleaching treatment was done according to Wu et al. (2019). They showed that by bleaching with H_2O_2 at elevated temperatures, more than 60 wt% of lignin is removed, with some additional removal of cellulose (4.4%) and hemicellulose (1.3%).
Lastly, the effect of NaOH treatment on protease treated biomass was investigated. The main interest here was in the possibility to recover proteins and protein fractions after protease treatment, which could be used as a precursor for the preparation of protein rich food. The subsequent NaOH treatment was then expected to yield similar tensile properties as NaOH treatment on its own.
The following experiments were conducted on *R. delemar* AIM ground once or on *R. delemar* biomass treated by protease and ground once. All samples were in water suspension with a 30 g/l dry weight concentration prior to treatment. All post-treatment materials were stored at +4°C until further use.

Alk + H_2SO_4

A 1% aqueous H_2SO_4 solution was prepared from 95%-98% stock solution (Sigma-Aldrich), assuming 100%. 200 ml AIM was mixed with 200 ml dilute sulfuric acid. The mixture was left static for 1 hour at room temperature. Ca. 200 ml of remaining alkali and acid insoluble material (AAIM) was then washed with 1 l tap water in a sieve.

Alk + H_2SO_4 + NaOH

100 ml of AAIM was mixed with 100 ml 2% NaOH solution. After 30 minutes of static treatment at room temperature, the biomass was separated via sieving and purged by pouring 1 l of tap water through the biomass collected in the sieve.

Alk + Cellulase

Cellulase treatment was done in a concentration of 45 µl/g dry biomass. 100 ml AIM was adjusted to pH 5.2. Cellulase was suspended in 1 ml ultrapure water and then added to the biomass and was then left for treatment in a static water bath at 50°C for 24 hours. Afterwards, the biomass was separated via sieving and washed by pouring 1 l tap water through the sieve.

Alk + H_2O_2 / Enz + H_2O_2

Bleaching solution was prepared according to the method by Wu et al. (2019, p. 2): 6 wt% H_2O_2 was mixed with 1 wt% trisodium citrate dihydrate, 1 wt% NaOH and 92 wt% ultrapure water. Bleaching solution was added to Alk and Enz (3% dry content concentration) in a ratio of 50 ml bleaching solution per g dry biomass. The mixture was kept at 60°C for 2 hours under constant stirring. Afterwards the bleaching solution was separated via sieving and the bleached biomass purged by rinsing it three times with 300 ml distilled water.

Pretests showed that heavy foaming occurs during bleaching of biomass, which requires beakers with 4-5 times of the initial volume of mixture to prevent overflow. All following bleaching treatments were therefore done by adding 0.1 ml of a commercial antifoam (fatty acid ester formulation) per 1 l biomass.

Alk + Protease

100 ml of AIM was treated with protease by first adjusting the biomass to pH 8.0 (optimal pH according to Olajuyigbe and Ajele (2008)) and then adding a 5 ml suspension of protease granulate in a concentration of 10 mg/g dry biomass. Enzymatic hydrolysis was done in a static 50°C water bath for 4 hours. Afterwards biomass was sieved and rinsed with 1 l tap water.

Enz + NaOH

50 ml of 2.4% (w/v) NaOH solution was added to 250 ml suspension of enzyme treated biomass to reach a final NaOH concentration of 4 g/l. The mixture was autoclaved at 121°C for 20 minutes and washed with tap water until pH was neutral.

Order of Treatments

After seeing promising results from tensile testing of films *Alk + H_2O_2* and *Enz + NaOH* films, the treatments were altered by switching the grinding sequence after bleaching and NaOH treatment respectively, to see if the order of treatments would yield different tensile properties. Additionally, these two experiments were used to see if a higher number of grinding cycles > 15 would further increase the tensile strength or stiffness of wet-laid films.

Alk was bleached via H_2O_2 treatment and then ground in multiple cycles. Samples after cycles 1, 10, 20, 30 and 40 were taken for film preparation.

Enz was subjected to the same treatment. However, biomass samples were taken after grinding cycles 1, 10, 15, 20 and 30.

2.7 ANALYSIS OF TREATED BIOMASS

2.7.1 WATER CONTENT

If not described differently, all water content, or inversely dry fraction, was determined by drying duplicates in aluminum dishes at 70°C over night in a ventilated oven. Aluminum dishes were first weighed empty, then filled with wet biomass and then a third time after drying over night. After subtracting the weight of empty aluminum dishes, the dry fraction was calculated by the following equation:

$$dry\ fraction = \frac{m_{post}}{m_{pre}} * 100\%$$

Where m_{pre} is mass of biomass pre drying and m_{post} is mass of biomass post drying. The mean average from both duplicates was calculated along with its standard deviation.

2.7.2 VISCOSITY

Viscosity of biomass suspensions after chemical and grinding treatments was measured with a sinewave vibro-viscometer (*SV-10,* A&D, Tokyo, Japan). The biomass suspension was equilibrated to room temperature (21 ± 1°C) before measurement. The displayed viscosity after 20 seconds of measurement was taken as the respective value for each specimen. Each sample was measured four times. Measurements of Alk, Enz and Aut showed very high deviations. Therefore, for measurement on AlkBG, the biomass was stirred in between measurements to avoid phase separation over time. The results report the mean average and standard deviation.

2.7.3 DIMENSIONS OF MYCELIAL FILAMENTS

Fiber length and width was estimated using a microscope (*Ocelloscope,* BioSense Solutions, Farum, Denmark) supported by image analysis software *Uniexplorer* v9.0.0.7805.

For sample preparation, biomass suspensions with a dry weight concentration of 3% were diluted with water (pH 10) in a volumetric ratio of 1:100. Using the image analysis software, the mycelium dimensions were measured on screen. Fiber width and length were measured at least 5 times per image, in cases were the fiber dispersion allowed, the number of measurements was increased up to 20. Since mycelium grows in branches, their maximum length was determined by adding up the distance from the beginning of the main branch to the end of the longest side-branch.

2.7.4 DETERMINATION OF CHEMICAL CELL WALL COMPOSITION

Duplicate samples from Alk1, AlkB1, EnzAlk1 and synthAlk1 were analyzed on their concentrations of glucosamine (GlcN) and N-acetyl-glucosamine (GlcNAc) monomers. The analysis was carried out according to the method described by Mohammadi et al. (2012). A two-step treatment with concentrated sulfuric acid at room

temperature and dilute acid at 120 ºC result in complete deacetylation of chitin and partial depolymerization of chitosan into acetic acid and GlcN oligosaccharides, respectively. Oligosaccharides are fully depolymerized via a nitrous acid treatment. The resulting 2,5-anhydromannose concentration is measured via colorimetric method and representative of total GlcN and GlcNAc concentration. Acetic acid concentration is determined via HPLC and directly converted into GlcNAc concentration.
All samples were taken from biomass ground once by the grinding treatment explained in section 2.6.4. Prior to analysis, the samples were freeze dried with a benchtop freeze dryer (*FreeZone 2.5L*, Labconco, Kansas City, USA) and pulverized using a rotor mill (*Pulverisette 14*, Fritsch GmbH, Idar-Oberstein, Germany).

2.8 ANALYSIS OF BIOMASS TREATMENT RESIDUES

To determine the fraction of recovered biomass residues per g dry biomass, the liquid residue of two batches of NaOH as well as protease treatments was separated from biomass via sieving and weighed. The residue was stored in glass bottles at +4°C until use. Of each batch, duplicate samples of 50 ml in plastic tubes were weighed and afterwards centrifuged at 5000 rcf for 5 minutes. Supernate and precipitate were separated from each other and freeze dried. The freeze-dried samples were weighed. Fractions of insoluble and soluble solids in respect to initial dry weight of fungal biomass were calculated by the following equation after subtracting empty weights of plastic tubes:

$$insoluble\ solid\ fraction = \frac{m_{IS} * m_{total\ residue}}{m_{residue} * m_{total\ biomass}} * 100\%$$

$$soluble\ solid\ fraction = \frac{m_{SS} * m_{total\ residue}}{m_{residue} * m_{total\ biomass}} * 100\%$$

Where m_{IS} is the weight of dry insoluble solid, m_{SS} is weight of dry soluble solid, $m_{total\ residue}$ is weight of the total recovered liquid of one batch, $m_{residue}$ is weight of one 50 ml sample and $m_{total\ biomass}$ is the total biomass weight of one batch.
Furthermore, the concentrations (g/l) of insoluble and soluble solids in the liquid residue were calculated by the following equations:

$$insoluble\ solid\ concentration = \frac{m_{IS}}{m_{residue}} * 100\%$$

$$soluble\ solid\ concentration = \frac{m_{SS}}{m_{residue}} * 100\%$$

Crude protein concentrations in insoluble and soluble solids were determined via total nitrogen measurement by Kjeldahl method (SS-EN ISO 3188, 1978). Nitrogen measurement was done using an *InKjel P* digestor and a *Behrotest S1* distiller (Behr Labor-Technik, Düsseldorf, Germany). The protein content was estimated by multiplying the nitrogen content with a factor of 6.25 (Hanne Mæhre et al., 2018).

2.9 WET-LAYING OF FILMS AND NONWOVEN COMPOSITES

Due to the world-wide outbreak of Covid-19, travel bans and limitations in everyday life caused a change of plans during the project. The initial plan of multiple wet-laying experiments at RISE Institutes in Stockholm could not be performed. The wet-laid process had to be remodeled in the labs of University of Borås. Because of a lack of specialized papermaking equipment, the process could not be reproduced to its full extend. However, the goal was to adhere to the initial process as closely possible. The initial papermaking method and the remodeled method are explained in the following sections.

2.9.1 WET-LAYING VIA HANDSHEET FORMER

Wet-laying was done according to SS-EN ISO 5269-1 (2005) with a handsheet former intended for lab scale paper making (see *Figure 11*). The handsheet former was equipped with a square screen with a size of 165 x 165 mm (= $272.25 \cdot 10^{-4}$ m²).
All films and nonwoven sheets were prepared with a target dry weight of 100 g/m². For this, a suspension with a dry biomass content of 0.3% w/w was prepared. For wet-laying of one film, 907 ml of 30 g/l biomass suspension was used. The sheet former's upper cylinder was filled about one fourth with tap water so that the wire screen was sufficiently submerged in water. Then the suspension was poured in and the cylinder was filled up with water to ca. 10 l total volume. This resulted in a final suspension with a biomass concentration of ca. 0.3% w/w. The suspension was mixed by an air bubble agitation system (outlets installed fixed, close to the wire screen) for 5 seconds. Then the draining of the handsheet former was initiated automatically until the water column was removed completely, leaving the wet fibrous biomass on the wire screen. All wet-laying experiments were done in duplicates.

Figure 11 Open handsheet former with phosphorous bronze wire screen installed (left) and closed handsheet former with a capacity above the wire screen of ca. 10 l (right)

2.9.1.1 WET-LAYING OF BIOMASS FILMS

The initial trials with autoclave treated biomass were done using a phosphorous bronze wire screen (pore size: 125 µm). The wet-laid biomass was sticking heavily to the bronze screen after pressing, which resulted in tearing of films when lifting the wet film from the screen (*Figure 12a, b*). Therefore, all subsequent trials with alkali and protease treated biomass were done with a nylon wire screen (pore size 125 µm).

Since pressing the sheets with the automatic pneumatic press caused too much sticking to the screen, an alternative was developed where 2 blotting sheets were put on top of the wet-laid film and then gently pressed with a plastic pin roll. This allowed for a better control of remaining water content in the wet-laid film. The wet film was then removed from the wire screen by leaving one of the blotting papers on the wet-laid film and then quickly rolling the pin roll over the entire area of the blotting paper. The quick rolling motion picked up the film together with blotting paper without causing any damage (*Figure 12c, d*).

For short term storage each wet-laid film was sandwiched between an acrylic sheet and a blotting paper and then stacked up for the following drying process.

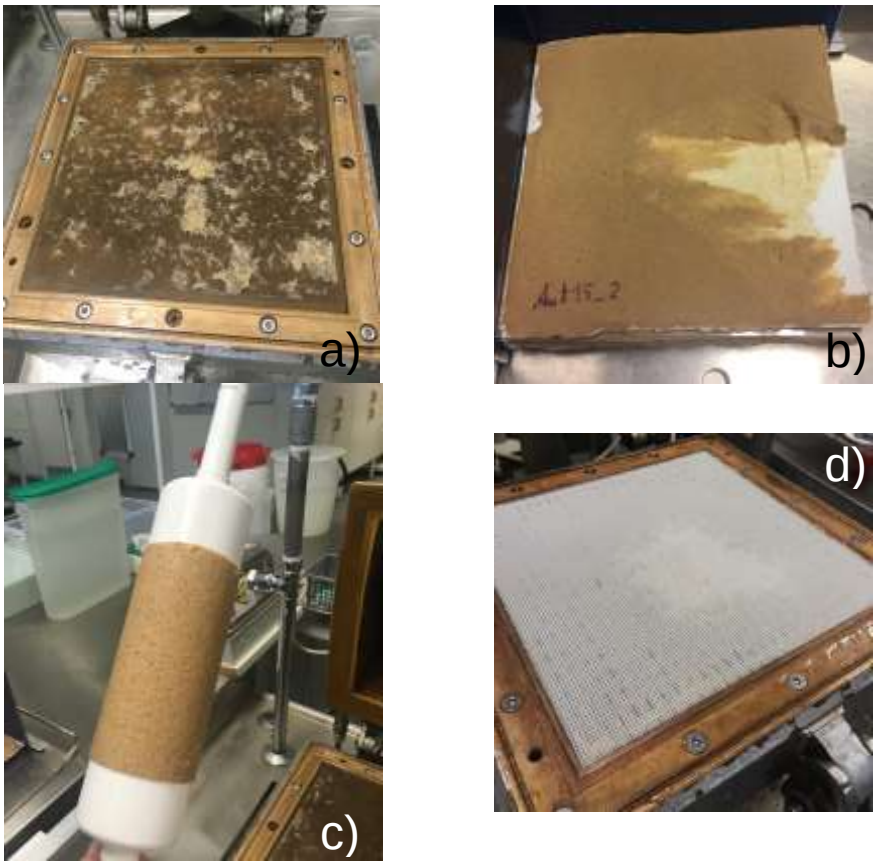

Figure 12 Biomass residue on phosphorous bronze wire screen (a), damaged biomass film due to sticking to wire screen (b), biomass film attached to pin roll for damage-free recovery (c), nylon wire screen without major biomass residue (d)

2.9.1.2 WET-LAYING OF VISCOSE-MYCELIA NONWOVEN COMPOSITES

In a second experiment, fungal biomass was mixed with viscose fibers (*Danufil KS*, Kehlheim Fibers, Germany) to create Viscose-mycelia nonwoven nomposites (VMNC). Viscose fibers had a length of 5 mm and a linear density of 1.7 dtex. For preparation of VMNC, Aut15 and Enz15 was used as biomass binder. Due to time constraints, VMNC with Alk15 as a binder was not prepared.
The viscose fibers were presoaked in water for ca. 2h. Then, the suspended viscose fibers and fungal biomass were mixed in dry weight ratios of 25:75, 50:50 and 75:25. The mixture was poured into a beaker and stirred with a blunt stirring rod at 1000 rpm for 30 seconds to create a homogeneous suspension. The sheet forming process was similar to the one described in section 2.9.1.1 for preparation of films. Except the pressing was done with a pneumatic press, which applied a weight of 3.8 kg over the full screen wire area (equivalent to 1.37 kPa) for 20 seconds as illustrated in *Figure 13*.

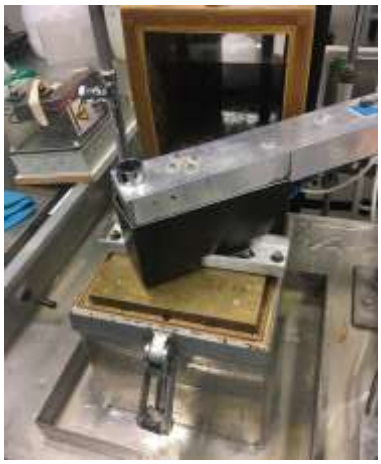

Figure 13 Pneumatic press on top of the wire screen to remove water from wet-laid films

Table 5 lists all nonwoven composite preparations and their respective sample code. The sample codes are used again in results, section 3.10.

Table 5 Sample codes for viscose-mycelia nonwoven composites (VMNC). All samples were prepared with biomass ground 15 times. Percentages are weight-related

Material Composition	Sample Code
75% Aut15 + 25% viscose fiber	Aut75Vc25
50% Aut15 + 50% viscose fiber	Aut50Vc50
25% Aut15 + 75% viscose fiber	Aut25Vc75
75% Enz15 + 25% viscose fiber	Enz75Vc25
50% Enz15 + 50% viscose fiber	Enz50Vc50
25% Enz15 + 75% viscose fiber	Enz25Vc75

2.9.1.3 DRYING OF FILMS AND COMPOSITE SHEETS

A stack of wet-laid films (stacking order shown in *Figure 14, left*) or VMNC was subjected to pressure of 0.395 MPa for 5.5 minutes with gradually increasing pressure, using a hydraulic press shown in *Figure 14, right* (Lorentzen & Wettre, Kista, Sweden). Afterwards the wet blotting papers were exchanged with dry ones. The stack was pressed a second time at 0.395 MPa for 2 minutes. This time maximum pressure was established in a few seconds.

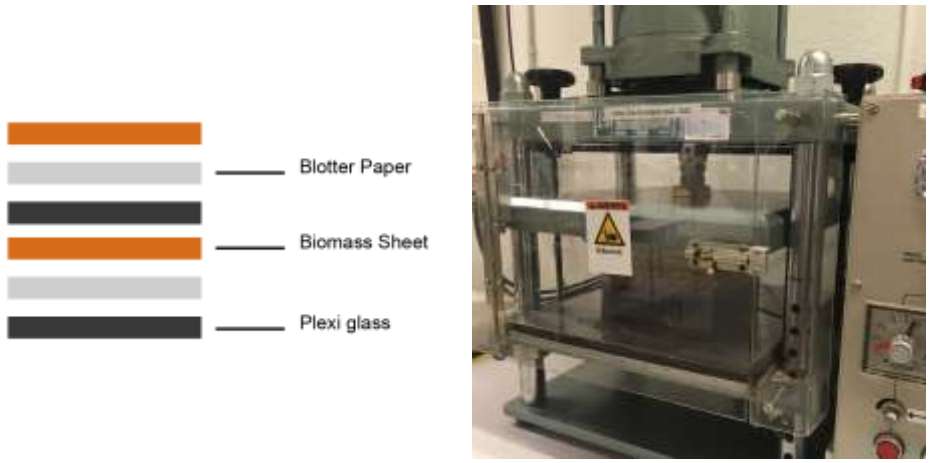

Figure 14 Schematic of stacking order of wet-laid films (left), stack of films in hydraulic press at 0.395 MPa for 7.5 minutes in total (right)

The final drying step was done by mounting an acrylic sheet, to which a wet-laid film adhered, into a drying frame (see *Figure 15*). The frame allows for unhindered airflow while preventing a shrinkage of the wet-laid samples. The drying was carried out at standardized climate (ISO 187, 1990) in a ventilation chamber.
Fully recovered and undamaged dry films and sheets were cut to a size of 150 x 150 mm using a hydraulic press and a cutting die. Partially destroyed samples were cut in rectangular shape so that the biggest intact area was recovered.

Figure 15 Wet-laid film after pressing mounted in drying rack (left), stacked drying rack with weight on top for fixation (right)

2.9.2 WET-LAYING VIA VACUUM FILTRATION

The alternative wet-laying process was performed using a vacuum filtration funnel. The cylindrical funnel had a maximum volume of 1 l and a circular PVDF-coated support screen with a diameter of 90 mm. The full setup is shown in *Figure 16*. The support screen was covered with a removable nylon mesh (30 µm pore size). Due to the limited funnel volume, the previous rate of dispersion (3 g/l) could not be reached while at the same time keeping the grammage of films similar. Therefore, an 8 g/l suspension was created for wet-laying of films. While for the handsheet former, the final dispersion rate was reached by filling the column to 10 l, here the final rate of dispersion was already prepared in a separate beaker by mixing biomass with tap water.

The wet-laying was done by vigorously stirring the biomass dispersion, then pouring it into the funnel and immediately after the dispersion had been fully poured in, vacuum was applied. Once the water was fully removed and biomass was collected on the nylon screen, the apparatus was taken apart to peel off the nylon screen together with the biomass collected on top of it.

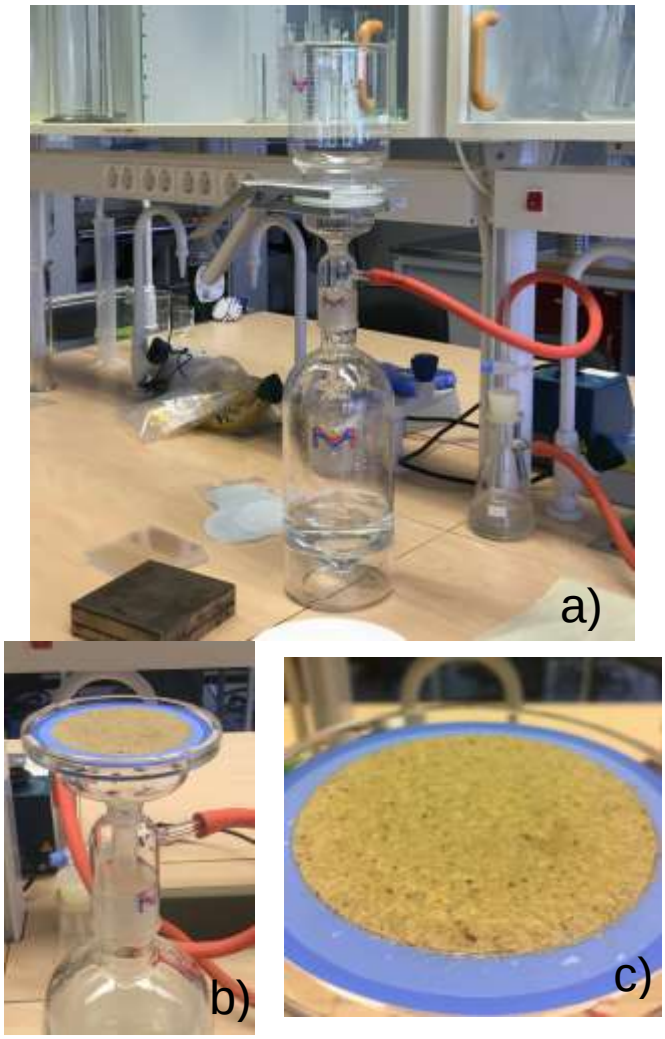

Figure 16 Full vacuum filtration setup with glass funnel clamped to the screen holder and flask (a), biomass film collected on nylon screen (b), close-up of biomass film on screen (c)

The nylon screen together with the wet-laid film was pressed for ca. 15 seconds between two 130 g/m^2 blotting papers, using a 3 kg weight, creating a pressure of ca. 6.9 kPa. Afterwards the biomass film was separated from the nylon mesh by peeling them apart. The wet-laid film was placed on a flat acrylic sheet. Multiple wet-laid films were stacked upon each other, by placing a fresh nylon mesh on the biomass film and on top of a paper to take up excess water. A stack of this arrangement was then placed in a manually operated hydraulic press, where a pressure of 9 kN over an area of 15 x 15 cm (≙ 0.4 MPa) was applied for 5 minutes. Since the films were much smaller compared to the ones prepared by initial papermaking, the pressing time was reduced from 7.5 to 5 minutes.

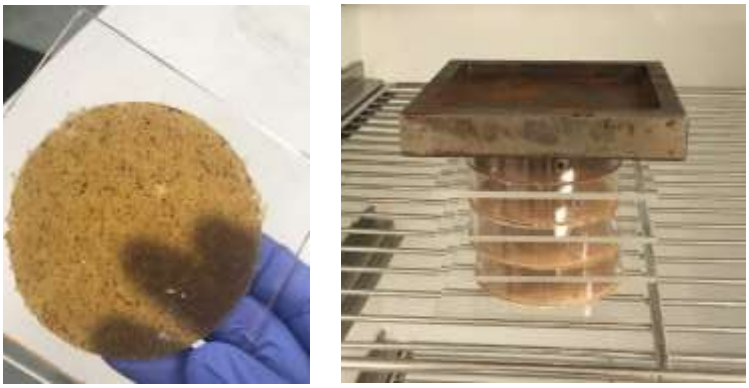

Figure 17 Biomass film adhering to acrylic sheet after pressing (left), stack of biomass films in drying setup with weight on top (right)

After pressing, the blotting papers and nylon screens were removed again and the biomass film, adhering to the acrylic sheet, was stacked up again by placing an acrylic ring of 2.5 cm height and an inner diameter of 70 mm on top of each film. The ring ensured fixation of the film during drying. The stack was placed in a fume hood over night under a weight of ca. 3 kg to ensure fixation of the films by the acrylic rings (see *Figure 17*). After drying, biomass films were cut manually into circular shaped specimens with a 70 mm diameter by using one of the acrylic fixation rings as a stencil.

2.10 CHARACTERIZATION OF FILMS AND NONWOVEN COMPOSITES

Measurement of grammage, thickness, air permeability, tensile properties, bending stiffness and water contact angle were carried out in standardized climate of 23 ± 2°C and 50 ± 4% relative humidity according to ISO 139 (2005).

2.10.1 GRAMMAGE

Grammage was determined using a digital balance (*160M*, Precisa, Dietikon, Switzerland) according to SS-EN ISO 536 (2012). Each sheet was weighed once and the grammage was calculated by the following equation:

$$g = \frac{m}{A}$$

Where g is grammage (g/m^2), m is mass and A is surface area.

2.10.2 THICKNESS

A fully recovered film or VMNC prepared via handsheet forming was measured on 13 spots using a digital micrometer (Lorentzen & Wettre, Kista, Sweden) according to SS-EN ISO 534 (2011). The measurement pattern is shown in *Figure 18a*. Films made by vacuum filtration were measured according to the schematic shown in *Figure 18b* using a thickness gauge (*EV 06B*, Elastocon AB, Brämhult, Sweden).

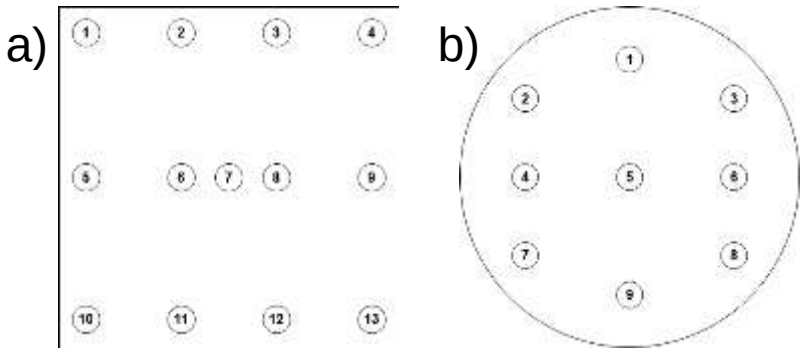

Figure 18 Points of measurement for determination of film thickness with numbers showing the order of measurement for samples made by (a) handsheet forming (a) and (b) vacuum filtration

2.10.3 DENSITY

Bulk density of films and VMNC was determined by the following equation:

$$\rho = \frac{g}{t}$$

Where ρ is bulk density (g/cm^3), g is grammage and t is average thickness.

2.10.4 AIR PERMEABILITY

Air permeability was measured with a digital air permeance tester (Lorentzen & Wettre, Kista, Sweden) according to the Gurley method described in SS ISO 5636-5 (2013). The size of the testing device required the full area of one film produced via the handsheet former. Due to time and resource limits, the test was therefore performed on one film (Enz5). A repetition of measurements was not possible, since the film was destroyed during the first test. This was due to the film's extremely low air permeability. The result was out of bounds, with an air permeability P = 0.00 µm/Pas. Air permeability can be arguably seen as an indirect measurement of porosity. Future studies should therefore focus on test methods, which directly determine porosity of films, i.e. measurement of skeletal density (Janesch et al., 2020; M. Jones et al., 2019; Nawawi et al., 2020a). A qualitative analysis of surface porosity is given in section 0, where SEM images of films are analyzed.

2.10.5 TENSILE PROPERTIESS

Tensile properties of specimens prepared by handsheet forming were tested using a tensile testing machine (*400/M*, MTS, Eden Prairie, MN, USA) according to SS ISO 1924-3 (2011). The machine was equipped with pneumatic grips (force capacity: 2 kN, clamp pressure: 3.6 bar). The deformation rate was set to 100 mm/min and the clamping distance to 100 mm. Test specimens were cut into sizes of 15 mm width and 150 mm length with a rectangular shape. To calculate tensile stress, the thickness of specimens was assumed to be the average thickness of the entire film they were cut out from. As some of the wet-laid films were partially destroyed during production, it was not always possible to produce the maximum sample size of 9 specimens from one film. Therefore, the sample size *n* varies in some instances.

Films prepared via vacuum filtration were cut into type 5A dog bone shape according to SS-EN ISO 527-2 (2012). From one film with a 70 mm diameter, 4 specimens were cut out. The specimens had a gauge length of 25 mm and a width at the narrowest part of 4 mm. The specimens were tested with a tensile testing machine (*H10KT*, Tinius Olsen, Horsham, USA). The grips had a force capacity of 100 N and the clamps were covered with silicon carbide P320 sanding paper to avoid premature damage by clamping. Testing speed was set to 10 mm/min and clamping distance to 40 mm.

For analysis and discussion of data, tensile index σ_{TI} (Nm/g) is used alongside ultimate tensile strength σ_{UTS} (MPa). Tensile index is commonly used for the analysis of paper products, which is calculated by the following equation:

$$\sigma_{TI} = \frac{F_{Peak}}{g * w} = \frac{\sigma_{UTS} * t}{g}$$

Where F_{Peak} is peak load (N), g is grammage and w is width of the specimen. By using the tensile index, a direct comparison between samples with different grammages is possible. In comparison to the tensile index, ultimate tensile strength is calculated by:

$$\sigma_{UTS} = \frac{F_{Peak}}{t * w}$$

Where F_{Peak} is peak load (N), t is thickness and w is the width of the specimen.

2.10.6 FLEXURAL RIGIDITY

Flexural rigidity was measured on specimens prepared by handsheet forming. It was determined using a manually operated cantilever with 1 mm measuring precision according to ISO 9073-7 (1995). The specimens were clamped from one side and then pushed over the edge of the plane area with a uniform speed until they met with a 41.5° slope. Many of the specimens showed prolonged elastic deformation under their own weight. Therefore, the initial point of contact with the slope was taken as the overhang length. To determine the flexural rigidity G (mN·cm), the following equation was used:

$$G = g * C^3$$

Where *g* is grammage and *C* half the overhang length.
Because of constraints in available specimens, destroyed specimens from previously conducted tensile tests were used again for this test. The above-mentioned norm calls for 6 specimens to be tested per sample set. Because obviously damaged specimens had to be sorted out, this number of specimens could not be met. While being fully aware that this greatly impedes the reliability of the results, the data is presented to give a first indication of bending stiffness. To verify the results presented in section 3.8.3 and 3.10.3, the bending stiffness experiment needs to be repeated in the future with unblemished specimens.

2.10.7 WATER CONTACT ANGLE

Water contact angle measurements were done with an optical tensiometer (*Attension Theta*, Gothenburg, Sweden) by sessile drop test (drop size: 3 µl) using ultrapure water. Since the water droplets were slowly absorbed during measurement, contact angle reading was done immediately after the drop was placed on the surface. Each specimen was tested on three random spots. Due to the drying method used after wet-laying, the films exhibit an even, shiny and a coarse, dull side. All samples were tested on their even surface side.

2.10.8 MICROSCOPY

For inspection of film surfaces, a microscope (*SMZ800*, Nikon, Tokyo, Japan) connected to a computer was used.

2.10.9 SCANNING ELECTRON MYCROSCOPY (SEM)

Scanning electron microscopy was performed externally by a project partner at KTH Royal Institute of Technology, Stockholm. Images were acquired on an ultra-high resolution field emission scanning electron microscope (FE-SEM) (*S-4800*, Hitachi, Tokyo, Japan) at an operating voltage of 2.0 kV. Specimens were attached to a carbon tape on the SEM stub and coated with 3 nm palladium/platinum.

2.11 STATISTICAL ANALYSIS

All experiments were performed in duplicates if not stated otherwise. Data was analyzed using statistical software Minitab 19 and Microsoft Excel 365. Regression analysis was carried out via Minitab 19. Variables with confidence levels above 95 % (p value < 0.05) were regarded as statistically significant.
Error bars depicted in graphs represent standard deviations in positive and negative direction. To avoid cluttering of graphs, some standard deviations are only depicted in positive or negative direction. The number of sample replicates is shown in Tables as *n*.

3 RESULTS AND DISCUSSION

3.1 PREPARATION OF CULTIVATION SUBSTRATE

3.1.1 SUBSTRATE ANALYSIS

A water content of 7.37 ± 0.03 wt% was determined for dried and milled bread. Bucuricova (2019) and Ghormade et al. (2017) arrived at water contents of 21.4% and 21.3% respectively. The stark difference can be explained by the additional drying step at 60°C for 6 hours after air-drying at room temperature. Previously established nutrient contents of bread are listed in section 2.2.2.

3.1.2 SUBSTRATE HYDROLYSIS

Bread particle size after hydrolysis largely influenced filtration time. Amylase treated bread showed larger particles, which did not clog the filter paper and therefore resulted in the shortest filtration time, with ca. 5 minutes needed to pass 50 ml of liquid through the filter paper. Other enzyme treatment combinations, such as *amylase + protease* and *amylase + cellulase + protease* showed much higher filtration times, taking up to 4 hours of 50 ml to pass the filtration paper. A visual comparison of filter cakes is shown in *Figure 19*, where amylase treatment resulted in a less dense filter cake, which did not clog the filter paper's pores as much.

Figure 19 Filter cakes of enzyme treated bread. From left to right: amylase, amylase + protease, amylase + cellulase + protease

Increasing bread concentrations (2%, 5%, 10%, 15% and 20% w/v) treated with amylase also increased filtration time. At 15% and 20% concentration, the filter paper ruptured after ca. half of filtrate passed through, causing increased numbers of macro-sized particles to be present in the filtrate. *Figure 20* shows a comparison of filtrate from 5% and 10% bread concentration and the resulting change in color and transparency of filtrate.

Figure 20 Filtrates after amylase treatment of bread. 5% (left) and 10% (right) w/v initial bread concentration

3.1.3 ANALYSIS OF HYDROLIZED SUBSTRATE

The first hydrolysis experiment was conducted to compare the yields of sugars and soluble solids resulting from different enzymatic treatments at 55°C for 15 hours, shown in *Table 6*. *Amylase + Protease* combination gave the highest recovery of soluble solids, followed by the combination of *Amylase + Protease + Cellulase*. Soluble solids were expected to consist mainly of starch, other carbohydrates and hydrolyzed proteins. The recovery fractions of soluble solids correlate with the respective concentrations of soluble solids.

In the first experiment, concentrations of glucose were also confirmed via HPLC. Here, the combination of *Cellulase + Protease* resulted in the highest glucose concentration of 6.59 g/l. Interestingly, *Amylase* and *Amylase + Cellulase* resulted in very low glucose concentrations (0.92 g/l), whereas *Cellulase* on its own had a much higher concentration (5.41 g/l).

Table 6 Soluble solid recovery after enzyme hydrolysis on 2% w/v bread suspensions at 55°C for 15 hours. Percentages are given in relation to initial weight of bread. The number of sample replicates is show in n

Treatment	Sol. solids (wt%)	Sol. solids (g/l)	Glucose (g/l)	*n*
Protease	73.65 ± 1.11	13.65 ± 0.21	0.24 ± 0.06	2
Cellulase	52.36 ± 0.99	9.70 ± 0.18	5.41 ± 1.03	2
Cellulase + Protease	76.38 ± 1.83	14.15 ± 0.34	6.59 ± 0.43	2
Amylase	77.70 ± 7.29	14.40 ± 1.35	0.92 ± 0.03	2
Amylase + Cellulase	80.67 ± 2.18	14.95 ± 0.40	0.92 ± 0.01	2
Amylase + Protease	88.17 ± 2.56	16.34 ± 0.47	5.53 ± 0.04	2
Amylase + Cellulase + Protease	86.53 ± 1.15	16.03 ± 0.21	5.47 ± 0.00	2

Verni et al. (2020) did extensive trials on the hydrolysis of bread waste by varying initial bread concentration, enzyme combinations as well as temperature and time of hydrolysis. 20 wt% bread suspension, hydrolyzed with amylase at 50°C for 24 hours, had a glucose concentration of 13.02 g/l and less than 1 g/l amino acids and peptides. Adding a protease to the treatment left the content of glucose and amino acids unchanged, while the concentration of peptides rose to 4.7 g/l. Furthermore, they

showed that by employing amyloglucosidase instead of amylase, the release of glucose was increased to up to 126 g/l, while keeping all other hydrolysis parameters the same. Considering that in the experiment at hand a 2% bread concentration was used and the hydrolysis time was 15 hours, the resulting glucose concentrations after amylase treatment (0.92 g/l) seem to correspond to the findings of Verni et al concerning the application of amylase.
Since in the experiment at hand, hydrolyzed bread was only analyzed on soluble solids and glucose concentrations, it's hard to tell how the concentration of nitrogen sources such as amino acids and peptides was.

Comparing the soluble solids recovery after amylase treatment on increasing bread concentrations, the highest average recovery rate was 12.49% for 10% bread suspension. Concentrations of 2% and 15% showed high standard deviations (see *Table 7*), which most probably was caused by non-sterile work in this experiment. This could have led to contaminations of some of the shake flasks, where microorganisms disturbed the hydrolysis of amylase.

Table 7 Soluble solid recovery after amylase treatment at 70°C for 2 hours on bread suspension in varying concentration. Percentages are given in relation to initial substrate weight. The number of sample replicates is show in n

Bread concentration (wt%)	Soluble Solids (wt%)	*n*
2	11.01 ± 5.04	2
5	7.99 ± 0.27	2
10	12.49 ± 0.85	2
15	10.45 ± 4.53	2
20	9.14 ± 1.15	2

To recall, *Table 6* shows results from 15 hour treatments while *Table 7* shows results from 2 hour treatments. Comparing the result of 2% bread suspension in *Table 7* against the result of amylase treatment in *Table 6* (also 2% bread suspension), shows that treatment time correlates directly with recovery of soluble solids.
Results from the third enzyme experiment, where bread was treated at 50°C for 4 hours, are shown in *Table 8*. Amylase + protease was used on bread concentrations of 5%, 7.5% and 10% w/v and yielded recovery soluble solid recovery fractions comparable to the first experiment (*Table 6*).
A comparison between experiment 1 and 3 (*Table 6* vs. *Table 8*) shows that agitation during amylase + protease treatment is not necessary to yield high soluble solid recoveries. Also, a treatment longer than 4 hours does not result in significantly higher recovery of soluble solids. To recall, experiment 1 was done with agitated water bath for 15 hours at 55°C. Experiment 3 was done with static water batch for 4 hours at 50°C.

Table 8 Soluble solid recovery after amylase + protease treatment on bread suspension at 50°C for 4 hours in varying concentration. Percentages are given in relation to initial substrate weight. The number of sample replicates is show in n

Bread concentration (wt%)	Soluble Solids (wt%)	*n*
5	90.61 ± 1.70	2
7.5	88.91 ± 0.12	2
10	89.01 ± 0.81	2

3.2 CULTIVATION OF RHIZOPUS DELEMAR

3.2.1 CULTIVATION ON BREAD PARTICLES IN 1.3 M³ BIOREACTOR

Cultivation of *R. delemar* on suspension of bread particles in water in a 1.3 m^3 bioreactor resulted in a total wet biomass harvest of 21.20 kg with a mean dry fraction of 20.20 wt%, which corresponds to a fungal biomass concentration in cultivation of 4.42 g/l. Bucuricova (2019) reported a biomass concentration of 7.92 g/l by 48 hour cultivation in the 26 l bioreactor with the same bread concentration (4.5%). This difference in cultivation time shows that a prolonged cultivation in 1.3 m^3 reactor would have probably resulted in higher biomass yield, while also reducing the presence of undigested bread particles.

Considering 45 kg of bread was used for cultivation, the dry biomass yield was 0.095 g/g bread. *Figure 21* shows the glucose concentration over time in cultivation medium. Glucose concentration was 11.46 g/l at inoculation and decreased rapidly afterwards, which indicates a healthy activity of fungi. The stark increase of glucose concentration to 8.66 g/l 11 hours after inoculation corresponds with a significant increase of ethanol concentration to 0.82 g/l (*Figure 22*), which is caused by starch hydrolysis by the fungi. The ethanol concentration reached a maximum of 4.45 g/l 21 hours after inoculation, which raised concerns in a possible contamination. Therefore, the cultivation was stopped prematurely and biomass was harvested 22 hours after inoculation.

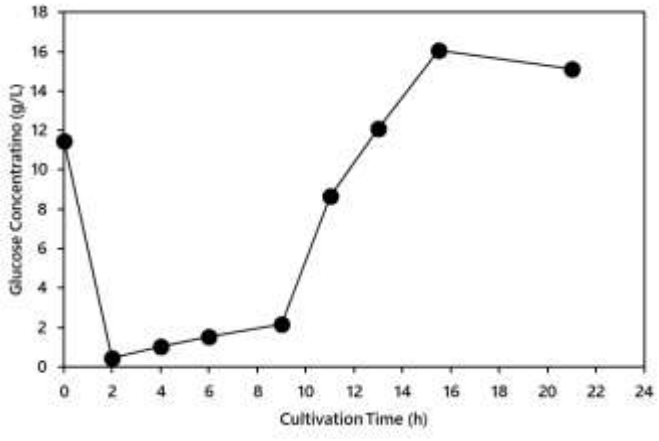

Figure 21 Glucose concentration over time in 1.3m^3 R. delemar *batch cultivation*

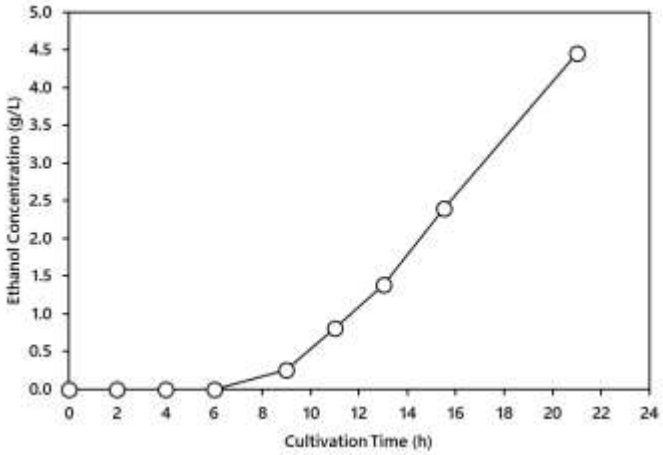

Figure 22 Ethanol concentration over time in 1.3m³ R. delemar *batch cultivation*

3.2.2 CULTIVATION ON SYNTHETIC MEDIUM IN 26 L BIOREACTOR

Four harvests of *R. delemar* biomass were successful, with an average harvest of 62.40 g dry biomass. The fifth harvest did not yield any useful biomass, due to an error in which the fourth harvest cleared the reactor almost completely of biomass and thereby not leaving enough fungi in the reactor as inoculum. The average biomass yield was 0.143 g/g glucose. Biomass concentration in cultivation medium was on average 4.30 g/l.

Göksungur (2004) reported a biomass concentration of > 4 g/l after cultivation of *R. oryzae* in 20 g/l glucose medium in a stirred-tank reactor at 28°C for 24 hours and a peak biomass concentration of 7.56 g/l after 72 hours. Zhou et al. (2011) reached a biomass concentration of 7.58 g/l for *R. delemar* at 20 g/l glucose and 6 g/l soybean peptone concentration in synthetic medium in batch cultivation at 30°C for 30 hours. However, cultivation volumes were much smaller, where Liao et al. worked with 100 ml medium in shake flasks. Nonetheless, the comparison shows, that cultivation time is a crucial factor in achieving high biomass concentrations. To recall, in the experiment at hand, *R. delemar* biomass was harvested after 8-16 hours.

Figure 23 Pellet growth of R. delemar *in synthetic medium. In 250 ml shake flask (left), a single large pellet from 26 l cultivation (middle), biomass harvest from 26 l cultivation with small and large pellets (right)*

The growth morphology of *R. delemar* exhibited spherical pellets, the majority of them 2-3 mm in diameter and some pellets reaching sizes of 5-15 mm, as shown in

Figure 23.Temperature, mode of agitation as well as aeriation can be ruled out as influencing factors for the growth morphology. This is because spherical pellet growth was already visible in shake flasks, where the same stock medium was used as for the large-scale cultivation (*Figure 23, left*).
Zhou et al. (2000) studied the effect of magnesium, zinc and iron concentrations in 50 g/l glucose medium and concluded, that high concentrations of magnesium and zinc have a positive effect on pellet size. An even bigger effect comes from the concentration of iron in cultivation medium, where 3000 ppb (parts per billion) resulted in pellet sizes of 3-4 mm. Furthermore, a dependency of morphology on the medium pH was observed. A pH of 5.59 led to pellet form. A pH of 3.93 and below resulted in dispersed filamentous form.

3.3 CULTIVATION OF FUSARIUM VENENATUM

3.3.1 CULTIVATION ON BREAD PARTICLES IN SHAKE FLASKS

It has to be noted that the cultivations, which are presented in the following sections will be mainly discussed according to their biomass yield (g dry biomass/g bread). This allows for a comparison of the cultivation's effectiveness, describing to which extend bread was converted to fungal biomass.
The initial *Fed-Batch non-sieved* experiment, in which the optimum cultivation time of *F. venenatum* was determined, showed that 48 and 72 hours resulted in the highest biomass yields: 0.382 ± 0.026 g/g bread and 0.407 ± 0.003 g/g bread respectively (see *Figure 24*).

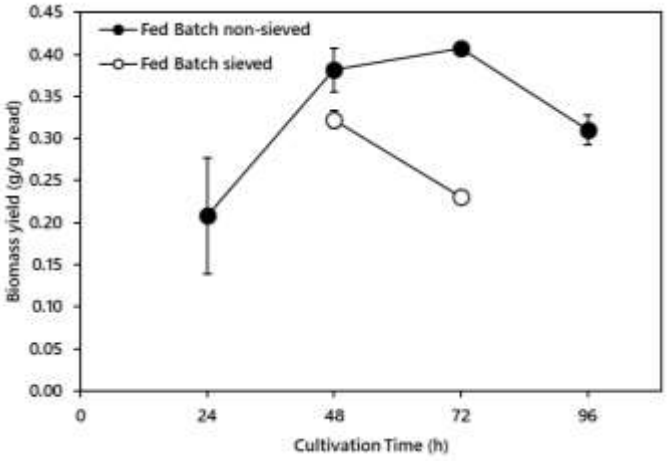

Figure 24 F. venenatum *biomass yields from fed-batch cultivation, starting with 1 wt% bread concentration and adding 1% bread in 24 hour steps. Cultivation on non-sieved and sieved bread is compared, where in the latter case, biomass was purged after harvest.*

The second fed-batch experiment was conducted with sieving of bread and purging after biomass harvesting to minimize bread residue in fungal biomass. As shown in *Figure 24*, biomass yields were generally lower for *Fed-Batch sieved* compared to *Fed-Batch non-sieved*, which stems from the removal of bread residue. For *fed-batch*

sieved, 72 hour cultivation showed a significant decrease of biomass yield compared to 48 hour cultivation (0.231 vs. 0.323g/g biomass respectively). This suggests a large fraction of bread added at t = 48 is not digested and remains in the 72 hours harvest, when using non-sieved bread.
Figure 25 shows a fed-batch cultivation of *F. venenatum* mycelium with sieved bread in Erlenmeyer flasks 24, 48 and 72 hours after inoculation. The mycelium shows evenly distributed growth with a slight tendency for a formation of spherical pellets. This is most evident after 48 hours cultivation time.

Figure 25 F. venenatum *mycelia in liquid medium with sieved bread particles. Cultivation time from left to right: 24 h, 48 h, 72 h*

A batch cultivation of *F. venenatum* under the same conditions as the second fed-batch cultivation was done to see how the presence of excess carbohydrates would influence mycelium growth. Biomass was harvested after 48 and 72 hours. *Table 9* shows the comparison of biomass yield (g biomass/g bread) between fed-batch and batch. Generally, harvesting after 48 hours resulted in higher yield, both for fed-batch as well as batch cultivation. However, fed-batch cultivation had a yield more than twice as high compared to batch cultivation with 0.323 g/g bread vs 0.139 g/g, bread respectively. In both cultivation modes, harvesting after 72 hours lead to a lower biomass yield. However, the difference for batch is not as high as compared to fed-batch cultivation.

Table 9 Biomass yield and concentration from fed-batch and batch cultivation of F. venenatum *after 48 and 72 hours. Total weight of bread added to medium was the same for batch and fed-batch (4 g for 48 h,6 g for 72 h cultivation). Bread was sieved to particle size < 1 mm prior to inoculation. Biomass concentration is given in reference to volume of medium. The number of sample replicates is show in* n

Media supply	Cultivation time (h)	Biomass yield (g/g bread)	Biomass conc. (g/l)	*n*
Fed-batch	48	0.323 ± 0.011	6.31 ± 0.21	2
	72	0.231 ± 0.003	6.92 ± 0.10	2
Batch	48	0.139 ± 0.014	2.78 ± 0.27	2
	72	0.117	3.51	1

Results of biomass metabolite concentrations via HPLC can be found in *Figure 26* for ethanol and *Figure 27* for glucose. Ethanol production was much more rapid in batch compared to fed-batch cultivations. This might be evidence for the Crabtree-effect, where a surplus of sugars in medium leads to ethanol production instead of biomass growth. Sieving the bread particles prior to cultivation led to higher amounts

of ethanol. This is because of the increased total amount of starch present in sieved bread, since by sieving, larger and indigestible particles containing lignocellulosic materials are removed.

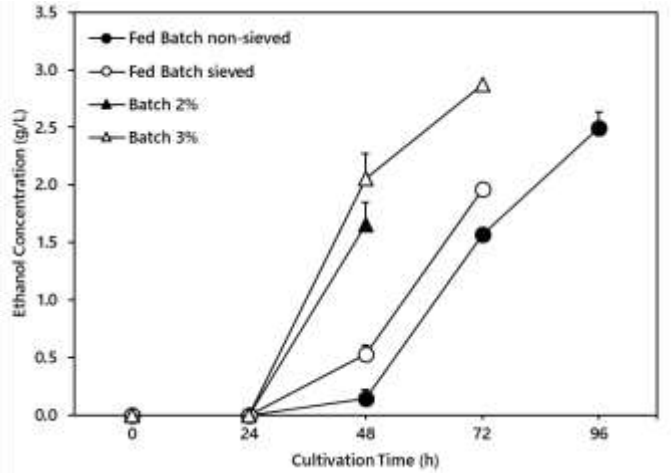

Figure 26 Ethanol concentrations in medium of F. venenatum *fed-batch and batch cultivations. All batch cultivations were carried out with sieved bread.*

Metabolization of starch to glucose and then absorption by the fungi can be tracked in *Figure 27*, most prominently for *Batch 3%*. The up and down trend of glucose concentration stems from the fungus alternating between decomposing starch to glucose and absorbing the glucose through its cell membrane to promote biomass growth. The *Fed Batch sieved* process gives a more stable glucose concentration throughout cultivation time, which makes for a lower ethanol production. This in turn leads to the higher biomass yield.

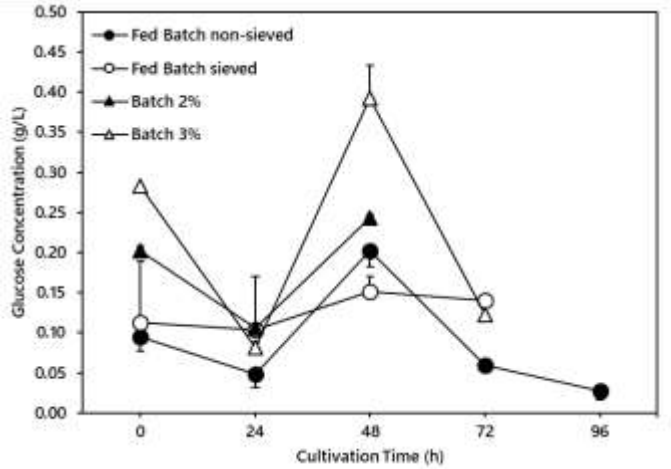

Figure 27 Glucose concentrations in medium of F. venenatum *fed-batch and batch cultivations. All batch cultivations were carried out with sieved bread.*

As a last experiment on batch cultivation, the bread concentration of cultivation medium was investigated. Since previous experiments established 48 hours as the optimum cultivation time, the same duration was chosen for this experiment. A 2% w/v

bread suspension was compared to 4% w/v suspension. 2% bread suspension resulted in higher yield (0.166 g/g bread) compared to 4% suspension (0.148 g/g bread).

Summarizing the cultivation of *F. venenatum* on bread particles in shake flasks, applying a 48 hour fed-batch process resulted in the highest biomass yield. Sieving bread particles and purging the biomass after harvest results in a great reduction of undigested bread particles. If a fed-batch process cannot be realized in scaled-up conditions, a batch cultivation at bread concentration of 2 wt% for 48 hours is the next best option in terms of biomass yield.
To date, no other study on the cultivation of *Fusarium* on bread waste has been published. Furthermore, most of the recent studies concerned with other strains of fungi cultivated on bread waste are employing a solid-state fermentation, by which a comparison of biomass yields or biomass concentrations is difficult (Gmoser et al., 2020; Melikoglu et al., 2015).
However, cultivation of *F. venenatum* on other types of liquid media have been investigated. Hoseyni et al. (2010) conducted research on cultivation of *F. venenatum* on 14 g/l date syrup medium and achieved a biomass concentration of 5.46 g/l after 72 hours cultivation at 30°C in 100 ml of medium.
Seyed Reihani and Khosravi-Darani (2019) also worked with date waste as the main component in cultivation medium. Cultivation in 41.81 g/l date sugar medium in a 3 l stirred tank bioreactor at 26°C for 73 hours, resulted in a biomass concentration of 8.07 g/l. According to their findings, *F. venenatum* grows well in media with higher concentrations of sugars. However, a date sugar concentration > 30 g/l led to a decrease of protein fraction in fungal biomass. How the protein fraction correlates with chitin fraction in fungal biomass is not described however.

3.3.2 CULTIVATION ON HYDROLYZED BREAD IN SHAKE FLASKS

In order to eliminate the presence of bread particles in harvested biomass, hydrolyzed bread particles were used as cultivation substrate for *F. venenatum*. The first experiment was a 24 hour batch cultivation on amylase treated liquid medium (20 g/l soluble solids concentration). As shown in *Table 10*, it resulted in an average biomass yield of 0.024 g/g substrate, which is only ca. 12% of yield from 24 hour cultivation on sieved bread (0.208 g/g substrate). An extension of cultivation time to 48 hours resulted in a biomass yield of 0.065 g/g substrate, which is ca. 46% of yield compared to batch cultivation with bread particles.

Table 10 F. venenatum *yield from cultivation on suspended bread particles vs. enzymatically treated bread particles. All cultivations were done in batch. The number of sample replicates is show in* n

Bread treatment	Medium conc. (wt%)	Cultivation time (h)	Biomass yield (g/g substrate)	Biomass conc. (g/l)	*n*
non-hydrolyzed	1	24	0.208 ± 0.069	2.08 ± 0.69	2
amylase	2	24	0.024 ± 0.008	0.46 ± 0.15	8
non-hydrolyzed	3	48	0.139 ± 0.014	2.78 ± 0.27	2
amylase	2	48	0.065 ± 0.021	1.25 ± 0.38	6
amylase + protease	2	48	0.116 ± 0.010	2.31 ± 0.20	4

A 2% liquid medium prepared from hydrolyzed bread via amylase and protease resulted in a yield of 0.116 g/g substrate. However, this is still significantly lower than cultivation on bread particles (see *non-hydrolyzed*). Further research is necessary to see if supplementation with salt- and nitrogen sources of hydrolyzed bread medium would result in comparable biomass yields. Additionally, Zhou et al. (2011) confirmed that the growth of *R. oryzae* in liquid-state medium is not only dependent on nitrogen concentration but also on the type of nitrogen source. Soybean peptone resulted in the highest biomass concentration (4.51 g/l), whereas the use of urea produced 1.91 g/l.

Verni et al. (2020) cultivated *Saccharomyces cerevisiae* yeast on liquified bread via enzyme treatment. Some of their results on glucose yield after enzyme treatment are discussed in section 3.1.3. Cultivation of *S. cerevisiae* on amylase treated bread (13.02 g/l glucose) without additional supplementation of nutrients already resulted in comparable biomass concentrations to cultivation in reference medium (optical density > 4). Cultivation on amylase and protease treated bread (13.02 g/l glucose, 4.7 g/l amino acids, 0.5 g/l peptides) did not yield a major improvement of biomass concentration.
However, the use of amyloglucosidase and a resulting glucose concentration of up to 126 g/l in cultivation medium resulted in an optical density > 9 of *S. cerevisiae* in suspension. While this shows that yeasts grow well on highly concentrated glucose-based media, the same is not necessarily true for *F. venenatum*. Nonetheless, as described earlier, Seyed Reihani and Khosravi-Darani (2019) reported a positive correlation of concentration of date sugar and biomass until 41.81 g/l.

3.4 BIOMASS TREATMENTS

Table 11 shows the decrease in *R. delemar* biomass weight after chemical treatments. Percentages indicate the relation of dry weight before and after treatment. Alkali treatment led to a much higher biomass loss than protease treatment (77.41% vs. 46.85%). This is probably because of alkali-soluble fractions, which are not hydrolyzed by protease and therefore remain in the biomass after treatment. Results of autoclave treatment show, that by heating the biomass in water suspension to 121°C for 20 minutes, 36.00% of cell wall fractions are removed. This reduction in weight is most probably due to a partial loss of bread particles and other fungal biomass

ingredients, such as lipids at increased temperatures. A subsequent bleaching treatment after alkali led to a slight increase in biomass loss (77.41% vs. 81.71%). This could be attributed to lignocellulosic fractions in bread particles being partly hydrolyzed and removed. EnzAlkG treatment resulted in the highest biomass loss of 94.02%. This could be due to biomass losing more bread particles after enzyme treatment compared to alkali treatment. A subsequent alkali treatment then results in a higher total biomass loss than alkali treatment on its own.
Furthermore, fractions of biomass have been lost during the different treatment steps. A three-step treatment (e.g. EnzAlkG) then causes a higher biomass loss than a two-step treatment (e.g. Alk).

Table 11 Dry biomass loss after various treatments on R. delemar *biomass. The number of sample replicates is show in* n

Treatment	Biomass loss (wt%)	*n*
Alk	77.41 ± 4.76	8
Enz	46.85 ± 2.04	4
Aut	36.00 ± 11.02	4
AlkBG	81.71 ± 0.41	2
EnzAlkG	94.02 ± 0.07	2
synthAlk	78.71 ± 0.92	2

Aut and Enz showed similar morphology. As illustrated in *Figure 28*, both had a clearly visible fibrous appearance, without a major change in color post-treatment. After alkali treatment, the biomass showed a hydrogel-like morphology. Bread residue was still visible after all treatments. However, it seemed like more bread was removed after enzyme treatment. It was suspected that the hydrolysis of protein fractions also caused the entanglements in biomass to open up and thereby allowing bread particles to be released from biomass.

Figure 28 R. delemar *biomass morphology after treatment via autoclave (left), protease (middle), NaOH (right) with subsequent washing and pressing*

After sieving and pressing, the average water content of Enz and Aut was reduced to 76.91% and 80.82% respectively (see *Table 12*). The alkali treatment apparently enabled a much higher water retention. Alk resembled a highly viscous hydrogel with an average water content of 96.52%. After alkali treatment, the biomass turned to a dark brown color, due to the starch contents in bread residues being hydrolyzed. AIM from *R. delemar* grown on synthetic medium (synthAlk) did not result in such

a change of color. Other combinations of treatments, which involved alkali treatment at some point, all resulted in water contents resembling hydrogels.

Table 12 Water content of R. delemar *biomass after various treatments. All treatments were done on biomass cultivated on bread particles, except synthAlk, where biomass was cultivated on synthetic medium. The number of sample replicates is show in* n

Treatment	Water Content (wt%)	*n*
Alk	96.52 ± 0.58	2
Enz	76.91 ± 1.13	2
Aut	80.82 ± 1.36	2
AlkBG	96.03 ± 0.35	2
EnzAlkG	97.11 ± 0.11	2
synthAlk	96.82 ± 0.09	2

The viscosity of biomass was measured on 3% w/v suspensions over the course of multiple grinding cycles. Where Aut and Enz resulted in fairly similar ranges of viscosity (*Figure 29*), Alk as well as AlkBG showed viscosities more than tenfold as high (*Figure 30*). However, regression analysis suggests, that due to high deviations in measurements, neither Enz nor Alk viscosity changes correlate with grinding cycles with respective *P*-values of .175 and .122. Only changes in viscosity for Aut and AlkBG are significant ($P = .039$ and $P < .001$ respectively).

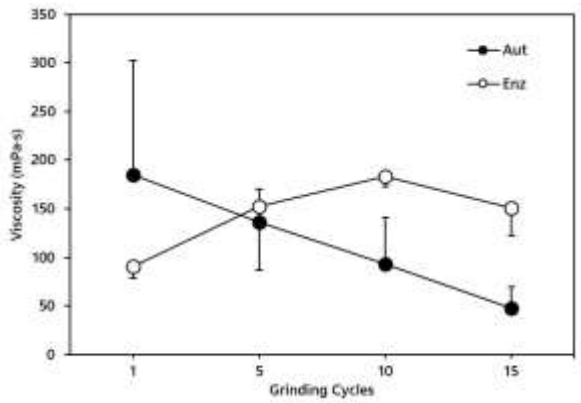

Figure 29 Change in viscosity by grinding treatment of autoclave and protease treated biomass. Standard deviations are depicted in one direction to avoid confusion

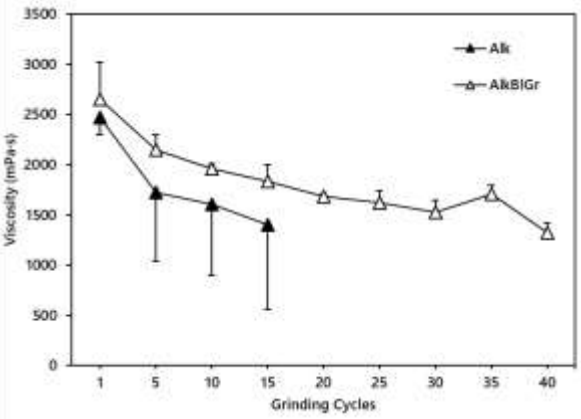

Figure 30 Change in viscosity by grinding treatment of NaOH and NaOH + H_2O_2 biomass. Standard deviations are depicted in one direction to avoid confusion

The results show that alkali treatment leads to a significant increase in viscosity. During post-treatment of AIM with dilute sulfuric acid, it was observed that viscosity was lowered drastically. While chitin and chitosan are insoluble in dilute sulfuric acid at room temperature, some crosslinking could have happened during the treatment. This might be due to the formation of a chitosan-sulfate complexes, caused by sulfuric acid treatment. Additionally, polyphosphate compounds are solubilized and removed by dilute sulfuric acid treatment. (Naghdi et al., 2014)
Both these factors could be an influence on the change in viscosity. The observation was made by stirring the biomass, so a verification of this observation needs to be made via viscosity measurements in the future. Additionally, viscosity measurements of Alk, Aut and Enz need to be repeated to arrive at more definitive results.

Microscope images in *Figure 31* show the effect of grinding treatment on biomass. After 1 grinding cycle, mycelia fibers are still highly entangled and appear as large clusters. After 10 grinding cycles the entanglements are partly broken up and clusters become smaller. After 15 grinding cycles a higher number of mycelia fragments are visible. Lignocellulosic bread residues appear as large flake-shaped fragments (*Figure 31 A3* and *B3*).
Measurements of fiber dimensions confirm that no significant change in length or width of fibers occurs during grinding treatment, even up to 40 grinding cycles in the case of AlkBG. Also, the type of chemical treatments does not seem to have a significant effect on fiber dimensions. Mycelia fragment length was ca. 60-300 µm with a width of ca. 4-8 µm.

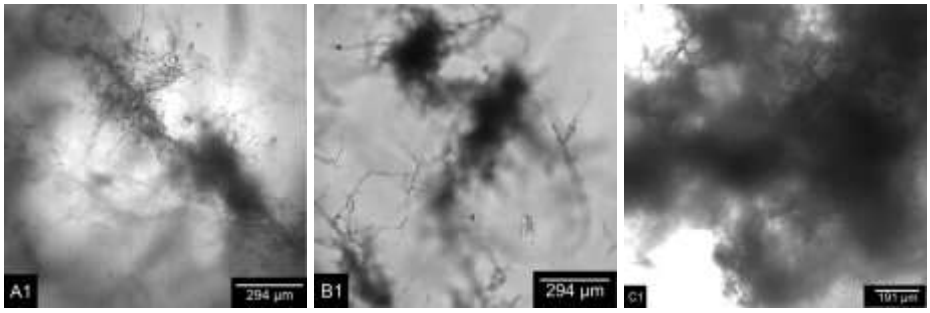

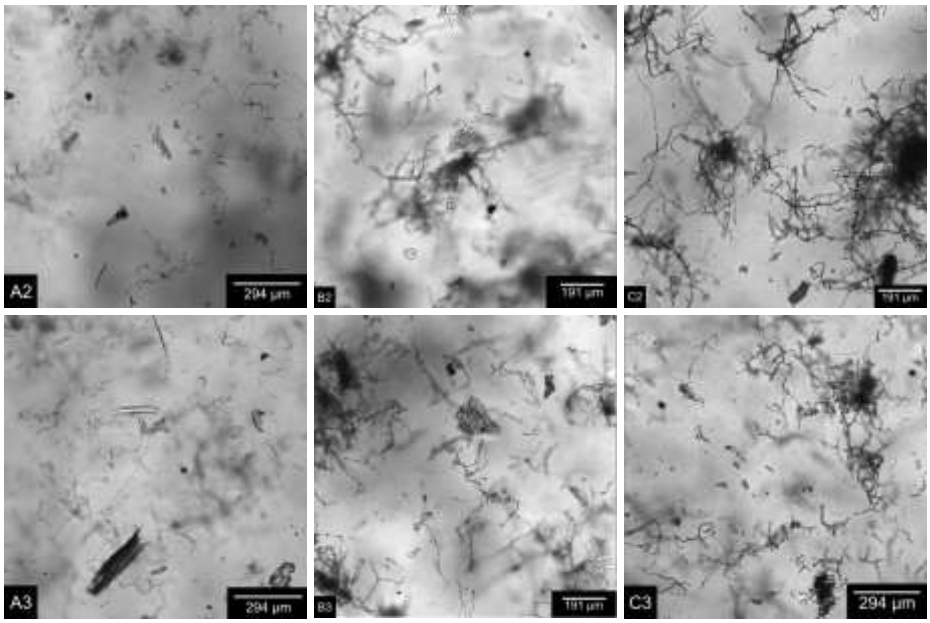

Figure 31 Microscope images of fungal biomass in suspension after treatment with alkali (A), protease (B), autoclave (C) and grinding cycles 1 (1), 10 (2), 15 (3)

Figure 32 shows AlkBG10, EnzAlkG10 and synthAlk15 biomass. A second chemical treatment seems to lead to more evenly dispersed fibers, with no clusters visible. It is important to note, that both AlkBG10 and EnzAlkG10 were ground after their second chemical treatment. It can be theorized that macro-sized bread particles have been broken down after the bleaching treatment, due to the removal of a large fraction of lignin. This in turn led to a greater energy absorption by mycelia during grinding and thereby a more even dispersion. Furthermore, studies show that removal of lignin via bleaching enhances the fibrillation of cellulose to nanofibrils (Berglund et al., 2017, 2016; Siqueira et al., 2016). Consequently, if nanofibrillated cellulose is present in the samples of AlkBG10 and EnzAlkG10, it is not visible at the magnification shown in *Figure 32*. A sample of synthAlk15 appears in a similar morphology, which acts as a control study with a total absence of bread particles.

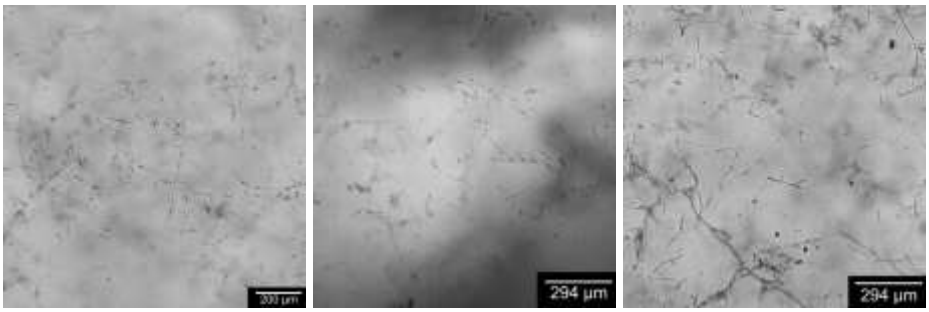

Figure 32 AlkBG10 (left), EnzAlkG10 (middle), synthAlk15 (right)

3.5 GLCN AND GLCNAC CONCENTRATION AFTER TREATMENTS

Table 13 shows the concentrations of glucosamine (GlcN) and N-acetyl-glucosamine (GlcNAc) from cell wall analysis. Percentages are given in reference to total dry biomass weight.

Table 13 GlcN and GlcNAc concentrations in fungal cell wall after treatment with Alk, AlkBG, Enz, synthAlk. The number of sample replicates is show in n

Sample	GlcN (wt%)	GlcNAc (wt%)	*n*
Alk1	8.05 ± 0.93	21.45 ± 0.80	2
AlkBG1	8.65 ± 0.50	18.92 ± 0.44	2
Enz1	4.77 ± 1.28	28.17 ± 0.18	2
synthAlk1	5.91 ± 1.42	19.72 ± 1.11	2

All treatments resulted in a much higher GlcNAc concentration compared to GlcN, which suggests that chitin was more prominent than chitosan. Much higher GlcNAc concentrations indicate that significant deacetylation during NaOH treatment at 121°C for 20 minutes does not occur. Concentrations of Enz1 biomass show significantly lower GlcN concentration (4.77%). However, this difference is most probably because other alkali-soluble polysaccharides largely remain in the biomass after enzyme treatment and thereby reduce the percentage of GlcN. GlcNAc concentration of enzyme treated biomass might not be accurate, since other polysaccharide components also release acetic acid, which is used as an indicator of GlcNAc concentration in the method used.

GlcN concentrations of Alk1 and AlkBG1 show an insignificant difference. However, a decrease in GlcNAc concentration can be observed by a bleaching treatment (21.45 vs. 18.92 wt%).

synthAlk shows lower GlcN and GlcNAc concentrations. This might be due to the shorter cultivation time in synthetic medium (8-16 hours) compared to bread medium (22 hours), where the short cultivation time reduced the biosynthesis of chitin and chitosan. Studies show that chitosan concentration in *R. oryzae* biomass increases rapidly over the 72-74 hour period after inoculation. (Göksungur, 2004; Tan et al., 1996) Furthermore, chitin is the precursor to chitosan, explaining the later onset of chitosan development and the general lower concentration of chitosan compared to chitin in zygomycete cell walls. (Davis and Bartnicki-Garcia, 1984).

Additionally, hyphae in the inner layer of pellets can show autolysis, meaning a breakdown of cells by the organism itself. (Gow et al., 2007) This might have had an effect on chitosan and chitin concentration in synthAlk, which grew in pellet form. For a true comparison of biomass with and without bread residue, the pellet growth has to be inhibited.

Jones et al. (2019) reported chitin and chitosan concentrations of 12.8 and 10.0 wt% for NaOH treated mycelia of *Mucor genevensis*. Since both Alk and synthAlk samples showed higher GlcNAc concentrations, it is plausible that *R. delemar* has higher chitin concentrations in its mycelia cell wall.

3.6 ANALYSIS OF BIOMASS TREATMENT RESIDUES

After storing liquid residues over several days at +4°C, a settling of insoluble solids was observed, which could be partly separated via decanting. However, the presented results are obtained from centrifuging samples and separating precipitate and supernate afterwards.
Results of liquid residue after NaOH and protease treatment are shown in *Table 14*. Soluble solids and insoluble solids are presented as recovered fractions in relation to initial dry biomass weight. Total residue is the cumulated percentage of soluble and insoluble solids.

Table 14 Recovered fractions in relation to initial dry biomass weight after chemical treatments of R. delemar *biomass. The number of sample replicates is show in* n

Treatment	Soluble Solids (wt%)	Insoluble Solids (wt%)	Total Residue (wt%)	*n*
NaOH	34.61 ± 0.70	1.12 ± 0.27	35.82 ± 0.97	4
Protease	24.13 ± 0.72	7.08 ± 0.87	31.22 ± 1.59	4

Recovery of NaOH treatment residues shows a higher yield of soluble solids (34.61%) and total residue (35.82%). Protease treatment leads to a much higher yield of insoluble solids, which could contain a high amount of bread particles.

Table 15 shows the concentration of soluble and insoluble solids in the recovered liquid residue after treatment of biomass. Of each treatment batch, 2.5-3 l of liquid residue were recovered.

Table 15 Concentration of soluble and insoluble solids in recovered liquid residue after chemical treatments of R. delemar *biomass. The number of sample replicates is show in* n

Treatment	Soluble Solids (g/l)	Insoluble Solids (g/l)	Total Residue (g/l)	*n*
NaOH	23.89 ± 1.47	0.84 ± 0.17	24.73 ± 1.60	4
Protease	11.60 ± 0.23	3.40 ± 0.33	15.01 ± 0.55	4

Determination of nitrogen contents of protease treatment residues by Kjeldahl method showed a nitrogen concentration in soluble solids and insoluble solids of 0.0904 g/g dry mass and 0.0531 g/g dry mass respectively. By the conversion factor of 6.25, the estimated protein concentration in soluble and insoluble solids resulted in 56.5 and 33.2 wt% respectively. Relating the percentages to the concentrations of protease treatment residues given in *Table 15*, estimated protein concentrations of 6.55 g/l are present in the soluble solids fraction and 1.13 g/l in the insoluble solids fraction. In total protein concentrations of 7.68 g/l are present in the liquid residue. These results give a promising start to studies on how to repurpose these fractions for the production of protein-rich foods.

3.7 WET-LAYING OF FILMS AND NONWOVEN COMPOSITES

Generally fungal biomass acts as a sticky substance and adheres to wire screens and blotting papers after wet-laying and pressing procedures. A high tendency to stick to surfaces was observed for all alkali treated and bleached materials. On uneven and structured surfaces, such as blotting paper and wire screens, a dual effect of physical entanglement and strong hydrogen bonding might be the cause of this. After pressing the films in between blotting papers, a separation of film and paper was often only partly accomplished. This led to paper residue on films in mild cases or destruction of films in severe cases. These damages could be greatly reduced by placing a thin nylon mesh (30 µm pore size) between film and blotting paper before pressing. However, a slight residue after pressing was also present on nylon films. Future work could investigate if a dilute sulfuric acid treatment on biomass would lessen the stickiness of biomass.

Figure 33 shows samples of films treated by alkali, protease and autoclave. The color change, which was observed in AIM, is not visible in the finished films anymore. However, bread residues appear as darker spots, which makes them more apparent in AIM films. A decrease in bread particle size with higher grinding cycles is clearly visible.

In terms of stiffness and haptic sensations, the films shared characteristics of a plastic-like film. The surface side which faced the acrylic sheet was smooth and shiny and at a grammage of ca. 100 g/m^2 they appeared slightly translucent. Initial tests of prolonged submersion of films in water showed that structural integrity is largely maintained, which is a distinction to conventional cellulosic paper sheets. This could be due to stronger hydrogen bonds in chitinous films. Also, the cationic nature of chitosan could further facilitate strong bonding, which remains in submersion of water.

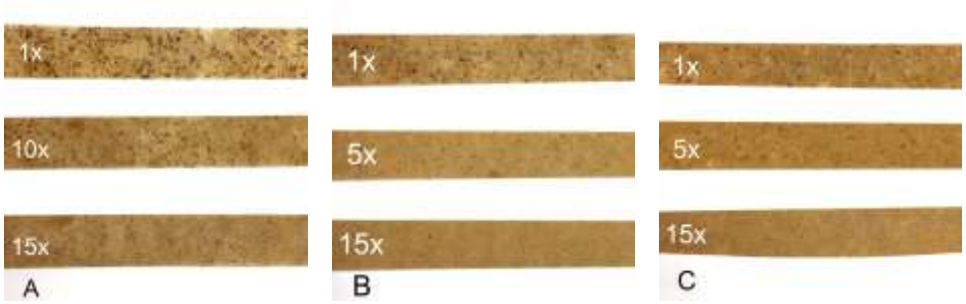

Figure 33 Samples of films made via handsheet former. Alkali treated (A), protease treated (B), autoclave treated (C). White numbers indicate the number of grinding cycles

Figure 34 shows samples of VMNC with Aut15 as a binder. With a 25 wt% concentration of viscose fibers, the nonwoven appears in a similar color as biomass films. Also, a slight translucence is still observable. With 50 and 75% viscose concentration, the sheets become more and more textile-like to the touch. However, the bending stiffness is much higher than for films, as will be explained in section 3.10.3.

Figure 34 Samples of VMNC prepared with Aut15. Viscose concentration from left to right: 25, 50, 75 wt%

In preliminary tests, film formation of *F. venenatum* biomass via vacuum filtration was confirmed. However, time constraints did not allow for a scaling up of cultivation. Properties of films derived from *F. venenatum* need to be investigated in future work. A first sample is shown in *Figure 35*. The biomass was derived via NaOH treatment from *Quorn™ Meatless Pieces*, which have a mycoprotein content of 93% (Marlow Food Ltd., 2020). Mycoprotein is directly derived from *F. venenatum* biomass (Wiebe, 2002). At the time of making, the improved wet-laid method via vacuum filtration was not developed yet. Therefore, large blotting paper residues remained on the film.

Figure 35 Wet-laying of F. venenatum *film via vacuum filtration (left), dry film with paper residue (middle) close-up of film (right)*

3.8 CHARACTERIZATION OF FILMS PREPARED VIA HANDSHEET FORMER

3.8.1 THICKNESS, GRAMMAGE, DENSITY

As shown in *Table 16*, films from Alk, Enz and Aut show generally a positive correlation between the number of grinding cycles and bulk density. This is most probably due to bread particles being pulverized by grinding and allowing a denser packing of fibers. The control study synthAlk confirms this, since no significant change in bulk density is observed between grinding cycles 1 and 15.

Another influence on density could be connected to the theory mentioned in section 3.4, that clusters of mycelia fibers are broken up by grinding and are more evenly dispersed in suspension. This in turn allows the fibers to settle more closely during wet-laying and allow for a higher bulk density.

Table 16 Thickness, grammage and bulk density of wet-laid biomass films from Alk, Enz and Aut. All films were prepared via handsheet former. The number of sample replicates is show in n

Treatment	Thickness (µm)	Grammage (g/m^2)	Density (g/cm^3)	*n*
Alk1	132 ± 27	84.43	0.64	1
Alk10	105 ± 8	83.24	0.80	1
Alk15	102 ± 6	85.30	0.84	1
Enz1	143 ± 3	99.11 ± 2.08	0.69 ± 0.00	2
Enz5	99 ± 1	81.73 ± 1.13	0.83 ± 0.01	2
Enz15	94 ± 2	84.89	0.90	1
Aut1	120 ± 6	93.73	0.78	1
Aut5	95 ± 4	85.24	0.90	1
Aut15	82 ± 1	78.21	0.96	1

3.8.2 TENSILE PROPERTIES

Tensile tests of films prepared via handsheet former showed that Alk films exhibit significantly higher tensile index and moduli than Aut or Enz films, as shown in *Table 17*. For 1 grinding cycle, the difference is at a maximum, where Alk1 shows more than double the tensile index than Enz1. Grinding treatment has a significant effect on tensile properties throughout all biomass treatments. Here, the greatest improvement is shown by Enz, where tensile index increases by more than 220% between 1 grinding cycle and 15. Both Aut15 films, were largely destroyed during their drying process. Therefore, the result of Aut15 is not representative, since tensile testing was performed on only two specimens.

Jones et al. (2019) reached an ultimate tensile strength for films derived from NaOH treated *M. genevensis* mycelia of σ_{UTS} = 24.7 MPa and a tensile modulus of E = 1.90 GPa. These are so far the highest reported tensile properties for mycelia derived films. Alk10 and Alk15 represent an improvement in tensile modulus with 2.23 and 2.20 GPa respectively. However, the reported ultimate tensile strength cannot be met by the results presented in this section. Jones et al. reported a chitin and chitosan concentration for *M. genevensis* films of 12.8 and 10.0 wt% respectively. In this study, chitin and chitosan was not directly determined. Instead determination of GlcNAc and GlcN in Alk1 resulted in 21.45 and 8.05 wt% respectively (see section 3.5). Generally, a higher GlcN content means a higher degree of deacetylation and therefore, most likely a higher content in chitosan. However, a part of the GlcN might also stem from partially deacetylated chitin. Nonetheless, a higher tensile strength might lie in a higher chitosan concentration. Jones et al. (2019) also reported highest tensile strength for mycelium derived films containing chitosan.

A secondary influence on tensile strength might lie in the drying method, which was applied by Jones et al. Instead of letting the films dry at room temperature after cold-pressing, they used a hot-press of 500 kg at 120°C for 15 minutes. Future research could validate the influence of hot-pressing on tensile properties of mycelia films.

*Table 17 Tensile index (σ_{TI}), Young's modulus (*E*), ultimate tensile strength (σ_{UTS}) and strain at break (ε) of Alk, Enz and Aut films prepared via handsheet former. The number of sample replicates is show in* n

Treatment	σ_{TI} (Nm/g)	*E* (GPa)	σ_{UTS} (MPa)	ε (%)	*n*
Alk1	14.73 ± 3.89	1.61 ± 0.05	9.44 ± 2.50	1.34 ± 0.26	7
Alk10	19.50 ± 5.52	2.23 ± 0.09	15.55 ± 4.39	1.45 ± 0.30	4
Alk15	21.64 ± 1.85	2.20 ± 0.09	18.14 ± 1.56	1.56 ± 0.12	7
Enz1	6.48 ± 1.58	0.90 ± 0.02	4.51 ± 1.09	1.07 ± 0.16	9
Enz5	12.66 ± 2.93	1.19 ± 0.03	10.46 ± 2.43	1.64 ± 0.28	9
Enz15	14.70 ± 1.35	1.33 ± 0.04	13.26 ± 1.23	1.88 ± 0.15	9
Aut1	9.94 ± 1.12	1.14 ± 0.03	7.76 ± 0.86	1.31 ± 0.07	9
Aut5	11.24 ± 3.03	1.37 ± 0.04	10.06 ± 2.72	1.40 ± 0.23	9
Aut15	9.49 ± 3.37	1.47 ± 0.01	9.10 ± 3.20	1.35 ± 0.35	2

Figure 36 shows examples of stress-strain curves of Alk, Enz and Aut films. The curves show the brittleness of films, since the films do not exhibit a plastic region in their stress-strain curves and their ultimate tensile strength is equal to strength at failure.

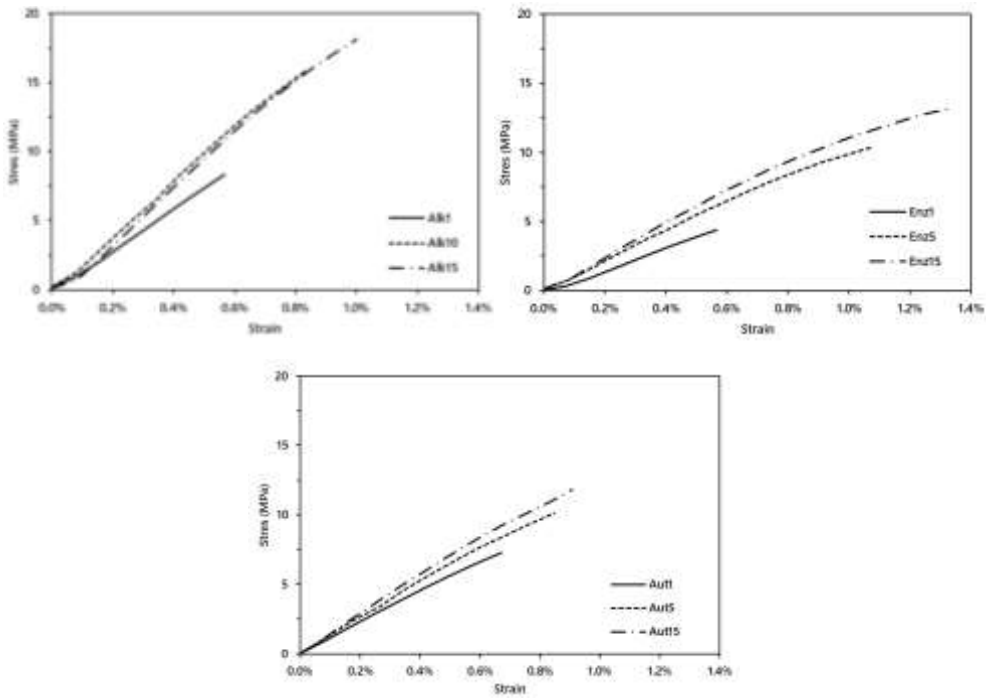

Figure 36 Examples of stress-strain curves for Alk films (top left), Enz films (top right) and Aut films (bottom middle)

3.8.3 FLEXURAL RIGIDITY

Analysis via fit regression models indicates a significant effect of both the biomass treatment and the number of grinding cycles on flexural rigidity ($P < .001$). A trend for a reduction in rigidity can be observed from 1 grinding cycle to 5 or 10, regardless of treatment, as seen in *Table 18*. Furthermore, alkali treatment seems to lead to higher rigidity of films, compared to protease or autoclave treatment. However, the small sample size as well as possible pre-damages due to the samples being used for tensile testing already, do not allow for a definitive conclusion. Future research should therefore validate the presented results.

Table 18 Flexural rigidity of fungal biomass films prepared from Alk, Enz and Aut. The number of sample replicates is show in n

Treatment	Flexural Rigidity (mN·cm)	*n*
Alk1	9.16 ± 0.66	2
Alk10	7.84	1
Alk15	8.37	1
Enz1	8.87 ± 0.35	4
Enz5	5.38 ± 0.10	3
Enz15	6.13 ± 0.31	3
Aut1	7.05 ± 0.76	3
Aut5	6.32 ± 0.31	3
Aut15	4.38	1

3.8.4 WATER CONTACT ANGLE

An effect of grinding treatment on the films' water contact angle is not observed. The average WCA for Enz and Aut are 73 - 77° (see *Table 19*). However, alkali treatment seems to have led to slightly higher contact angles with a maximum average of 94° for Alk15. Comparing these results to previous findings, the films produced in this study show inferior WCA results. Appels et al. (2020) reported WCA of 129° for untreated films from mycelia of *S. commune*. Since no hydrolysis step was performed, this exceptionally high WCA could be due to hydrophobic compounds in the biomass, such as lipids. Jones et al. (2019) reported WCA on NaOH treated mycelia films of 106° (*A. arbuscula*) and 101° (*M. genevensis*). The significantly lower WCA presented here are most probably due to bread residues in films. Since they contain at least partly cellulose, they could act as hydrophilic particles and lower the overall WCA of films.

Table 19 Results of water contact angle measurements of films from alkali (Alk), protease (Enz) and autoclave (Aut) treated biomass prepared via handsheet former. The number of sample replicates is show in n

Sample	WCA (°)	*n*
Alk1	85 ± 8	3
Alk10	82 ± 10	3
Alk15	94 ± 1	3
Enz1	73 ± 4	3
Enz5	73 ± 1	3
Enz15	73 ± 1	3
Aut1	77 ± 7	3
Aut5	74 ± 4	3
Aut15	73 ± 5	3

3.9 CHARACTERIZATION OF FILMS PREPARED VIA VACUUM FILTRATION

3.9.1 THICKNESS, GRAMMAGE, DENSITY

As shown in *Table 20*, films which were prepared from biomass subjected to two chemical treatments did not show significant changes of bulk density with grinding treatment. This is in line with the visual observations from microscopy in section 3.4, where a second chemical treatment of biomass leads to more evenly dispersed fibers in suspension and a lessened disturbance of bread particles. As a control study, synthAlk films confirm the disturbing factor of bread particles, since they show the highest bulk density of all films (ca. 1.00 g/cm^3) and an unchanged density between 1 and 15 grinding cycles.

Table 20 Thickness, grammage and bulk density of wet-laid films with varying chemical and grinding treatment. All films were prepared via vacuum filtration. The number of sample replicates is show in n

Treatment	Thickness (µm)	Grammage (g/m^2)	Density (g/cm^3)	*n*
AlkGB1	58 ± 22	67.47 ± 23.05	0.85 ± 0.06	3
AlkGB5	46 ± 2	59.70 ± 1.03	0.77 ± 0.02	4
AlkGB10	48 ± 3	60.74 ± 0.86	0.79 ± 0.04	4
AlkGB15	51 ± 1	65.22 ± 0.64	0.78 ± 0.01	4
AlkBG1	71 ± 2	53.13 ± 13.11	0.75 ± 0.18	4
AlkBG10	51 ± 3	44.77 ± 0.08	0.88 ± 0.06	4
AlkBG20	43 ± 2	37.83 ± 1.95	0.88 ± 0.04	4
AlkBG30	44 ± 4	39.38 ± 5.28	0.89 ± 0.05	3
AlkBG40	43 ± 3	37.87 ± 02.09	0.88 ± 0.06	4
EnzGB1	71 ± 12	44.71 ± 1.35	0.64 ± 0.09	3
EnzGB5	50 ± 5	35.71 ± 0.57	0.72 ± 0.07	4

Treatment	Thickness (µm)	Grammage (g/m^2)	Density (g/cm^3)	*n*
EnzGB10	46 ± 1	37.94 ± 0.52	0.83 ± 0.02	4
EnzGB15	43 ± 28	47.72 ± 0.74	0.83 ± 0.05	4
EnzAlkG1	80 ± 3	57.04 ± 1.05	0.71 ± 0.04	4
EnzAlkG10	60 ± 4	49.64 ± 1.07	0.83 ± 0.06	4
EnzAlkG15	55 ± 1	48.27 ± 1.35	0.88 ± 0.02	4
EnzAlkG20	52 ± 1	46.82 ± 0.31	0.89 ± 0.02	4
EnzAlkG30	55 ± 3	48.40 ± 0.71	0.89 ± 0.03	4
synthAlk1	55 ± 3	57.03 ± 1.62	1.03 ± 0.02	3
synthAlk15	49 ± 2	47.84 ± 1.40	0.99 ± 0.03	4

3.9.2 TENSILE PROPERTIES

Alk1 and Enz1 biomass were used for further chemical treatments, to see if tensile properties of wet-laid films could be further improved. The results from tensile testing are shown in *Table 21*. Alk + H_2SO_4 lead to a decrease in tensile index. However, Alk + H_2SO_4 + NaOH resulted in a significant increase in tensile index compared to pure NaOH treatment. Also, its tensile modulus increased by almost 0.5 GPa to 2.06 GPa. Films prepared from Alk + H_2O_2 showed the highest tensile moduli out of all treatments (2.42 GPa).

Subsequent enzyme treatments of Alk1 with cellulase and protease were mainly done to see if bread particle residues could be removed from biomass without harsh chemical treatment. Interestingly, both treatments lead to a decrease in tensile index. While *R. delemar* does not contain any cellulosic components (Bartnicki-Garcia, 1968; Griffin, 1996), studies shows that chitosan is hydrolyzed by non-specific enzymes, such as amylase, lipase, protease and especially cellulase. (Ike et al., 2007; Xia et al., 2008) Also polyglucuronic acid components, which are present in zygomycete cell walls, could have been hydrolyzed via cellulase. Therefore, it is highly probable that major cell wall components have been broken down by the enzyme treatment and thereby weakening the structural integrity of films.

*Table 21 Tensile index (σ_{TI}), Young's modulus (*E*), ultimate tensile strength (σ_{UTS}) and strain at break (ε) of films after various chemical treatments of* R. delemar *biomass. Maxima are highlighted in bold. The number of sample replicates is show in* n

Treatment	σ_{TI} (Nm/g)	*E* (GPa)	σ_{UTS} (MPa)	ε (%)	*n*
Alk1	24.72 ± 3.03	1.58 ± 0.11	25.27 ± 3.80	2.50 ± 0.41	8
Alk1 + H_2SO_4	15.38 ± 4.55	1.74 ± 0.30	17.19 ± 5.09	1.50 ± 0.58	12
Alk1 + H_2SO_4 + NaOH	28.05 ± 3.34	2.06 ± 0.18	32.29 ± 3.58	2.80 ± 0.71	8
Alk1 + Cellulase	14.04 ± 2.85	1.52 ± 0.13	15.40 ± 3.71	1.29 ± 0.31	16
Alk1 + Protease	20.49 ± 1.57	1.66 ± 0.06	22.45 ± 2.24	1.90 ± 0.25	8
Alk1 + H_2O_2	24.87 ± 3.98	**2.42 ± 0.18**	24.53 ± 10.12	1.40 ± 0.77	12
Enz1 + NaOH	36.91 ± 5.20	2.20 ± 0.24	38.17 ± 5.36	**2.70 ± 0.33**	8
Enz1 + H_2O_2	**52.33 ± 5.93**	1.96 ± 0.21	33.39 ± 5.68	2.41 ± 0.40	12

From this pre-study, the following treatments were selected to be further investigation by applying the grinding treatment on them: Alk+H_2O_2, Enz + NaOH and Enz + H_2O_2.

Table 22 shows the results of tensile testing from films, which were selected for further investigation. As a control study, synthAlk was added as a bread particle free biomass to see the influence of bread particles on films. The numbers at the end of sample codes indicate the number of grinding cycles. *Figure 37* shows exemplary stress-strain curves of films prepared from AlkGB10, AlkBG10, EnzGB10, EnzAlk10 and synthAlk15. In comparison to previous stress-strain curves of Alk, Enz and Aut, these curves show a more distinct plastic deformation, especially EnzAlkG10 and synthAlk15.

Out of all samples, EnzGB15 reached the highest tensile index σ_{TI} = 61.41 Nm/g. The highest tensile modulus was reached for AlkGB10 films (3.38 GPa) and highest ultimate tensile strength was reached by AlkGB15 films (σ_{UTS} = 71.50). This constitutes the highest ultimate tensile strength as well as tensile modulus of mycelia derived films reported to date. As already discussed in section 3.8.2, future research could investigate if a drying of films via hot-pressing leads to a further increase of tensile properties. Since analysis of GlcN and GlcNAc concentration showed no significant change from before and after bleaching treatment (see section 3.5), their influence on tensile properties can be ruled out in this case.

Lastly, synthAlk shows no significant change in tensile property from 1 grinding cycle to 15. This suggests that a grinding treatment helps in breaking down bread particles and thereby lessening their detrimental effect on tensile properties of films. Additionally, the higher entanglement in biomass grown on bread particles is broken up by grinding. Furthermore, it seems that bread particles present in cultivation medium lead to a higher entanglement of mycelia. This might be due to the fungi enclosing the particles in order to digest them.

*Table 22 Tensile index (σ_{TI}), Young's modulus (*E*), ultimate tensile strength (σ_{UTS}) and strain at break (ε) of films prepared via vacuum filtration. Maxima are highlighted in bold. The number of sample replicates is show in* n

Treatment	σ_{TI} (Nm/g)	*E* (GPa)	σ_{UTS} (MPa)	*ε* (%)	*n*
AlkGB1	24.87 ± 3.98	2.46 ± 0.12	29.29 ± 4.95	1.42 ± 0.77	12
AlkGB5	44.90 ± 3.53	3.01 ± 0.18	57.58 ± 4.74	2.82 ± 0.55	12
AlkGB10	51.80 ± 5.01	**3.38 ± 0.25**	56.70 ± 7.24	2.94 ± 0.43	12
AlkGB15	54.74 ± 9.76	3.20 ± 0.49	**71.50 ± 9.39**	3.13 ± 0.73	12
AlkBG1	36.95 ± 3.69	1.46 ± 0.08	31.27 ± 3.13	2.87 ± 0.52	12
AlkBG10	49.92 ± 3.64	2.06 ± 0.13	44.12 ± 4.03	2.98 ± 0.33	12
AlkBG20	51.98 ± 3.55	2.18 ± 0.12	46.59 ± 3.93	3.17 ± 0.16	12
AlkBG30	51.93 ± 4.57	2.20 ± 0.13	46.35 ± 4.91	3.91 ± 0.58	12
AlkBG40	51.41 ± 6.20	2.24 ± 0.13	45.73 ± 6.89	2.71 ± 0.51	12
EnzGB1	52.32 ± 5.93	1.96 ± 0.21	33.39 ± 5.68	2.41 ± 0.40	12
EnzGB5	51.92 ± 4.29	2.60 ± 0.26	36.39 ± 5.56	2.65 ± 0.38	12
EnzGB10	57.68 ± 2.71	2.59 ± 0.29	48.14 ± 2.70	2.73 ± 0.40	12
EnzGB15	**61.41 ± 3.43**	2.80 ± 0.17	51.09 ± 3.05	3.14 ± 0.37	12
EnzAlkG1	36.76 ± 4.04	1.54 ± 0.10	25.78 ± 3.26	2.15 ± 0.31	12
EnzAlkG10	50.39 ± 3.54	1.93 ± 0.14	41.41 ± 4.56	3.42 ± 0.57	12
EnzAlkG15	53.80 ± 1.86	2.15 ± 0.06	47.36 ± 2.09	3.78 ± 0.36	12
EnzAlkG20	54.20 ± 6.23	2.30 ± 0.10	48.80 ± 5.82	3.62 ± 0.70	12
EnzAlkG30	56.79 ± 3.40	2.35 ± 0.07	51.30 ± 2.69	3.99 ± 0.55	12
synthAlk1	46.41 ± 1.26	1.65 ± 0.08	47.98 ± 1.58	**5.45 ± 0.60**	12
synthAlk15	44.39 ± 8.30	1.94 ± 0.13	44.65 ± 8.08	4.02 ± 1.47	12

Unfortunately, previous papers on the topic do not disclose individual data on grammage and thickness. Otherwise a more direct comparison via the tensile index would have been possible. Still, an estimate for films produced by Nawawi et al. (2020a) is possible, since they mention the film thickness ranging from 60-80 µm and a goal grammage of 80 g/m^2. Assuming a thickness of 80 µm and a grammage of 80 g/ m^2, a tensile index of ca. 20 Nm/g was reached for films which exhibited an ultimate tensile strength of 204.4 MPa (see section 2.10.5 for equation of tensile index). This tensile index is lower than any result presented in *Table 22*. Future research could therefore investigate, if 80 g/m^2 films prepared from any of the biomasses listed in *Table 22*, would result in similarly high tensile strengths > 200 MPa.

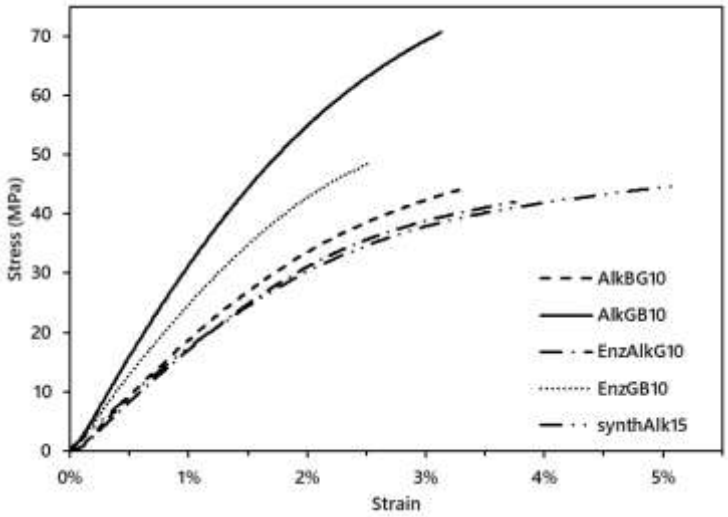

Figure 37 Exemplary stress-strain curves of films prepared from various biomass via vacuum filtration

The above presented results suggest EnzGB treatment of *R. delemar* biomass as one of the most favorable treatments. This makes an enzymatic hydrolysis for deproteinization of fungal cell wall a viable alternative to alkali treatment. In fact, biomass which is first treated via protease poses another significant advantage compared to biomass first treated via alkali: Hydrolyzed protein fractions can be recovered after enzyme treatment and possibly used for repurposing to food-products.

The effect of treatment sequence was studied by a comparison between results of AlkGB10 and AlkBG10. For AlkGB, the biomass was first NaOH treated, then ground and afterwards bleached. For AlkBG, the biomass was NaOH treated, bleached and ground at the end. Regression analysis showed that the sequence of treatments does not have a significant effect on tensile index ($P = .521$) but it does have a significant effect on tensile modulus ($P < .001$). Following the grinding treatment by bleaching yields a higher tensile modulus than doing the bleaching first and then performing the grinding.

3.9.2.1 DETERMINATION OF GRINDING OPTIMUM

Analysis of various regression models showed that the chemical treatment of biomass is insignificant in a comparison of tensile properties between AlkBG and EnzAlkG. The only significant effect is attributed to the grinding treatment, where the regression models for tensile index and tensile modulus as a function of grinding cycles show $P < .001$. *Figure 38* and *Figure 39* show the plotted regression curves for tensile index and tensile modulus as a function of grinding cycles, respectively. Response optimization of regression functions predict a maximum tensile index (55.63 MPa) is reached at 26 grinding cycles and a maximum tensile modulus (2.33 GPa) at 29 grinding cycles. A compromised maximum for tensile index (55.58 MPa) and modulus (2.33 GPa) is predicted at 27 grinding cycles, with insignificant declines from their individually predicted maximum. Future studies could investigate if grinding cycles > 15 are also favorable for tensile properties of EnzGB films.

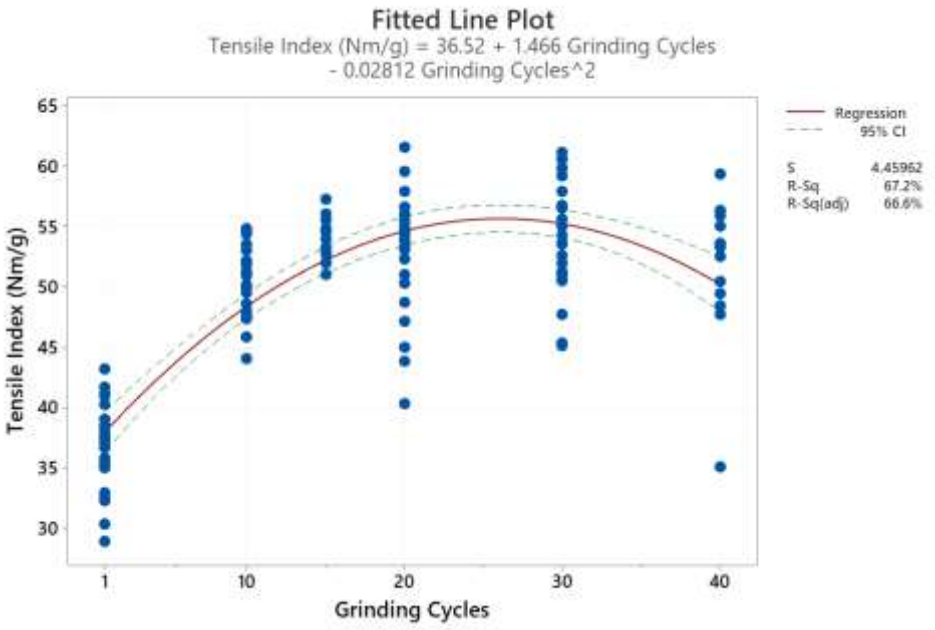

Figure 38 Cumulated tensile indices of AlkBG and EnzAlkG as a function of grinding cycles

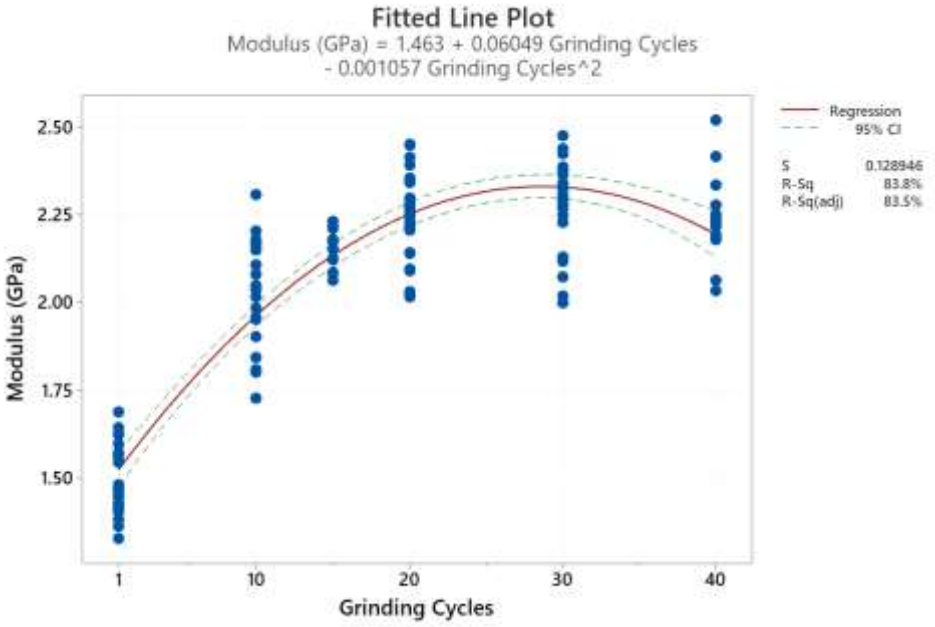

Figure 39 Cumulated tensile moduli of AlkBG and EnzAlkG as a function of grinding cycles

3.9.2.2 EFFECT OF SPECIMEN SHAPE ON TENSILE RESULTS

From the first film trials to the next developments, the mode of film preparation, film size and thereby specimen shape changed drastically. In order to create a more direct connection between the first films (Alk, Enz, Aut) and further developments (EnzGB, AlkGB, EnzAlkG, AlkGB), dog bone shaped specimens were made from previously used specimens from tensile testing. *Table 23* shows the results of tensile testing of dog bone shaped films prepared via handsheet former.

*Table 23 Tensile index (σ_{TI}), Young's modulus (*E*), ultimate tensile strength (σ_{UTS}) and strain at break (ε) of films prepared via handsheet former cut into dog bone shape. Previously tested rectangular specimens were cut into dog bone shape to measure the effect of specimen shape on tensile results. The number of sample replicates is show in* n

Treatment	σ_{TI} (Nm/g)	*E* (GPa)	σ_{UTS} (MPa)	ε (%)	*n*
Alk1_db	22.43 ± 3.84	1.20 ± 0.06	14.38 ± 2.46	1.38 ± 0.27	9
Alk10_db	28.59 ± 3.11	1.65 ± 0.08	22.77 ± 2.47	1.64 ± 0.19	9
Alk15_db	25.18 ± 3.27	1.65 ± 0.07	21.09 ± 2.73	1.38 ± 0.27	9
Enz1_db	9.27 ± 2.01	0.76 ± 0.03	6.44 ± 1.40	0.97 ± 0.20	9
Enz5_db	13.65 ± 2.30	1.02 ± 0.02	11.26 ± 1.90	1.33 ± 0.25	9
Enz15_db	14.35 ± 1.39	1.13 ± 0.03	12.93 ± 1.25	1.38 ± 0.19	9

Figure 40 and *Figure 41* show the comparisons of tensile index and modulus respectively. Dashed graphs represent values of dog bone shaped specimens while solid lines represent values of rectangular shaped specimens. Tensile index is significantly higher for Alk films in dog bone shape ($P < .001$), while the difference for Enz specimen shape is insignificant ($P = .287$). Moduli are significantly higher ($P < .001$) for rectangular shaped specimens from both Alk and Enz. While being aware, that the results of dog bone shaped specimens may be skewed due to pre-damages of tensile testing, a comparison was still regarded necessary in order to relate the results of rectangular to dog bone shaped specimens.

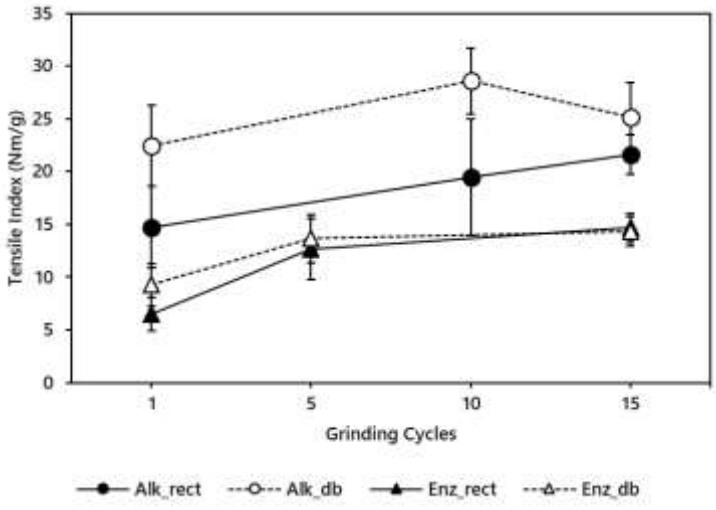

Figure 40 Comparison of tensile index between rectangle shaped specimens (Alk_rect, Enz_rect) and dog bone shaped specimens (Alk_db, Enz_db)

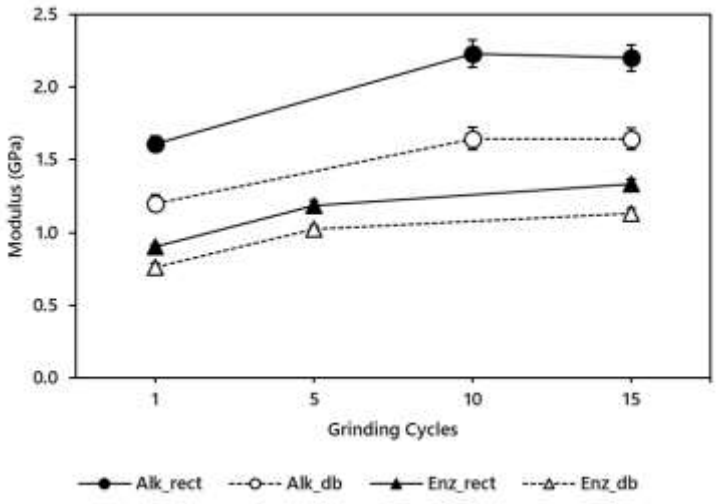

Figure 41 Comparison of Young's modulus between rectangle shaped specimens (Alk_rect, Enz_rect) and dog bone shaped specimens (Alk_db, Enz_db)

3.9.2.3 EFFECT OF BREAD RESIDUE ON TENSILE PROPERTIES

To verify the effect of bread particles on films, synthAlk films were prepared. The biomass from which they were derived, was cultivated on synthetic medium. Therefore, a presence of bread particles could be excluded. For the analysis, synthAlk specimens were compared against Alk_db specimens. The respective results from 1 grinding cycle and 15 were cumulated to plot the regression line shown in *Figure 42*. The regression analysis confirms the negative effect of bread particles on the tensile index of biomass films ($P < .001$). synthAlk showed an average tensile index of σ_{TI} = 45.45 Nm/g whereas average tensile index of Alk_db was σ_{TI} = 23.80 Nm/g.

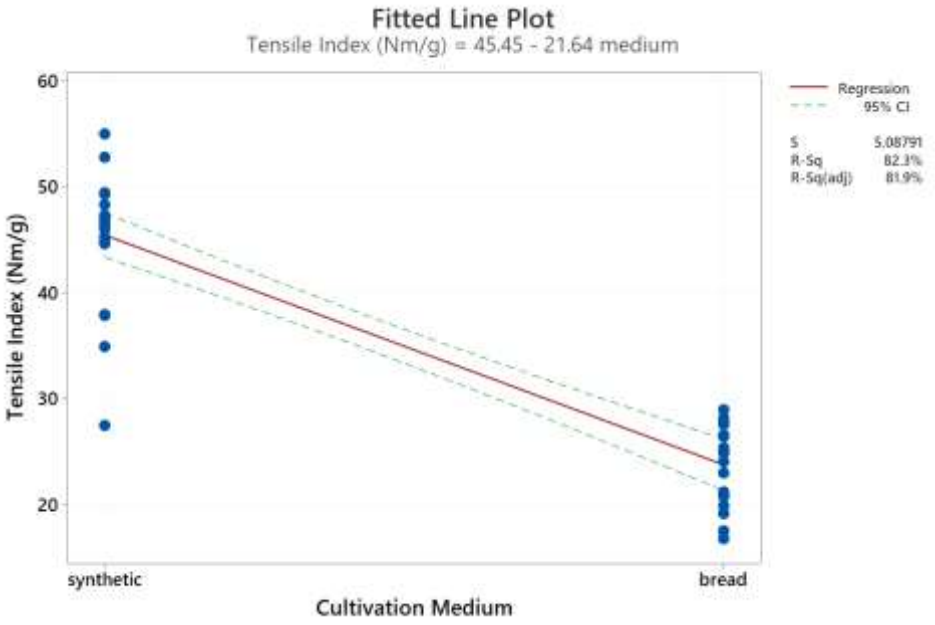

Figure 42 Tensile index of alkali treated films as a function of cultivation medium

However, a comparison between synthAlk and EnzGB films indicate that by bleaching, lignin of bread particles is largely removed and the remaining cellulose fibrils might take on a reinforcing function after they have been subjected to a bleaching treatment.
Regression analysis showed, that while synthAlk1 and EnzGB1 do not show a significant difference in tensile index, the difference grows to a significant size after 15 grinding cycles ($P < .001$). The scatterplot shown in *Figure 43* illustrates this growth in difference. Average tensile indices of synthAlk15 and EnzGB15 were 44.49 Nm/g and 56.89 Nm/g respectively.

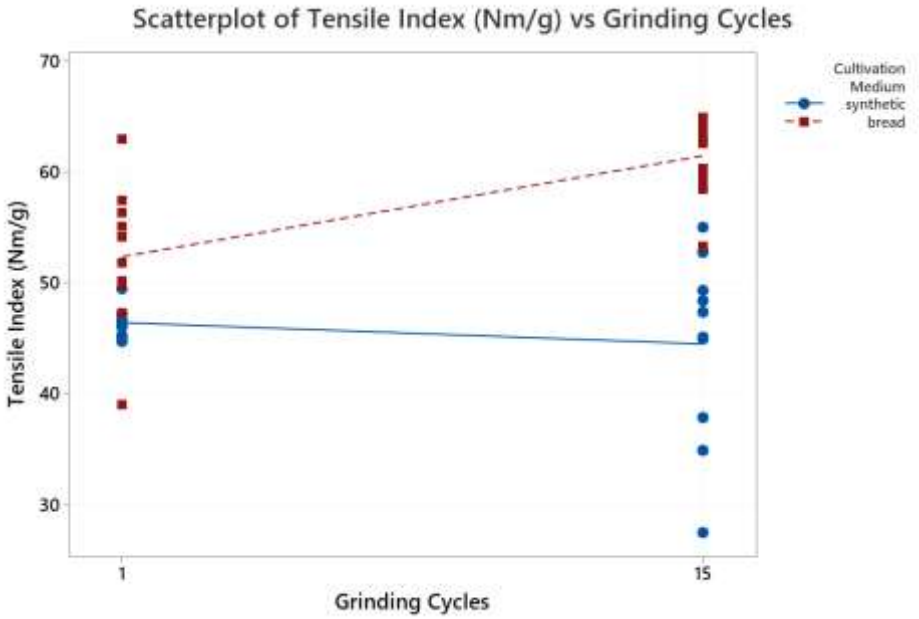

Figure 43 Tensile index scatterplot for synthAlk (cultivation medium = synthetic) and EnzGB (cultivation medium = bread)) as a function of grinding cycles

By the hypothesis of bread as reinforcement, bread particles remain as smaller, cellulosic fractions after bleaching treatment. Through grinding, these fractions are further decreased in size and are evenly distributed in the biomass. These cellulosic fractions are able to take up tensile forces and increase the overall tensile strength of the biomass film. *Figure 44* shows microscopic images at 1x magnification of Alk15 film (left) and EnzGB15 film (right). In Alk15 bread particles are large enough to cause disruptions in the continuous fungal film. In EnzGB15, the bread particles have been significantly reduced in size and are assumed to appear in some cases as singular fibers (white arrow).

Considering the previously established concentrations of GlcN and GlcNAc (see section 3.5), synthAlk1 showed average results of 5.91% GlcN and 19.72% GlcNAc, while AlkBG1 showed 8.65% GlcN and 18.92% GlcNAc. The significantly lower concentrations of both monomers in synthAlk contradict the hypothesis of cellulosic reinforcement. Its antithesis would then be that bread particles are a disturbance in fungal biomass. This disturbance is lessened by further grinding. In the comparison of synthAlk15 and EnzGB15, the higher chitin and chitosan concentrations then dominate and are the main reason for a higher tensile index.

For a conclusion on the hypothesis, *R. delemar* biomass needs to be cultivated on synthetic medium in a way that chitin and chitosan concentrations are similar to Alk1 and AlkBG1 results.

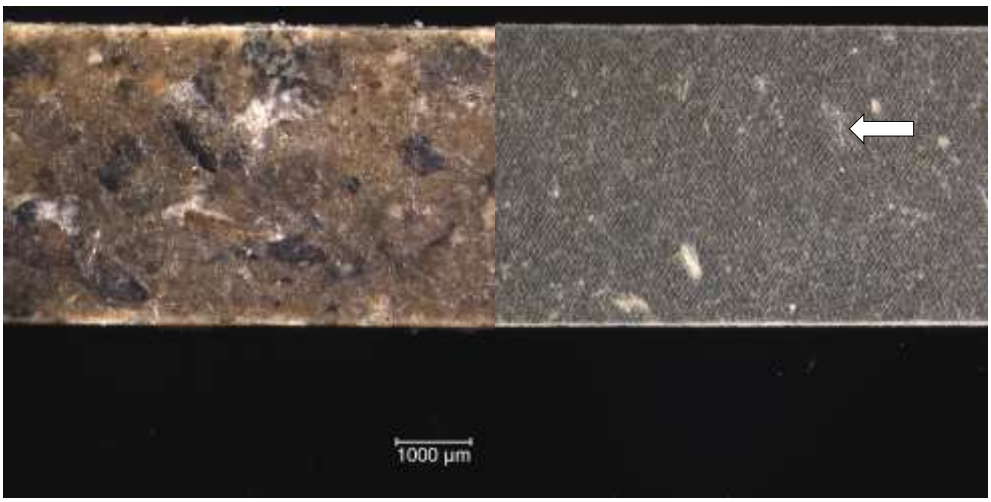

Figure 44 Microscopic images at 1x magnification of Alk15 film (left) and EnzGB15 film (right). The white arrow marks the position of an assumed singular cellulosic fiber

3.9.2.4 EFFECT OF BIOMASS DEGRADATION OVER TIME

Since the project continued over the span of several months, an investigation of the effect of storage time on fungal biomass and its tensile properties of wet-laid films was made. It was assumed that at the end of storage time, biomass would have experienced degradation and thereby a worsening in tensile properties.
Films were prepared from 15 week old Alk10 biomass via vacuum filtration method explained in section 2.9.2. Tensile results obtained from these films were compared against Alk10_db films (cut out in dog bone shape), which were prepared from ca. 3 weeks old biomass at that time and stored in airtight zip-lock bags. Tensile results are presented in *Table 24*. A clear effect of storage time on films from can be observed. The degraded biomass films showed only 43% of their former tensile index and 67% of their former tensile modulus. Since the 15 week old biomass had an unpleasant smell, it was assumed that some form of degradation occurred. The main reason for the lower tensile results of 15 weeks old biomass is most probably be due to the extended storage of biomass in water suspension.

*Table 24 Tensile index (σ_{TI}), Young's modulus (*E*), ultimate tensile strength (σ_{UTS}) and strain at break (ε) of Alk10 films prepared from 3 weeks old biomass and 15 weeks old biomass. The number of sample replicates is show in* n

Storage Time (weeks)	σ_{TI} (Nm/g)	*E* (GPa)	σ_{UTS} (MPa)	ε (%)	*n*
3	28.59 ± 3.11	1.65 ± 0.08	22.77 ± 2.47	1.64 ± 0.19	9
15	12.35 ± 1.52	1.10 ± 0.10	14.62 ± 1.50	1.49 ± 0.19	12

3.9.3 SCANNING ELECTRON MYCROSCOPY (SEM)

Wet-laid films showed similar surface morphologies under SEM (see *Figure 45*). From their even surface side, films appear as one continuous layer, without an apparent fibrous structure. An exception here is Alk1 (*Figure 45a*), where cavities between the fibers are still visible. However, Alk1 is the only out of all presented SEM images, where the film was prepared via handsheet forming. The difference in morphology could be caused by the different wet-laid and drying method.
In EnzGB films (*Figure 45c, e*), mycelia are more fused together and singular fibers are barely visible anymore. Even under 8000x magnification, a distinct fibrous structure is not visible (*Figure 45g*). synthAlk1 (*Figure 45b*) appears as an almost completely smooth surface. AlkGB10 from its coarse surface side (*Figure 45d*) shows that individual mycelia fibers are still present but are very closely pressed together by the two-step pressing process during drying of films. *Figure 45f* shows an encapsulated bread residue particle after protease and bleaching treatment. A mycelial film is laid on top of the particle, while its bottom right corner lays bare (white arrow).
Future studies could rely on cross sectional images to reveal more about the fiber bonding and the disturbance of bread particles in films.

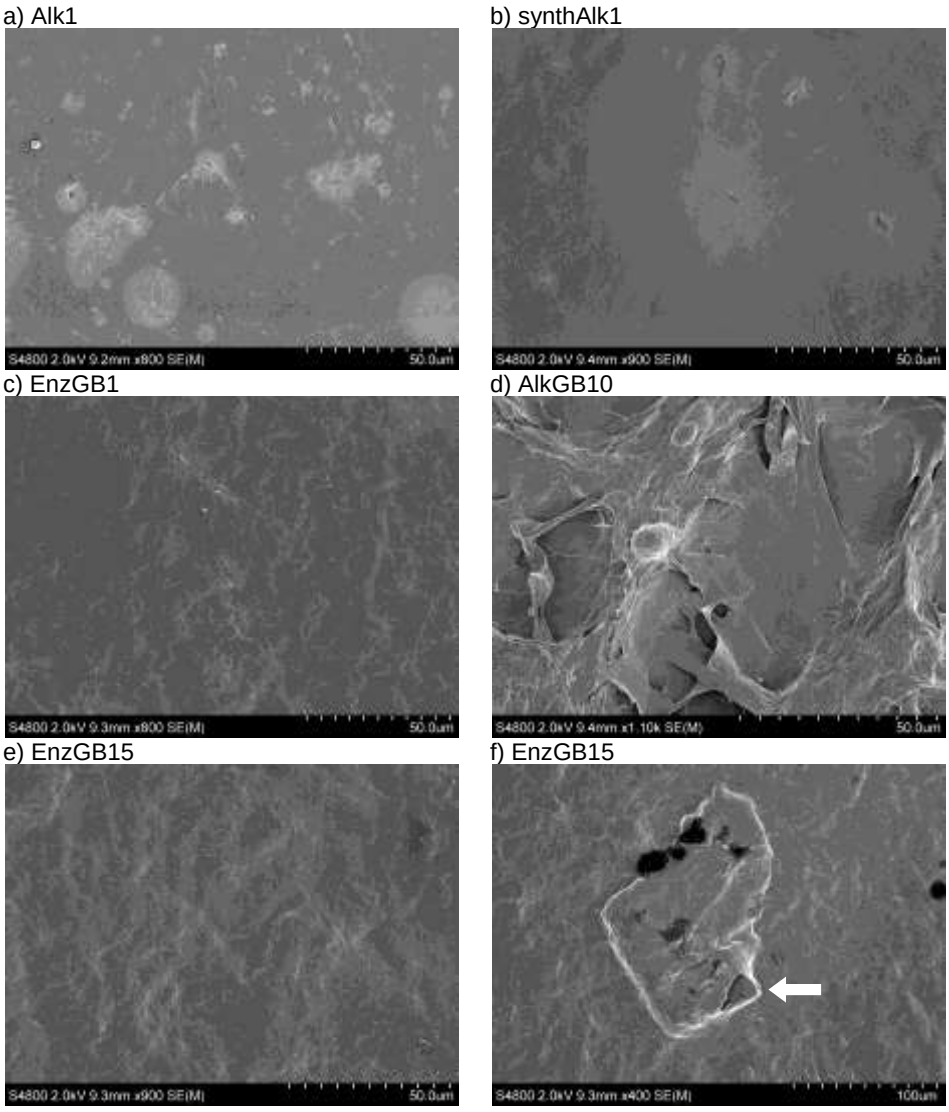

g) EnzGB15

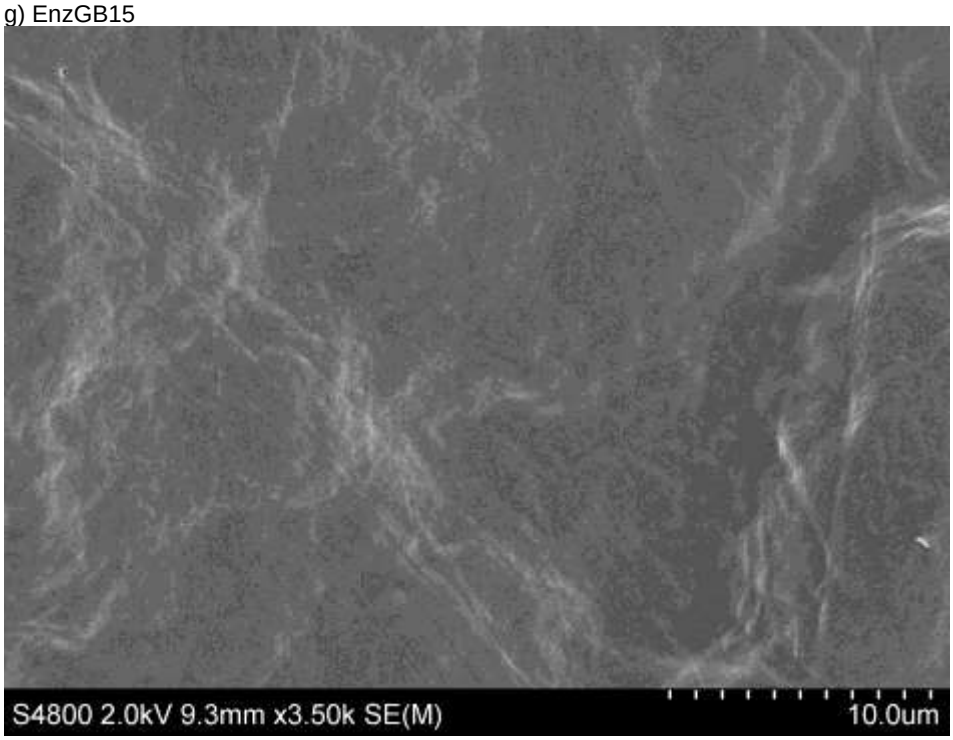

Figure 45 SEM images depicting the surface morphology of wet-laid mycelia films. Images were taken at 400x (f), 800x (a, c) 900x (b, e), 1100x (d) and 8000x (g) magnification. The respective scales show the depicted reading in µm as the distance between one dash to the next

3.10 CHARACTERIZATION OF VISCOSE-MYCELIA NONWOVEN COMPOSITES

3.10.1 THICKNESS, GRAMMAGE, DENSITY

Table 25 shows thickness, grammage and density of VMNC, prepared from Aut15 and Enz15. Generally, thickness and density seem to correlate inversely. With 75 wt% viscose concentration, density is at its lowest while thickness at its highest. Since viscose fibers have a higher fiber length (5 mm) than fungal fibers (ca. 300 µm), their packing density in an amorphous structure is much lower. Viscose fiber concentration correlates thereby positively with high porosity. This relationship between density and thickness can be seen as an indirect measurement of porosity.
However, porosity of VMNC was not measured in this project. It is an important attribute for nonwovens, i.e. when investigating for filtration properties, as was done by Janesch et al. (2020) and Wales and Sagar (1990).

Table 25 Thickness, grammage and bulk density of wet-laid VMNC with varying viscose concentration. The number of sample replicates is show in n

Composition	Thickness (µm)	Grammage (g/m^2)	Density (g/cm^3)	*n*
Aut75Vc25	28 ± 3	72.49	2.62	1
Aut50Vc50	43 ± 1	80.00 ± 0.31	1.87 ± 0.03	2
Aut25Vc75	63 ± 2	77.07	1.22	1
Enz75Vc25	31 ± 1	83.13 ± 1.54	2.70 ± 0.07	2
Enz50Vc50	44 ± 1	82.91 ± 2.29	1.91 ± 0.01	2
Enz25Vc75	65 ± 4	81.53 ± 3.61	1.26 ± 0.02	2

3.10.2 TENSILE PROPERTIES

Table 26 shows the results of tensile testing of VMNC. Tensile index and strain at break are generally highest at a viscose concentration of 50 wt%. Tensile modulus is at its peak at 25% viscose concentration. For a comparison between films and VMNC, tensile results of Aut15 and Enz15 are presented again. The drastic increase of ultimate tensile strength between pure biomass films and VMNC with 25% viscose concentration, suggests that the biomass acts as a binding matrix, while viscose fibers are the main load bearing component. At 50% viscose concentration, the relation of binder to load bearing fiber seems to reach its preliminary maximum. At 75% viscose, the biomass concentration is presumably too low to ensure sufficient binding between viscose fibers.

Figure 46 shows exemplary stress-strain curves for VMNC prepared with Enz15 and varying viscose concentrations. Enz50Vc50 shows a prolonged plastic phase after elastic deformation.

*Table 26 Tensile index (σ_{TI}), Young's modulus (*E*), ultimate tensile strength (σ_{UTS}) and strain at break (ε) of VMNC. Aut15 and Enz15 are recited results of pure biomass films, taken from Table 21. The number of sample replicates is show in* n

Composition	σ_{TI} (Nm/g)	*E* (GPa)	σ_{UTS} (MPa)	ε (%)	*n*
Aut15	9.49 ± 3.37	1.47 ± 0.01	9.10 ± 3.20	1.35 ± 0.35	2
Aut75Vc25	16.06 ± 0.93	3.94 ± 0.12	42.14 ± 2.47	2.72 ± 0.31	5
Aut50Vc50	19.24 ± 1.00	2.97 ± 0.24	36.28 ± 1.86	3.58 ± 0.66	9
Aut25Vc75	15.10 ± 1.71	1.81 ± 0.12	18.01 ± 2.04	2.27 ± 0.30	9
Enz15	14.70 ± 1.35	1.33 ± 0.04	13.26 ± 1.23	1.88 ± 0.15	9
Enz75Vc25	16.83 ± 0.54	3.99 ± 0.12	44.69 ± 1.44	2.68 ± 0.18	9
Enz50Vc50	18.58 ± 0.70	3.05 ± 0.11	35.49 ± 1.35	3.27 ± 0.32	9
Enz25Vc75	15.06 ± 0.72	1.90 ± 0.07	19.17 ± 0.91	2.27 ± 0.22	9

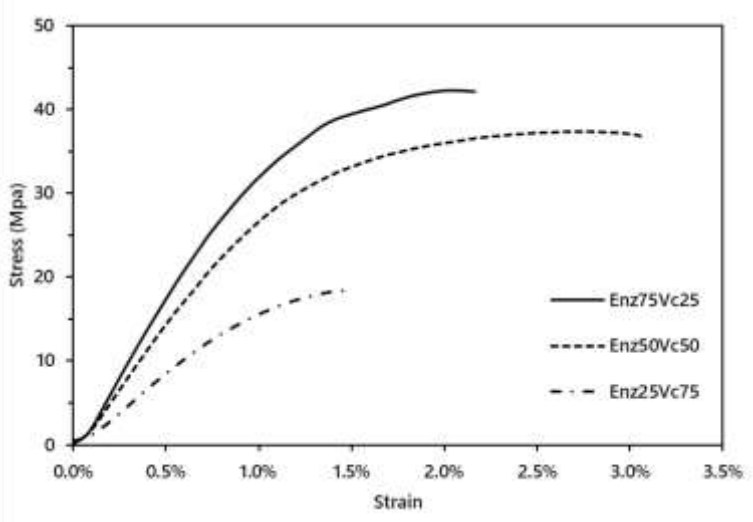

Figure 46 Examples of stress-strain curves of VMNC prepared from Enz15 with varying viscose concentration

Regression analysis suggests that Aut and Enz treatment of biomass are no significant contributors to tensile index (P = .624) and tensile modulus (P = .126) of VMNC. *Figure 47* and *Figure 48* show fitted line plots of tensile index and tensile modulus as a function of viscose concentration respectively. For plotting, results of Enz and Aut composites were cumulated.

The P-values of both regression functions are $P < .001$. Since Alk15 films showed a significantly higher tensile index than Enz15 and Aut15, future research should investigate the influence of alkali treated biomass as a binder. If Alk15 as a binder shows a significant increase in tensile strength, biomass treated by a two-step chemical (i.e. AlkGB and EnzGB) is then a strong candidate for further research into VMNC.

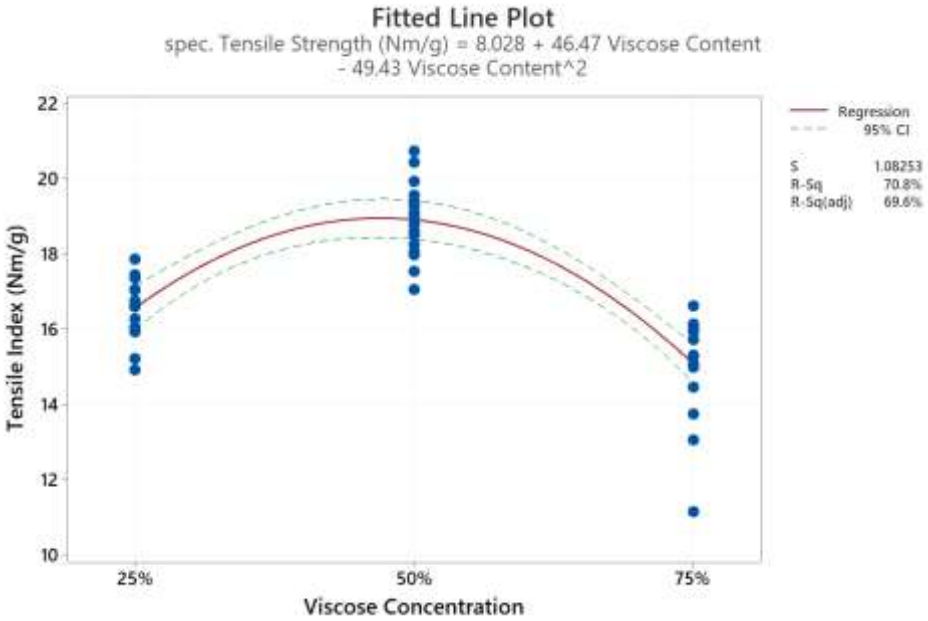

Figure 47 Tensile index of VMNC as a function of viscose concentration

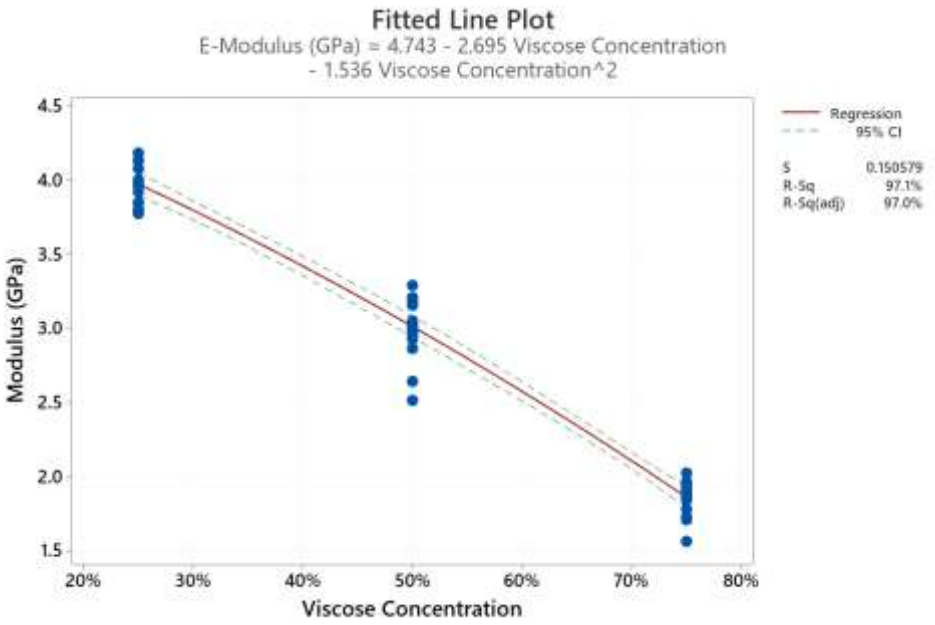

Figure 48 Tensile modulus of VMNC as a function of viscose concentration

3.10.3 FLEXURAL RIGIDITY

Analysis of flexural rigidity in response to viscose content of VMNC resulted in a much clearer outcome compared to biomass films. *Table 27* shows the results of measurements. Regression analysis resulted in a cubic function, in which concentrations of viscose fibers > 25 wt% lead to a rapid increase of flexural rigidity. Measurement of VMNC with a viscose concentration of 75% were out of bounds, because the full length of specimens was not enough to cause a bending of 41.5°. To plot the regression function (see *Figure 49*), a flexural rigidity of 43.00 mN·cm was assumed for 75% viscose concentration. However, the true value is expected to be higher than that. To determine the true flexural rigidity at 75 wt% viscose concentration, a three-point-bending method could be employed (Nawawi, 2016).

Table 27 Flexural rigidity of VMNC with Enz15 as a binder with varying viscose concentration. Enz15 represents pure biomass film. The number of sample replicates is show in n

Composition	Flexural Rigidity (mN·cm)	*n*
Enz15	6.13 ± 0.43	3
Enz75Vc25	8.10 ± 0.75	4
Enz50Vc50	21.02 ± 1.43	4
Enz25Vc75	> 43*	4

* out of bounds

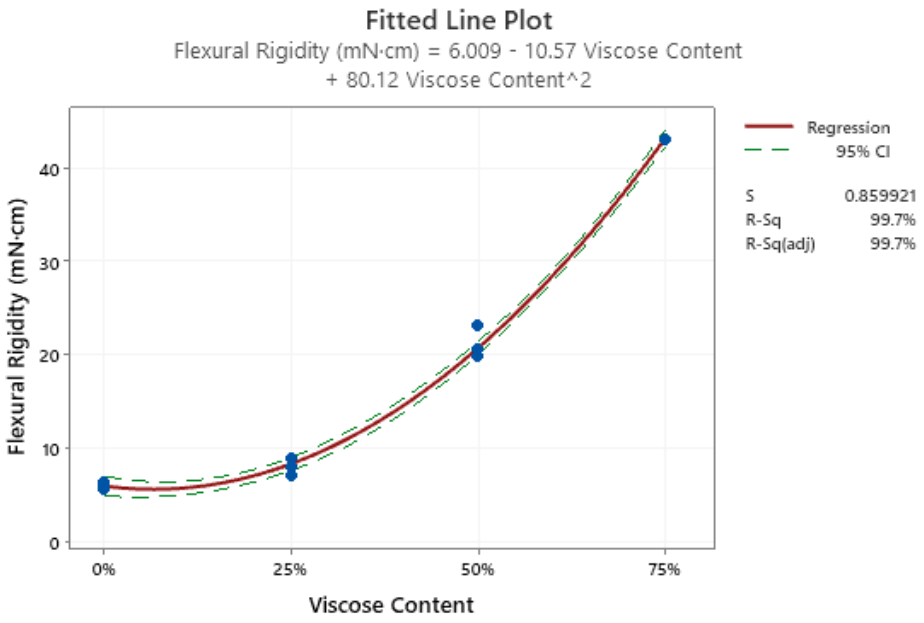

Figure 49 Flexural rigidity of VMNC as a function of viscose concentration

When comparing results of tensile modulus and flexural rigidity of VMNC, the properties seem to run inverse to each other. This shows, that while VMNC show low tensile stiffness, they can take up high lateral forces at high viscose concentrations. Since viscose fibers are expected to be non-self-binding, a rapid decrease of flexural rigidity is expected with extreme viscose concentrations (> 95 wt%). Nonetheless, future studies could investigate the optimum viscose fiber content and binding properties between fungal biomass and other fibrous materials, i.e. PLA.
Since flexural rigidity tests have been conducted on specimens previously used for tensile testing, future research should validate the presented results.

3.10.4 WATER CONTACT ANGLE

Table 28 shows the influence of viscose concentration on WCA. With viscose > 25%, water drops are immediately absorbed after being placed on the surface. Therefore, measurements are presented as 0°. Already at 25% viscose, WCA is decreased significantly in comparison to fungal biomass films.

Table 28 Results of water contact angle measurements of VMNC prepared with autoclaved (Aut) and enzyme treated (Enz) biomass at varying viscose fiber concentrations. The number of sample replicates is show in n

Sample	WCA (°)	*n*
Aut75Vc25	80 ± 4	3
Aut50Vc50	0	3
Aut25Vc75	0	3
Enz75Vc25	61 ± 9	3
Enz50Vc50	0	3
Enz25Vc75	0	3

3.11 DISCUSSION OF ENVIRONMENTAL ISSUES

Of course, the proposition to prioritize the reduction of occurring bread waste in supermarkets is valid. Certainly, this issue needs to be addressed as well. However, the issue of food waste is a multi-faceted one. As already discussed in section 1.3.1, freshly baked bread is very susceptible to being removed from shelves due to non-disclosed best-before dates as well as the customer's expectation of full shelves at any operating hour. In fact, Stenmarck et al. (2011) showed that retailers often produce 7% more than the expected sales in order to keep shelves full during opening hours. However, Stenmarck et al. (2011) further claim the largest causes for food ending up as waste are outside the control of retailers. Sales are dependent upon the weather, special offers and even the mood of customers on a given day. So, while there is certainly potential to reduce the amount of bread waste in supermarkets, it remains probable that even in retailing conditions optimized for minimum food loss, a significant amount of bread waste still occurs. Therefore, the investigation of reusing bread waste for the cultivation of filamentous fungi is considered valid.

Furthermore, the current disposal of unsold bread is suboptimal. Dorward (2012) claims that greenhouse gas (GHG) emissions are greatest when food waste is landfilled, where anaerobic digestion leads to great emissions of methane. The smallest emission of GHG is found in the repurposing of animal feed. However, the possibility of using food waste for fungal cultivation is not discussed by Dorward and is therefore not included in the ranking of GHG emissions.

Ferreira et al. (2020) discuss the critical role of filamentous fungi in global pollution mitigation. They propose the use of filamentous fungi for the creation of closed loop scenarios in which various waste streams can be used for the cultivation of fungi. These are then employed for the production of a wide array of high-value products, such as enzymes, acids or alcohols via secretion. The remaining fungal biomass could be utilized for the sourcing of chitin and chitosan or further processed into animal feed or even food fit for human consumption. The thesis at hand even goes one step further, in which the separation of fungal cell wall into chitinous and protein-rich matter is proposed to maximize the yield of high-value products.

As for the films and nonwoven composites prepared in the study at hand, they could be used to tackle several problems regarding environmental issues. The films prepared from fungal mycelia share characteristics with plastic sheets and similar fungal films are in fact proposed as alternatives to packaging applications, where commonly non-degradable plastics are used (Nawawi et al., 2020b). Furthermore, by tailoring the appearance and tensile properties of films, they could be used as biodegradable wound healing applications, as was examined in previous studies (Su et al., 1999, 1997). The use of fungal biomass as a binder in nonwoven composites also poses a promising start for the production of environmentally friendly and fully biodegradable composite structures. Furthermore, previous research showed the promising application of similar composites for the filtration of water from metal ions (Janesch et al., 2020; Wales and Sagar, 1990).

4 CONCLUSIONS

Applying a wet-laid papermaking process for the production of *R. delemar* biomass films was successful. However, the papermaking process needed to be adapted to fungal biomass. The binding of wet-laid biomass to wire screens and blotting papers posed a major issue in the recovery of dried films. Improvements in the process were made by using a nylon wire screen for wet-laying and a thin nylon mesh as a separating layer between blotting paper and film during drying. An adaption of the conventional papermaking method to a vacuum filtration process was also successful.
Preparation of viscose-mycelia nonwoven composite sheets by the papermaking process was also successful. Fungal biomass seems to take over the role of a binding matrix while viscose fibers are the load bearing component. Nonwoven composite sheets exhibit far greater flexural rigidity than pure biomass films.

To remove protein fractions from the fungal cell wall, enzymatic hydrolysis via protease showed promising results. The solely enzyme treated biomass did not meet the tensile properties of alkali treated biomass. However, a subsequent bleaching treatment leads to major improvements of tensile properties and the difference between alkali and enzyme treated films is greatly reduced. Protease treatment of fungal biomass poses a significant advantage to NaOH treatment: About 30% of biomass weight after protease treatment are recovered as liquid and solid residue. By the Kjeldahl method an estimated protein concentration of 7.68 g/l was determined in the liquid residue after protease treatment

Bread particles, which remained as cultivation residues in films, caused disturbances in film structures of alkali, protease and autoclave treated biomass. A grinding treatment on biomass lessened the detrimental effect of bread particles while also leading to a more homogeneous distribution of fungal fibers in suspension. Both factors led to an increase in tensile properties. Regression analysis predicts a maximum result of tensile properties at 27 grinding cycles.
Experiments on removing bread residue via protease or cellulase resulted in a significant reduction of tensile properties of films. However, bread particles were at least partly removed by a subsequent bleaching treatment on biomass. A hypothesis was stated, in that bleached bread particles remain as smaller cellulosic fractions and act as reinforcements in the film structure. The reinforcement then increases the overall tensile properties of films.
The highest average tensile index σ_{TI} = 61.41 Nm/g was recorded for EnzGB15 films. AlkGB10 films showed the highest tensile modulus E = 3.38 GPa, while AlkGB15 showed the highest ultimate tensile strength σ_{UTS} = 71.50 MPa. These are the highest reported tensile properties of mycelia derived films to date.

As a control study, *R. delemar* was cultivated on synthetic medium to investigate how fungal biomass films would perform without the presence of bread particles. However, the short cultivation time in synthetic medium (8-16 hours) most probably caused a significant decrease of chitin and chitosan concentrations in fungal cell walls. Nonetheless, the control study suggests that a grinding treatment on biomass is mainly responsible for breaking down bread particles and thereby lessening their negative effect on tensile properties of films.

Water contact angle measurements showed that fungal films have hydrophobic characteristics. However, the results do not meet reported values of previous studies, where WCA of 101° - 106° (M. Jones et al., 2019) and even 129° (Appels et al., 2020) were reported. The lessened hydrophobicity is probably caused by cellulosic bread residues in films. For viscose-mycelia nonwoven composites, a hydrophobic surface is only observed at a biomass concentration of 75 wt%. At 50 and 75%, water drops are immediately absorbed.

Regarding the cultivation of *Fusarium venenatum* on suspended bread particles, a fed-batch cultivation for 48 hours with a continuous supply of 1 wt% bread, resulted in the highest biomass yield. If a fed-batch process cannot be realized in bigger cultivation vessels, a batch cultivation for 48 hours at 2% bread concentration is the next best option. Cultivation of *F. venenatum* on hydrolyzed bread did not turn out successful. It is hypothesized, that missing nitrogen and salt sources are the reason for the low outcome in biomass yield.

5 FUTURE RESEARCH

During the course of the project, many ideas and could not be realized due to time constraints. As cultivation parameters for *F. venenatum* on bread particles have been established by the research at hand, future work needs to look into the scaling up of cultivation. Furthermore, since the intention of the project was to compare chitin-chitosan films against chitin-glucan films, *F. venenatum* biomass needs to be used for wet-laying of films as well.

Regarding further development of treatment on *R. delemar* biomass, a preliminary treatment with dilute sulfuric acid and a subsequent second alkali treatment showed promising results in improving tensile properties. This treatment should be further investigated. Regression analysis of tensile properties as a function of grinding cycles predicted an optimum of 27 grinding cycles on biomass. This statement needs to be verified by experiments.

About the preparation of wet-laid films, future studies could investigate the influence of a hot pressing treatment for drying of films. Previous studies applied this method. However, a direct comparison between the two methods has not been done yet.
Since Alk15 films showed a significantly higher tensile index than Enz15 and Aut15, future research should investigate the influence of alkali treated biomass as a binder for viscose nonwoven composites. If Alk15 shows a significant increase in tensile strength, biomass treated by a two-step chemical (i.e. AlkGB and EnzGB) is then a strong candidate for further research into VMNC. Additionally, an investigation into nonwoven composites prepared with other fibrous materials could be made. A suggestion here would be PLA fibers, since they can be sources from renewable resources.

Films and nonwoven composites can be further characterized by additional test methods. A promising lead would be the tensile properties of films in wet condition. Since a preliminary test showed, that structural integrity is maintained after submerging films in water, this characterization could help in order to further differentiate the films from paper products.
Porosity of films was tested via Gurley method. However, the test result was out of bounds. Therefore, future studies should focus on test methods, which directly determine porosity of films, i.e. measurement of skeletal density (Janesch et al., 2020; M. Jones et al., 2019; Nawawi et al., 2020a). Nonwoven composites were not tested on their porosity due to time constraints. Since their porosity seems to be far greater than that of biomass films, an air-flow method such as the Gurley test should be suitable.
To verify the results of bending stiffness, the measurements need to be repeated in the future with unblemished specimens. Since results for nonwoven composites were out of bounds, a three-point-bending test could be applied to measure their bending stiffness.

Chitosan has recently been the object of research for applications of flame retardant coatings on textiles (Li et al., 2020; Zhang et al., 2019). Future research could investigate if fungal biomass shows flame-retardant properties as a binder in nonwoven composites.

6 REFERENCES

Adney, B., Baker, J., 2008. Measurement of Cellulase Activities: Laboratory Analytical Procedure (LAP); Issue Date: 08/12/1996. Tech. Rep. 11.

Appels, F.V.W., van den Brandhof, J.G., Dijksterhuis, J., de Kort, G.W., Wösten, H.A.B., 2020. Fungal mycelium classified in different material families based on glycerol treatment. Commun. Biol. 3, 334. https://doi.org/10.1038/s42003-020-1064-4

Barbosa, I.P., Kemmelmeier, C., 1993. Chemical Composition of the Hyphal Wall from Fusarium graminearum. Exp. Mycol. 17, 274–283. https://doi.org/10.1006/emyc.1993.1026

Barran, L., Schneider, E., Wood, P., Madhosingh, C., Miller, R., 1975. Cell wall of Fusarium sulphureum: I. Chemical composition of the hyphal wall. Biochim. Biophys. Acta BBA - Gen. Subj. 392, 148–158. https://doi.org/10.1016/0304-4165(75)90175-0

Bartnicki-Garcia, S., 1968. Cell Wall Chemistry, Morphogenesis, and Taxonomy of Fungi. Annu. Rev. Microbiol. 22, 87–108. https://doi.org/10.1146/annurev.mi.22.100168.000511

Benjamin, M., Douglass, I.B., Hansen, G.A., Major, W.D., Navarre, A.J., Yerger, H.J., 1969. A General Description of Commercial Wood Pulping and Bleaching Processes. J. Air Pollut. Control Assoc. 19, 155–161. https://doi.org/10.1080/00022470.1969.10466471

Berglund, L., 2019. From bio-based residues to nanofibers usingmechanical fibrillationfor functional biomaterials (Doctoral Thesis). Luleå University of Technology.

Berglund, L., Anugwom, I., Hedenström, M., Aitomäki, Y., Mikkola, J.-P., Oksman, K., 2017. Switchable ionic liquids enable efficient nanofibrillation of wood pulp. Cellulose 24, 3265–3279. https://doi.org/10.1007/s10570-017-1354-2

Berglund, L., Noël, M., Aitomäki, Y., Öman, T., Oksman, K., 2016. Production potential of cellulose nanofibers from industrial residues: Efficiency and nanofiber characteristics. Ind. Crops Prod. 92, 84–92. https://doi.org/10.1016/j.indcrop.2016.08.003

Brancoli, P., Rousta, K., Bolton, K., 2017. Life cycle assessment of supermarket food waste. Resour. Conserv. Recycl. 118, 39–46. https://doi.org/10.1016/j.resconrec.2016.11.024

Bucuricova, L., 2019. Production of Edible Fungi Using Bread Waste (Master Thesis). University of Borås, Borås.

Chung, L.Y., Schmidt, R.J., Hamlyn, P.F., Sagar, B.F., Andrew, A.M., Turner, T.D., 1994. Biocompatibility of potential wound management products: Fungal mycelia as a source of chitin/chitosan and their effect on the proliferation of human F1000 fibroblasts in culture. J. Biomed. Mater. Res. 28, 463–469. https://doi.org/10.1002/jbm.820280409

Chung, L.Y., Schmidt, R.J., Hamlyn, P.F., Sagar, B.F., Andrews, A.M., Turner, T.D., 1998. Biocompatibility of potential wound management products: Hydrogen peroxide generation by fungal chitin/chitosans and their effects on the proliferation of murine L929 fibroblasts in culture. J. Biomed. Mater. Res. 39, 300–307. https://doi.org/10.1002/(SICI)1097-4636(199802)39:2<300::AID-JBM18>3.0.CO;2-G

Davis, L.L., Bartnicki-Garcia, S., 1984. Chitosan synthesis by the tandem action of chitin synthetase and chitin deacetylase from Mucor rouxii. Biochemistry 23, 1065–1073. https://doi.org/10.1021/bi00301a005

De Deken, R.H., 1966. The Crabtree Effect: A Regulatory System in Yeast. J. Gen. Microbiol. 44, 149–156. https://doi.org/10.1099/00221287-44-2-149

Desbrières, J., Guibal, E., 2018. Chitosan for wastewater treatment. Polym. Int. 67, 7–14. https://doi.org/10.1002/pi.5464

Dorward, L.J., 2012. Where are the best opportunities for reducing greenhouse gas emissions in the food system (including the food chain)? A comment. Food Policy 37, 463–466. https://doi.org/10.1016/j.foodpol.2012.04.006

Ek, M., Gellerstedt, G., Henriksson, G., 2009. Pulp and paper chemistry and technology. Volume 3: Paper Chemistry and Technology. Walter de Gruyter, Berlin.

El-Enshasy, H.A., 2007. Filamentous Fungal Cultures – Process Characteristics, Products, and Applications, in: Bioprocessing for Value-Added Products from Renewable Resources. Elsevier, pp. 225–261. https://doi.org/10.1016/B978-044452114-9/50010-4

Eriksson, M., Strid, I., Hansson, P.-A., 2015. Carbon footprint of food waste management options in the waste hierarchy – a Swedish case study. J. Clean. Prod. 93, 115–125. https://doi.org/10.1016/j.jclepro.2015.01.026

Ferreira, A., Rocha, F., Mota, A., Teixeira, J.A., 2017. Nonmechanically Agitated Bioreactors, in: Current Developments in Biotechnology and Bioengineering. Elsevier, pp. 217–233. https://doi.org/10.1016/B978-0-444-63663-8.00008-2

Ferreira, J.A., Varjani, S., Taherzadeh, M.J., 2020. A Critical Review on the Ubiquitous Role of Filamentous Fungi in Pollution Mitigation. Curr. Pollut. Rep. https://doi.org/10.1007/s40726-020-00156-2

Garnett, T., 2011. Where are the best opportunities for reducing greenhouse gas emissions in the food system (including the food chain)? Food Policy 36, S23–S32. https://doi.org/10.1016/j.foodpol.2010.10.010

Ghormade, V., Pathan, E.K., Deshpande, M.V., 2017. Can fungi compete with marine sources for chitosan production? Int. J. Biol. Macromol. 104 B, 1415–1421. https://doi.org/10.1016/j.ijbiomac.2017.01.112

Gmoser, R., Fristedt, R., Larsson, K., Undeland, I., Taherzadeh, M.J., Lennartsson, P.R., 2020. From stale bread and brewers spent grain to a new food source using edible filamentous fungi. Bioengineered 11, 582–598. https://doi.org/10.1080/21655979.2020.1768694

Gmoser, R., Sintca, C., Taherzadeh, M.J., Lennartsson, P.R., 2019. Combining submerged and solid state fermentation to convert waste bread into protein and

pigment using the edible filamentous fungus N. intermedia. Waste Manag. 97, 63–70. https://doi.org/10.1016/j.wasman.2019.07.039

Göksungur, Y., 2004. Optimization of the production of chitosan from beet molasses by response surface methodology. J. Chem. Technol. Biotechnol. 79, 974–981. https://doi.org/10.1002/jctb.1065

Goldstein, D.B., 1986. Effect of alcohol on cellular membranes. Ann. Emerg. Med. 15, 1013–1018. https://doi.org/10.1016/S0196-0644(86)80120-2

Gow, N.A., Gadd, Geoffrey M, Gow, N. a, Gadd, Geoffrey Michael, 2007. The Growing Fungus.

Griffin, D.H., 1996. Fungal Physiology. John Wiley & Sons.

Hamlyn, P.F., Schmidt, R.J., 1994. Potential Therapeutic Application of Fungal Filaments in Wound Management. Mycologist 8, 147–152.

Hanne Mæhre, Lars Dalheim, Guro Edvinsen, Edel Elvevoll, Ida-Johanne Jensen, 2018. Protein Determination—Method Matters. Foods 7, 5. https://doi.org/10.3390/foods7010005

Hoseyni, S.M., Mohammadifar, M.A., Khosravi-Darani, K., 2010. Production and rheological evaluation of mycoprotein produced from fusarium venenatum ATCC 20334 by surface culture method 7.

Hubbe, M.A., Koukoulas, A.A., 2016. Wet-Laid Nonwovens Manufacture – Chemical Approaches Using Synthetic and Cellulosic Fibers. BioResources 11. https://doi.org/10.15376/biores.11.2.Hubbe

Ike, M., Ko, Y., Yokoyama, K., Sumitani, J.-I., Kawaguchi, T., Ogasawara, W., Okada, H., Morikawa, Y., 2007. Cellobiohydrolase I (Cel7A) from Trichoderma reesei has chitosanase activity. J. Mol. Catal. B Enzym. 47, 159–163. https://doi.org/10.1016/j.molcatb.2007.05.004

Islam, S., Bhuiyan, M.A.R., Islam, M.N., 2017. Chitin and Chitosan: Structure, Properties and Applications in Biomedical Engineering. J. Polym. Environ. 25, 854–866. https://doi.org/10.1007/s10924-016-0865-5

ISO 139, 2005. Textiles – Standard atmospheres for conditioningand testing.

ISO 187, 1990. Paper, board and pulps - Standard atmosphere for conditioning and testing and procedure for monitoring the atmosphere and conditioning of samples.

ISO 9073-7, 1995. Textiles - Test for nonwovens - Part 7: Determination of bending length.

Janesch, J., Jones, M., Bacher, M., Kontturi, E., Bismarck, A., Mautner, A., 2020. Mushroom-derived chitosan-glucan nanopaper filters for the treatment of water. React. Funct. Polym. 146, 104428. https://doi.org/10.1016/j.reactfunctpolym.2019.104428

Johnson, M.A., Carlson, J.A., 1978. Mycelial paper: A potential resource recovery process? Biotechnol. Bioeng. 20, 1063–1084. https://doi.org/10.1002/bit.260200708

Jones, M., Kujundzic, M., John, S., Bismarck, A., 2020. Crab vs. Mushroom: A Review of Crustacean and Fungal Chitin in Wound Treatment. Mar. Drugs 18, 64. https://doi.org/10.3390/md18010064

Jones, M., Weiland, K., Kujundzic, M., Theiner, J., Kählig, H., Kontturi, E., John, S., Bismarck, A., Mautner, A., 2019. Waste-Derived Low-Cost Mycelium Nanopapers with Tunable Mechanical and Surface Properties. Biomacromolecules 20, 3513–3523. https://doi.org/10.1021/acs.biomac.9b00791

Jones, M.P., Lawrie, A.C., Huynh, T.T., Morrison, P.D., Mautner, A., Bismarck, A., John, S., 2019. Agricultural by-product suitability for the production of chitinous composites and nanofibers utilising Trametes versicolor and Polyporus brumalis mycelial growth. Process Biochem. 80, 95–102. https://doi.org/10.1016/j.procbio.2019.01.018

Kim, S.-K. (Ed.), 2011. Chitin, chitosan, oligosaccharides and their derivatives: biological activities and applications. CRC Press, Boca Raton.

Kinsey, G., Paterson, R., Kelley, J., 2003. Filamentous fungi in water systems, in: Handbook of Water and Wastewater Microbiology. Elsevier, pp. 77–98. https://doi.org/10.1016/B978-012470100-7/50006-6

Kjeldahl, J., 1883. Neue Methode zur Bestimmung des Stickstoffs in organischen Körpern. Fresenius Z. Für Anal. Chem. 22, 366–382. https://doi.org/10.1007/BF01338151

Knezevic-Jugovic, Z., Petronijevic, Z., Smelcerovic, A., 2010. Chitin and Chitosan from Microorganisms, in: Kim, S.-K. (Ed.), Chitin, Chitosan, Oligosaccharides and Their Derivatives. CRC Press, pp. 25–36. https://doi.org/10.1201/EBK1439816035-c3

Kumirska, J., X., M., Czerwicka, M., Kaczyski, Z., Bychowska, A., Brzozowski, K., Thming, J., Stepnowski, P., 2011. Influence of the Chemical Structure and Physicochemical Properties of Chitin- and Chitosan-Based Materials on Their Biomedical Activity, in: Laskovski, A. (Ed.), Biomedical Engineering, Trends in Materials Science. InTech. https://doi.org/10.5772/13481

Li, P., Wang, B., Liu, Y.-Y., Xu, Y.-J., Jiang, Z.-M., Dong, C.-H., Zhang, L., Liu, Y., Zhu, P., 2020. Fully bio-based coating from chitosan and phytate for fire-safety and antibacterial cotton fabrics. Carbohydr. Polym. 237, 116173. https://doi.org/10.1016/j.carbpol.2020.116173

Liao, W., Liu, Y., Frear, C., Chen, S., 2008. Co-production of fumaric acid and chitin from a nitrogen-rich lignocellulosic material – dairy manure – using a pelletized filamentous fungus Rhizopus oryzae ATCC 20344. Bioresour. Technol. 99, 5859–5866. https://doi.org/10.1016/j.biortech.2007.10.006

Ma, M., Xu, L., Qiao, L., Chen, S., Shi, Y., He, H., Wang, X., 2020. Nanofibrillated Cellulose/MgO@rGO composite films with highly anisotropic thermal conductivity and electrical insulation. Chem. Eng. J. 392, 123714. https://doi.org/10.1016/j.cej.2019.123714

Mariotti, F., Tomé, D., Mirand, P.P., 2008. Converting Nitrogen into Protein—Beyond 6.25 and Jones' Factors. Crit. Rev. Food Sci. Nutr. 48, 177–184. https://doi.org/10.1080/10408390701279749

Marlow Food Ltd., 2020. Quorn Meatless Pieces [WWW Document]. Quorn. URL https://www.quorn.us/products/quorn-meatless-chicken-pieces (accessed 8.14.20).

Martinou, A., Bouriotis, V., Stokke, B.T., Vårum, K.M., 1998. Mode of action of chitin deacetylase from Mucor rouxii on partially N-acetylated chitosans. Carbohydr. Res. 311, 71–78. https://doi.org/10.1016/S0008-6215(98)00183-9

Maya, Rike, 2013. Cell wall structure of Fungi (licensed under CC BY 3.0) [WWW Document]. Wikimedia Commons. URL https://commons.wikimedia.org/wiki/File:Cell_wall_structure_of_Fungi.png#filehistory (accessed 12.10.19).

Melikoglu, M., Lin, C.S.K., Webb, C., 2015. Solid state fermentation of waste bread pieces by Aspergillus awamori: Analysing the effects of airflow rate on enzyme production in packed bed bioreactors. Food Bioprod. Process. 95, 63–75. https://doi.org/10.1016/j.fbp.2015.03.011

Michalenko, G.O., Hohl, H.R., Rast, D., 1976. Chemistry and Architecture of the Mycelial Wall of Agaricus bisporus. J. Gen. Microbiol. 92, 251–262. https://doi.org/10.1099/00221287-92-2-251

Mohammadi, M., Zamani, A., Karimi, K., 2012. Determination of Glucosamine in Fungal Cell Walls by High-Performance Liquid Chromatography (HPLC). J. Agric. Food Chem. 60, 10511–10515. https://doi.org/10.1021/jf303488w

Money, N.P., 2016. Fungi and Biotechnology, in: The Fungi. Elsevier, pp. 401–424. https://doi.org/10.1016/B978-0-12-382034-1.00012-8

Morin-Crini, N., Lichtfouse, E., Torri, G., Crini, G., 2019. Applications of chitosan in food, pharmaceuticals, medicine, cosmetics, agriculture, textiles, pulp and paper, biotechnology, and environmental chemistry. Environ. Chem. Lett. 17, 1667–1692. https://doi.org/10.1007/s10311-019-00904-x

Muñoz, I., Rodríguez, C., Gillet, D., M. Moerschbacher, B., 2018. Life cycle assessment of chitosan production in India and Europe. Int. J. Life Cycle Assess. 23, 1151–1160. https://doi.org/10.1007/s11367-017-1290-2

Naghdi, M., Zamani, A., Karimi, K., 2014. A sulfuric–lactic acid process for efficient purification of fungal chitosan with intact molecular weight. Int. J. Biol. Macromol. 63, 158–162. https://doi.org/10.1016/j.ijbiomac.2013.10.042

Nair, R.B., Theimya, E.-H.N., Taherzadeh, M.J., Lennartsson, P., 2017. Waste Bread Valorization Using Edible Filamentous Fungi. Presented at the EUBCE 2017 – 25th European Biomass Conference and Exhibition, Stockholm, p. 5.

Nawawi, W., 2016. Renewable chitin based nanomaterials from fungi. https://doi.org/10.25560/67286

Nawawi, W., Jones, M., Kontturi, E., Mautner, A., Bismarck, A., 2020a. Plastic to elastic: Fungi-derived composite nanopapers with tunable tensile properties. Compos. Sci. Technol. 198, 108327. https://doi.org/10.1016/j.compscitech.2020.108327

Nawawi, W., Jones, M., Murphy, R.J., Lee, K.-Y., Kontturi, E., Bismarck, A., 2020b. Nanomaterials Derived from Fungal Sources—Is It the New Hype? Biomacromolecules 21, 30–55. https://doi.org/10.1021/acs.biomac.9b01141

Nawawi, W., Lee, K.-Y., Kontturi, E., Bismarck, A., 2015. Strong and tough fungal based Chitin-Glucan thin film. Presented at the 20th International Conference on Composite Materials, Copenhagen, p. 8.

Nawawi, W., Lee, K.-Y., Kontturi, E., Bismarck, A., Mautner, A., 2020c. Surface properties of chitin-glucan nanopapers from Agaricus bisporus. Int. J. Biol. Macromol. 148, 677–687. https://doi.org/10.1016/j.ijbiomac.2020.01.141

Nawawi, W., Lee, K.-Y., Kontturi, E., Murphy, R.J., Bismarck, A., 2019. Chitin Nanopaper from Mushroom Extract: Natural Composite of Nanofibers and Glucan from a Single Biobased Source. ACS Sustain. Chem. Eng. 7, 6492–6496. https://doi.org/10.1021/acssuschemeng.9b00721

Olajuyigbe, F.M., Ajele, J.O., 2008. Some Properties of Extracellular Protease from Bacillus licheniformis Lbbl-11 Isolated from "iru", A Traditionally Fermented African Locust Bean Condiment. Glob. J. Biotechnol. Biochem. 3, 42–46.

Piepenbring, M., 2015. Biologische Schemata, gezeichnet und freigegeben von M. Piepenbring (licensed under CC BY-SA 3.0) [WWW Document]. Wikimedia Commons. URL https://commons.wikimedia.org/wiki/File:06_05_sporangiophores,_sporangia,_conidia,_liberation_of_spores,_Mucorales,_Zygomycota_(M._Piepenbring).png (accessed 12.8.19).

Roberts, G.A.F., 1992. Chitin Chemistry.

Ruggiero, M.A., Gordon, D.P., Orrell, T.M., Bailly, N., Bourgoin, T., Brusca, R.C., Cavalier-Smith, T., Guiry, M.D., Kirk, P.M., 2015. A Higher Level Classification of All Living Organisms. PLOS ONE 10, e0119248. https://doi.org/10.1371/journal.pone.0119248

Sagar, B., Hamlyn, P., Wales, D., 1991. Wound Dressing. EP0460774B1.

Sagar, B., Hamlyn, P., Wales, D., 1987. Production of textile and other articles. GB2188135A.

Seyed Reihani, S.F., Khosravi-Darani, K., 2019. Mycoprotein Production from Date Waste Using Fusarium venenatum in a Submerged Culture. Appl. Food Biotechnol. 5. https://doi.org/10.22037/afb.v5i4.23139

Siqueira, G., Oksman, K., Tadokoro, S.K., Mathew, A.P., 2016. Re-dispersible carrot nanofibers with high mechanical properties and reinforcing capacity for use in composite materials. Compos. Sci. Technol. 123, 49–56. https://doi.org/10.1016/j.compscitech.2015.12.001

Smelcerovic, A., Knezevic-Jugovic, Z., Petronijevic, Z., 2008. Microbial Polysaccharides and their Derivatives as Current and Prospective Pharmaceuticals. Curr. Pharm. Des. 14, 3168–3195. https://doi.org/10.2174/138161208786404254

Spatafora, J.W., Chang, Y., Benny, G.L., Lazarus, K., Smith, M.E., Berbee, M.L., Bonito, G., Corradi, N., Grigoriev, I., Gryganskyi, A., James, T.Y., O'Donnell, K., Roberson, R.W., Taylor, T.N., Uehling, J., Vilgalys, R., White, M.M., Stajich, J.E., 2016. A phylum-level phylogenetic classification of zygomycete fungi based on genome-scale data. Mycologia 108, 1028–1046. https://doi.org/10.3852/16-042

SS ISO 1924-3, 2011. Paper and board – Determination of tensile properties – Part 3: Constant rate of elongation method (100 mm/min).

SS ISO 5636-5, 2013. Paper and board – Determination of air permeance (medium range) – Part 5: Gurley method.

SS-EN ISO 527-2, 2012. Plastics – Determination of tensile properties – Part 2: Test conditions for moulding and extrusion plastics.

SS-EN ISO 534, 2011. Paper and board – Determination of thickness, density and specific volume.

SS-EN ISO 536, 2012. Paper and board – Determination of grammage.

SS-EN ISO 3188, 1978. Starches and derived products - Determination of nitrogen content by the Kjeldahl method - Titrimetric method.

SS-EN ISO 5269-1, 2005. Pulps – Preparation of laboratory sheets for physical testing – Part 1: Conventional sheet-former method.

SS-EN ISO 9092, 2019. Nonwovens - Vocabulary.

Stenmarck, Å., Hanssen, O.J., Werge, M., 2011. Initiatives on prevention of food waste in the retail and wholesale trades. Nordic Council of Ministers, Copenhagen.

Su, C.-H., Sun, C.-S., Juan, S.-W., Ho, H.-O., Hu, C.-H., Sheu, M.-T., 1999. Development of fungal mycelia as skin substitutes: Effects on wound healing and fibroblast. Biomaterials 20, 61–68. https://doi.org/10.1016/S0142-9612(98)00139-2

Su, C.-H., Sun, C.-S., Juan, S.-W., Hu, C.-H., Ke, W.-T., Sheu, M.-T., 1997. Fungal mycelia as the source of chitin and polysaccharides and their applications as skin substitutes. Biomaterials 18, 1169–1174. https://doi.org/10.1016/S0142-9612(97)00048-3

Swart, R.M., le Roux, F., Naude, A., de Jongh, N.W., Nicol, W., 2020. Fumarate production with Rhizopus oryzae: utilising the Crabtree effect to minimise ethanol by-product formation. Biotechnol. Biofuels 13, 22. https://doi.org/10.1186/s13068-020-1664-8

Tai, C., Li, S., Xu, Q., Ying, H., Huang, H., Ouyang, P., 2010. Chitosan production from hemicellulose hydrolysate of corn straw: impact of degradation products on Rhizopus oryzae growth and chitosan fermentation. Lett. Appl. Microbiol. 51, 278–284. https://doi.org/10.1111/j.1472-765X.2010.02893.x

Tan, S., Tan, T., Wong, S., Khor, E., 1996. The chitosan yield of zygomycetes at their optimum harvesting time. Carbohydr. Polym. 30, 239–242. https://doi.org/10.1016/S0144-8617(96)00052-5

TAPPI T 205 sp-12, 2018. Forming handsheets for physical tests of pulp.

Van Horn, W.M., Shema, B.F., Shockley, W.H., Conkey, J.H., 1957. Sheets comprising Filaments of Fungi. US2811442.

Verni, M., Minisci, A., Convertino, S., Nionelli, L., Rizzello, C.G., 2020. Wasted Bread as Substrate for the Cultivation of Starters for the Food Industry. Front. Microbiol. 11, 293. https://doi.org/10.3389/fmicb.2020.00293

Wales, D.S., Sagar, B.F., 1990. Recovery of Metal Ions by Microfungal Filters. J. Chem. Technol. Biotechnol. 49, 345–355. https://doi.org/10.1002/jctb.280490407

White, C., 2007. Wet-laid web formation, in: Handbook of Nonwovens. Elsevier, pp. 112–142. https://doi.org/10.1533/9781845691998.112

Wiebe, M., 2002. Myco-protein from Fusarium venenatum : a well-established product for human consumption. Appl. Microbiol. Biotechnol. 58, 421–427. https://doi.org/10.1007/s00253-002-0931-x

Wilson, A., 2010. The formation of dry, wet, spunlaid and other types of nonwovens, in: Applications of Nonwovens in Technical Textiles. Elsevier, pp. 3–17. https://doi.org/10.1533/9781845699741.1.3

Wu, Y., Wu, J., Yang, F., Tang, C., Huang, Q., 2019. Effect of H2O2 Bleaching Treatment on the Properties of Finished Transparent Wood. Polymers 11, 776. https://doi.org/10.3390/polym11050776

Xia, W., Liu, P., Liu, J., 2008. Advance in chitosan hydrolysis by non-specific cellulases. Bioresour. Technol. 99, 6751–6762. https://doi.org/10.1016/j.biortech.2008.01.011

Zamani, A., 2010. Superabsorbent Polymers from the Cell Wall of Zygomycetes Fungi. Chalmers University of Technology, Göteborg.

Zamani, A., Edebo, L., Sjöström, B., Taherzadeh, M.J., 2007. Extraction and Precipitation of Chitosan from Cell Wall of Zygomycetes Fungi by Dilute Sulfuric Acid. Biomacromolecules 8, 3786–3790. https://doi.org/10.1021/bm700701w

Zhang, Z., Ma, Z., Leng, Q., Wang, Y., 2019. Eco-friendly flame retardant coating deposited on cotton fabrics from bio-based chitosan, phytic acid and divalent metal ions. Int. J. Biol. Macromol. 140, 303–310. https://doi.org/10.1016/j.ijbiomac.2019.08.049

Zhou, Y., Du, J., Tsao, G.T., 2000. Mycelial Pellet Formation by Rhizopus oryzae ATCC 20344. Appl. Biochem. Biotechnol. 84, 11.

Zhou, Z., Du, G., Hua, Z., Zhou, J., Chen, J., 2011. Optimization of fumaric acid production by Rhizopus delemar based on the morphology formation. Bioresour. Technol. 102, 9345–9349. https://doi.org/10.1016/j.biortech.2011.07.120